Fall 2021

The Immune Modulatory Role of Endocannabinoid Anandamide to Suppress Inflammation Through Regulation of Microrna and Microbiome

Muthanna Ali Sultan

THE IMMUNE MODULATORY ROLE OF ENDOCANNABINOID ANANDAMIDE TO SUPPRESS INFLAMMATION THROUGH REGULATION OF MICRORNA AND MICROBIOME

by

Muthanna Ali Sultan

Bachelor of Veterinary Medicine and Surgery
University of Mosul Iraq, 2005

Master of Science in Veterinary Public Health
University of Mosul Iraq, 2007

Submitted in Partial Fulfillment of the Requirements

For the Degree of Doctor of Philosophy in

Biomedical Science

School of Medicine

University of South Carolina

2021

Accepted by:

Mitzi Nagarkatti, Major Professor

Prakash Nagarkatti, Major Professor

Susan Lessner, Committee Member

Brandon Busbee, Committee Member

Ehsan Jabberzadeh, Committee Member

Tracey L. Weldon, Interim Vice Provost and Dean of the Graduate School

DEDICATION

This work is dedicated to everyone who has helped me throughout my life, particularly my colleagues who shared this journey with me. I want to also dedicate this work to all my family and friends for offering their much-appreciated love and support. I first extend a deep heartfelt thank you to my father and my mother who always encouraged me to reach for the stars, and made me believe that I could be anything I wanted to be, as long as I worked hard towards my goals.

ACKNOWLEDGMENTS

I would like to thank my mentors, Dr. Mitzi Nagarkatti and Dr. Prakash Nagarkatti, for their tremendous support and leadership. I want to thank my committee members, Dr. Brandon Busbee, Dr. Susan Lessner, and Dr. Ehsan Jabberzadeh for their guidance and support. I would like to thank my dear country, Iraq, for all support during my entire life. Importantly, I would like to thank all my family members in Iraq including my father, mother, brothers, and sisters who spiritually supported me throughout my years of study. Thanks for all your prayers and wishes. Many people have helped me throughout my journey at the University of South Carolina, and even though I cannot mention all their names due to space, I am grateful for all that they have done!

ABSTRACT

Cannabinoids are group of compounds that exert their anti-inflammatory action through activation of cannabinoid 1 receptor (CB1) and cannabinoid receptor 2 (CB2), as well as other minor receptors. In the current study, we investigated the effect of anandamide (AEA) on Acute Respiratory Distress Syndrome (ARDS) induced by exposure to Staphylococcus enterotoxin B (SEB) intranasally. We found that C57BL/6 mice treated with AEA showed improvement in the clinical functions of the lungs, accompanied by a decrease in the infiltration of inflammatory cells in the lung tissue, and a decrease in the secretion of pro-inflammatory cytokines. Furthermore, AEA regulated the miRNA profile of the mononuclear cells in the lungs leading to significant downregulation of miRNA-23a-3p which led to upregulation of Arginase 1 (Arg1) and Transforming Growth Factor-beta 2 (TGFB2), which are markers of Myeloid Derived Suppressor Cells (MDSCs) and T regulatory cells (Tregs), respectively. Another miRNA that was downregulated after AEA treatment was miRNA-34a-5p which led to induction of FOXP3, a defining transcription factor for Tregs. All the miRNA markers and their target genes were validated by quantitative RT-PCR (RT-qPCR). Additionally, flow cytometry data indicated that AEA caused a decrease in CD4+T cells, CD8+T cells, V□8+ T cells, and natural killerT cells (NKT) in ARDS mice. On the other hand, AEA caused induction of MDSCs, Tregs (CD4+FOXP3+), and type 1 regulatory T cells (Tr1)

(CD4+IL10+) subpopulations. Additionally, proliferation assays demonstrated that AEA-induced MDSCs were indeed highly immunosuppressive and blocked T cell proliferation in vitro.

Next, we investigated whether AEA attenuated ARDS through modulation of the microbiome profile in the Gut-Lung Axis (GLA) in mice treated with SEB. AEA caused a decrease in the leakage of the gut and lungs, and decreased pathology in these organs based on histopathological analysis. Furthermore, data obtained from flow cytometry demonstrated that T cell subsets in the mesenteric lymph nodes (MLN) including CD4+ T cells, CD8+ T cells, Vβ8+ T cells, and NK+ T cells were significantly decreased in the AEA treated mice, when compared to SEB+VEH-treated mice.

In addition, single cell RNA sequencing (sc-RNAseq) of the cells derived from the lungs demonstrated upregulation of the gene expression of antimicrobial peptides (AMPs) in the lung epithelial cells including tracheal anti-microbial peptide 1 and 2 (TAP1,TAP2), lysozyme 2 (LYZ2), murine beta defensin 2 (MBD2) , and serum protease leukocyte inhibitor (SLPI), as well as tight junction proteins including claudin 1 (CLDN1) and cadherin 1 (CDH1), which were all significantly increased post-AEA treatment. Also, gene expression was validated by performing qRT-PCR. These data suggested that AEA was inducing the AMPs to kill pathogenic bacteria as well as stabilizing the epithelial cell functions disrupted by SEB.

Furthermore, we investigated the nature of microbial dysbiosis in the Gut-Lung Axis. The results obtained from 16S rRNA sequencing on the MiSeq platform demonstrated significant changes in the microbiome of the gut and lungs in the AEA-treated group of mice when compared to the disease controls treated with vehicle

(SEB+VEH). Also, upon analysis using both Nephele and linear discrimination analysis (LDA), there was an increase in butyrate-producing bacteria such as S-247 in both the gut and the lungs and Lachnospiraceae in the lungs. In addition, we observed that short chain fatty acids (SCFAs), especially butyrate, valeric acid, and isovaleric acid, were significantly increased in the AEA-treated group mice, when compared to SEB+VEH-treated group. Lastly, direct treatment of mice with butyrate led to attenuation of SEB-mediated ARDS, improved the clinical lung respiratory functions, and decreased the infiltration of the inflammatory cells.

Together, these studies demonstrate for the first time that endogenous cannabinoids play a critical role in suppressing cytokine storm and ARDS. These studies are highly significant considering that ARDS is difficult to treat as seen in COVID-19 patients with ARDS and thus, direct use of endocannabinoids or increasing their levels in vivo with agents such as fatty acid amide hydrolase (FAAH) an integral membrane enzyme that hydrolyzes AEA, may constitute a novel therapeutic modality to treat ARDS.

TABLE OF CONTENTS

LIST OF TABLES

LIST OF FIGURES

CHAPTER 1

INTRODUCTION

1.1 The Endocannabinoid System (ECS)

The endocannabinoid system consists of three components including, endogenous ligands (endocannabinoids), cannabinoid receptors, and the enzymes that degrade the ligands. The identification of these components has triggered interest among scientists to further investigate their role in health and disease (Pacher et al., 2006). The endogenous cannabinoids (endocannabinoids) are anandamide (AEA), also known as arachidonoyl ethanolamide, and 2 arachidonoyl glycerol (2-AG), while there are two G-protein coupled receptors (GPRs) that are considered as a part of this system. The endocannabinoid system (EC system) was unknown to the scientists until the 1990s. Studies at the National Institute of Drug Abuse (NIDA) reported cloning the G-protein coupled receptor which binds the cannabinoid-associated ligands, which they referred to as cannabinoid receptor CB1 receptor or cannabinoid receptor 1. A few years later, another receptor was identified, which was named as cannabinoid receptor 2 (CB2) (Pertwee, 2015).

AEA was first identified in 1992 as an arachidonic acid derivative, which were endogenous ligands found in porcine brain (Devane et al., 1992). These endogenous

ligands activate cannabinoid receptors in the brain and lead to behavioral effects similar to Δ9-tetrahydrocannabinol (THC), but less potent (Smith et al., 1994). Anandamide is also a part of the endocannabinoid system (ECS) which has been found in all mammalian species, as well as in the invertebrate species except the phyla protozoa and Insecta (De Petrocellis et al., 1999) .

1.2 Arachidonoyl Ethanol Amide (Anandamide, AEA)

AEA is a signaling endogenous lipid that binds to and activates cannabinoid receptors in different part of the body including the brain and the peripheral tissues (Astarita et al., 2008). The endogenous precursor of AEA is N arachidonoyl phosphatidylethanolamines (NarPE),which is considered as a family of complex glycerophospholipids derived from the arachidonoyl group (Astarita et al., 2008). AEA plays an important role in the central nervous system as well as in peripheral nervous system (Fride, 2002). The role by which AEA mediates its effect is through activating several receptors that are considered as pharmacological targets including the CB1 receptor (Dasilva et al., 2014) , CB2 receptor (Malek et al., 2015), as well as other receptors including G protein coupled receptor 55 (Sharir et al., 2012), G protein coupled receptor 119 (Im, 2021), peroxisome proliferator activated receptor (PPAR)(O'Sullivan, 2016), and Transient Receptor Potential Valid (TRPV1) (Fenwick et al., 2017).

In the immune level, endocannabinoids play an important role in immune system homeostasis mainly through interactions with the CB1 and CB2 receptors which are both expressed on immune cells. It is important to note that the CB2 receptor is expressed about 100 times more on immune cells than CB1 receptor however (Pacher et al., 2006). AEA binds with higher affinity to the brain cells through CB1 receptor and mimics the behavioral actions of the THC when injected into rodents. Our laboratory has conducted several studies on the effect of endocannabioids on immune cells, for example investigating the role of exogenous 2-AG in inflammation during induction of delayed type hypersensitivity (DTH) in mice (Sido et al., 2016). In this study, administration of 2-AG (40 mg/kg) attenuated the methylated Bovine Serum Albumin (mBSA)-DTH response by decreasing Th1 and Th17-associated cytokines such as IL-6, IL-2, TNF-α, and the IgG response. In this study, it was shown for the first time that that naïve T cells and B cells expressed low levels of 2-AG, while their activation leads to enhanced expression of 2-AG. Another study from our lab has found that exogenous AEA plays a critical role in the amelioration of DTH through the induction of myeloid derived suppressor cells (MDSCs) (Jackson et al., 2014a). Additionally, it was shown that blocking fatty acid amide hydrolyze (FAAH), an enzyme that hydrolyzes AEA in vivo, can lead to elevation in the level of endogenous AEA, which in turn protects the mice against colitis by suppressing inflammation (Shamran et al., 2017).

1.3 COVID-19 and acute respiratory distress syndrome.

Severe acute respiratory syndrome /Coronvirus disease 19 (SARS/COVID 19) has been the main cause of respiratory failure and/or death for millions of people recently due to the pandemic which has caused huge economic losses and social disruptions globally (Hodgson et al., 2021). COVID-19 Acute Respiratory Distress Syndrome (ARDS) causes typical pathological changes and diffuse alveolar damage in the lungs (Konopka et al., 2020). ARDS is considered an acute phenomenon at the onset of hypoxemia that occurs after damage to the respiratory tract (Voshaar et al., 2021). ARDS is characterized by infiltration of inflammatory cells in the lungs and cytokine storm (Umbrello et al., 2016). About 25% of the patients usually have mild form of ARDS, while 75% of the patients have medium or severe form of ARDS (Rubenfeld et al., 2005). There are many risk factors associated with ARDS such as pneumonia, sepsis, shock, trauma, and multi-organ failure (Umbrello et al., 2016). While the pathophysiology of the ARDS is still unclear, the main characteristic of ARDS is an increased pulmonary capillary permeability as well as accumulation of protein rich fluid inside the alveoli, which is considered the main result of the damages of the capillary endothelium and capillary epithelium and release of cytokines causing diffuse alveolar damage (Martin, 1999). T cells subsets are one of the main target cells during ARDS caused by an infection. CD4+ T helper cells are the main activated T cells subsets when compared to the CD8+ cytotoxic T cells, and thus the ratio of CD8+/CD4+ is significantly increased in the patients with ARDS compared to normal healthy people (Umbrello et al., 2016). Another study observed there are other T cell subsets activated during ARDS, such as NKT cells (Tumurkhuu et al., 2008). Cytokines are one of the most important clinical factors that are released after the activation of

immune cells, which causes the destruction of the lung tissue. One of the key cytokines is interleukin-6 (IL-6), which is significantly increased in the patients with ARDS compared to normal healthy people (Swaroopa et al., 2016).

1.4 Staphylococcus Enterotoxin B (SEB)

Staphylococcus Enterotoxin B (SEB) is an exotoxin that is produced by *Staphylococcus aureus* which can cause food poisoning or respiratory infections through ingestion or inhalation (Rozynska and Plusa, 2015). SEB is considered the most potent bacterial super antigen which can activate a large proportion of T cells expressing certain V□ specificities, thereby hyperactivating the immune system and leading to massive cytokine release often called "cytokine storm", resulting in systemic inflammation which is often lethal (Fries and Varshney, 2013). The cytokines produced primarily include IL6 and interferon-gamma (IFN-γ). SEB directly interacts with major histocompatibility class (MHC II) molecules expressed on antigenic presenting cells (APCs) without being processed and presented like other antigens, and the SEB+MHC II complex can directly activate T cells that express a certain type of T cell receptor (TCR). In the mouse, SEB+MHC II activates T cells that express the V□8 TCR (Newell et al., 1991;Miethke et al., 1992).

1.5 MicroRNA

MicroRNAs (miRNAs) are small endogenous molecules that have the main function of regulating the gene expression post-transcriptionally. There are many methods including in vivo and in vitro for isolation, identification, quantification,

profiling, and detection of miRNA (Lu and Rothenberg, 2018).The majority of miRNAs are transcribed directly from DNA into primary RNAs, then into precursor miRNA, and finally a mature miRNA (O'Brien et al., 2018). There are several studies that focused on miRNAs biogenesis (Bartel, 2009;Carthew and Sontheimer, 2009). MiRNAs precursors (pri-miRNAs) are transcribed by either RNA polymerase II from independent genes or represent introns and hairpins which are the resulting of fold of miRNAs are acting as a substrate of Drosha and Pasha, while Drosha cleavage which is about 70 nucleotide pre-miRNA that exported to cytoplasm and Dicer which is about 20 bp miRNA/miRNA duplex (Krol et al., 2010)

Micro-RNAs interact with the 3' untranslated region (3' UTR) of messenger RNAs (mRNAs) to induce degradation and translation repression. There are many factors that determine the interaction of the miRNAs with their target genes, such as location, abundancy, and affinity between miRNA and mRNA (O'Brien et al., 2018). Many studies have been found that miRNAs bind to specific sequence of the 3' UTR of their target miRNA to induce translational repression (Huntzinger and Izaurralde, 2011;Ipsaro and Joshua-Tor, 2015). As miRNAs bind to specific regions of the 3' UTR, there are many other studies which show miRNAs also bind to other mRNAs region such as 5' UTR region, coding sequences, and parts of the promotor regions which results in silencing of gene expression (Forman et al., 2008;Zhang et al., 2018). Recent studies have shown that miRNA play a central role as novel therapeutic against inflammation (Tahamtan et al., 2018). MicroRNA may mediate anti-inflammatory action by interacting with other factors such as transcription factors, signaling proteins, and regulators of the cell death (Tsitsiou and Lindsay, 2009). In addition to these aforementioned factors, miRNA can act

as key regulators of inflammation by controlling the signaling of initiation or termination of the inflammation thereby either promoting or suppressing inflammation (Alam and O'Neill, 2011;O'Connell et al., 2012). Many studies performed in our lab suggested the role of miRNA in the initiation of inflammation by SEB to trigger ARDS (Rao et al., 2014;Rao et al., 2015a), or even in the suppression of the inflammation such as the role of cannabinoids in the amelioration of experimental model of multiple sclerosis (Al-Ghezi et al., 2019;Tejman-Yarden et al., 2019), as well as the role of 2,3,7,8 - Tetrachlorodibenzo-p-dioxin (TCDD, "dioxin") in the amelioration of the DTH response (Abdulla et al., 2021b). In an earlier study, miRNA-132 was found to target High Mobility Group Box 1 (HMGB1) which regulates FoxP3+ Treg differentiation. Thus, upregulation of miRNA-132 caused downregulation of HMGB1, which in turn caused an increase in FoxP3+ Treg differentiation and suppression of Th-17 cells (Abdulla et al., 2021b). Resveratrol was shown to decrease the expression of several miRs (miR-31, Let7a, miR-132) which were found to target cytokines and transcription factors that regulated the functions of Foxp3 and TGF-β thereby suppressing inflammation (Alrafas et al., 2020).

1.6 Microbiome

All mammals are inhabited by a large population of microorganisms numbering in the trillions which are essential and referred to as the microbiome. This microbiome is a diverse collection of bacteria, viruses, fungi, protozoa, and archaea that contribute to the overall health and homeostasis of the host (Shreiner et al., 2015;Hillman et al., 2017). The microbiome are dynamic and are affected by many important factors such as diet,

health status, environment and other factors (Barko et al., 2018). In the gut, the microbial composition is distributed along the gut lumen, colonic mucus layer, and colon crypts (Donaldson et al., 2016). The microbiome is not limited to only the gut, but is also present in other organs such as the lungs (Moffatt and Cookson, 2017). Bacteria are classified taxonomically into phyla, genera, and species based on differences in phenotype characteristics. Carl and others optimized sequencing of small subunit of 16S ribosomal RNA (rRNA) polymerase chain reaction with next gene sequencing of amplicons which led to better characterization of the microbiome (Chakravorty et al., 2007)

In recent years, studies have shown that there is a vital cross talk between the gut microbiome and the lung microbiome, known as gut–lung axis that plays an important role in mediating the immune response and reshaping inflammation (Zhang et al., 2020). There is evidence showing gut microbiome affecting pulmonary immunity through the vital cross talk of the gut-lung axis (Keely et al., 2012). Studies have also shown that many respiratory infections involve significant alterations in the composition of the microbiome in the gut and lung (Dumas et al., 2018).

Short chain fatty acids (SCFAs) are a subset of fatty acids that are produced by the gut bacteria during fermentation of partially and non-digestible polysaccharides (Tan et al., 2014). SCFAs a play a major role in the health homeostasis (Tan et al., 2014). They are considered important in terms of the communication between gut microbiome and immune system, and the signal they produce are transferred amongst immune cells

via free fatty acids receptors (FFARs). They also mediate homeostasis not only for the digestive system but also for other organs including the lungs (Ratajczak et al., 2019).

1.7 Antimicrobial Peptides (AMPs)

Antimicrobial peptides (AMPs) are proteins with broad range of antimicrobial and immune modulatory activities against bacterial infections. Therefore, there are many pharmaceutical companies that are conducting clinical trials of these AMPs as therapeutic drugs (Toriyama, 1992). Making it difficult for microbes like bacteria to develop drug resistance, AMPs interact with cell membrane through electrostatic interactions (Hollmann et al., 2018;Pfalzgraff et al., 2018). There are some AMPs that interact with the lipid bilayer and bind with DNA, inhibiting synthesis of the bacterial cell wall. Thus, AMPs display intracellular inhibitory activity (Steckbeck et al., 2014). AMPs have been shown to be successful in treating infectious diseases, being both safe and effective (Toriyama, 1992). Airways epithelial cells contribute in the synthesis of AMPs and the relevance of these AMPs has been shown host-mediated defense against respiratory infections. Inasmuch, these peptides have served as a potential alternative for antibiotics and immune modulators (Hiemstra et al., 2016). In the lungs, there are large AMPs that play a role in the immune homeostasis of the respiratory system such as lysozyme, lactoferrin, and secretory leukocyte proteinase inhibitor (Amatngalim et al., 2015).

1.8 Tight Junction Proteins

Tight junction proteins are continuous intercellular barrier molecules between epithelial cells that mediate the regulation of movements of the solutes across the

epithelial cells (Schneeberger and Lynch, 2004). The intestinal barriers maintain and regulate the permeability of ions through epithelial tight junctions, water, and nutrients (Turner, 2006). Besides the intestine, the lung also contains tight junctions, and the barrier function of the lung depends on these proteins at the interface of the adjacent epithelial cells (Schlingmann et al., 2015). There are many types of tight junctions that have been identified (Flesch et al., 2017). Claudin is one of the tight junctions identified in the lungs of humans and animals, and these proteins have been shown to play an important role in protection against lung injury in various respiratory models (Schlingmann et al., 2015). Another type of tight junction protein is Epithelial Cadherin (or E-Cadherin) whichplays an important role in the regulation of the airway epithelial structure, barrier function, and immune response (Nawijn et al., 2011). There are studies demonstrating E-Cadherin plays an important role in the mediation of lung respiratory diseases (Post et al., 2018). Beta Defensins are some of the most important proteins which play a defense role against pathogens, and are produced by both epithelial cells and immune cells. Beta defensins manage cross talk between the host and microbes while maintaing the homeostasis and healthy status. For example murine beta defensin 2 (mBD2) is one of these important factors which has been shown to protect against lung diseases (Meade and O'Farrelly, 2018).

CHAPTER 2

THE ENDOCANNABINOID ANANDAMIDE ATTENUATES ACUTE RESPIRATORY DISTRESS SYNDROME BY DOWNREGULATION OF MIRNA THAT TARGET INFLAMMATORY PATHWAYS

2.1 ABSTRACT

Acute respiratory distress syndrome (ARDS) is defined as a type of respiratory failure that is caused by a variety of insults such as pneumonia, sepsis, trauma and certain viral infections. In this study, we investigated the effect of an endocannabinoid, anandamide (AEA), on ARDS induced in the mouse by SEB Administration of a single intranasal dose of SEB in mice and treated with exogenous AEA at a dose of 40mg/kg body weight led to the amelioration of ARDS in mice. Clinically, plethysmography results indicated that there was an improvement in lung function after AEA treatment accompanied by a decrease of inflammatory cell infiltrate. There was also a significant decrease in pro-inflammatory cytokines IL-2, TNF-α, and IFN-□□ and immune cells including $CD4^+$ T cells, CD8+ T cells, $V\beta8^+$ T cells, and NK^+ T cells in the lungs. Concurrently, an increase in anti-inflammatory phenotypes such as CD11b+Gr1+ Myeloid-derived Suppressor Cells (MDSCs), CD4+FOXP3+ Tregs, and $CD4^+$IL10+ cells was observed in the lungs. Microarray data showed that AEA treatment in ARDS mice significantly altered

numerous miRNA including downregulation of miRNA-23a-3p, which caused an upregulation of arginase (ARG1), which encodes for arginase, a marker for MDSCs, as well as TGF-β2, which induces Tregs. AEA also caused down-regulation of miRNA-34a-5p which led to induction of FoxP3, a master regulator of Tregs. Transfection of T cells using miRNA-23a-3p or miRNA-34a-5p mimics and inhibitors confirmed that these miRNAs targeted ARG1, TGFβ2 and FoxP3. In conclusion, the data obtained from this study suggests that endocannabinoids such as AEA can attenuate ARDS induced by SEB by suppressing inflammation through down-regulation of key miRNA that regulate immunosuppressive pathways involving the induction of MDSCs and Tregs.

2.2 INTRODUCTION

ARDS, a pulmonary disease characterized by an exudation of protein-rich fluid into alveolar space (Zhao et al., 2017), has a high morbidity rate approaching 200,000 cases each year with an approximate mortality rate of 27 – 45% depending on disease severity (Diamond et al., 2020). ARDS is defined as a type of respiratory failure which is caused by a variety of insults such as pneumonia, sepsis, trauma, and certain viral infections. ARDS is usually accompanied by systemic hyperactivation of the immune system leading to inflammation in the lungs, development of pulmonary edema, alveolar damage, and often respiratory failure (Fan et al., 2018). As there are no pharmacological agents currently approved by the FDA to treat ARDS, there is a high rate of mortality associated with this disease.

Recently, the severe form of COVID-19 caused by infection with the SARS-CoV-2 virus has also been shown to elicit ARDS (Li and Ma, 2020), although the nature of pathogenesis may be different from other forms of ARDS. Nevertheless, ARDS is also

accompanied by the release of inflammatory cytokines such as IL-6. IFN-γ and TNFα (Matthay and Zimmerman, 2005;Mohammed et al., 2020a;Mohammed et al., 2020b). In this context, suppressing pro-inflammatory responses is critical for attenuating disease severity.

The endocannabinoid system consists of the endocannabinoids, their metabolic enzymes and the cannabinoid receptors (Di Marzo, 2018). The analgesic effects of these endocannabinoids are primarily mediated through the CB1 which has been shown to have a significant role in the presynaptic modulation of pain (Walker and Huang, 2002). In contrast, CB2 is primarily expressed on immune cells, and activation of CB2 has been shown to suppress inflammation (Ameri, 1999;Pandey et al., 2009), However, it should be noted that CB1 is also expressed on immune cells and its activation by cannabinoids can also induce immunosuppression (Sido et al., 2015b). Two of the best-characterized endocannabinoids are AEA and 2-AG (Devane et al., 1992;Mechoulam et al., 1995;Fan et al., 2018), which can bind to both CB1 and CB2 receptors (Barrie and Manolios, 2017). The main enzymes responsible for the hydrolysis of AEA and 2-AG are FAAH and Monoacylglycerol lipase (MAGL), respectively (van Egmond et al., 2021) This has enabled the synthesis of many distinct classes of FAAH and MAGL inhibitors that have been shown to increase the levels of endocannabinoids when administered in vivo, thereby offering an opportunity to treat certain clinical disorders (van Egmond et al., 2021). Such FAAH and MAGL inhibitors have also been shown to effectively attenuate lipopolysaccharide (LPS)-induced acute lung inflammation (Costola-de-Souza et al., 2013;Wu et al., 2019;Abohalaka et al., 2020).

As recently reviewed, both AEA and 2-AG work in tandem as 'master regulators' of the innate-adaptive immune axis, governing numerous immune responses (Chiurchiu et al., 2015). For example, we have shown that AEA attenuates type-IV delayed-type hypersensitivity (DTH) mediated by Th17 cells via the induction of IL-10 and miRNA (Jackson et al., 2014b) and that activated T and B cells produce 2-AG, thereby inhibiting T-cell activation and proliferation, and thus attenuating DTH (Sido et al., 2016). Taken together, the immunoregulatory effects of endocannabinoids are manifold, and may yet provide a suitable pharmacological intervention in the treatment of ARDS.

SEB is a superantigen produced by the gram-positive bacterium, *Staphylococcus aureus* that causes many diseases ranging from food poisoning to toxic shock syndrome. SEB is known to stimulate T cells via binding to the Major Histocompatibility Complex II (MHC II) outside the conventional antigen-binding site that shares the variable region of the T cell receptor causing a robust proliferation of T cells (Pinchuk et al., 2010). Because SEB is easily aerosolized, it is considered as a bioterrorism agent, and the Centers for Disease Control and Prevention (CDC) has classified SEB as Category B (Pinchuk et al., 2010).

MicroRNAs are highly conserved small non-coding RNA molecules (21-25 nucleotides) that are expressed in most organisms from plants to vertebrates and regulate gene expression by degrading or silencing their targeted mRNA (Millar and Waterhouse, 2005;Macfarlane and Murphy, 2010). Specifically, miRNAs use their seed sequence to interact with the 3' untranslated region (3'UTR) found in the mRNA target via imperfect matching (Cannell et al., 2008). While many parameters govern miRNA-mRNA interactions, what adds to the inherent complexity between these interactions are the

numerous bindings sites per miRNA and the potential of each mRNA to be targeted by multiple miRNAs (Krol et al., 2010;O'Neill et al., 2011). Consequently, miRNAs are involved in the regulation of several cellular processes including the regulation of immunity, particularly as it relates to innate immune responses in the process of pathogen clearance and tissue restitution (O'Neill et al., 2011). There is only one previous report, that from our laboratory, investigating whether the anti-inflammatory action of anandamide is associated with miRNA (Jackson et al., 2014b). Additionally, we have also reported that the use of FAAH inhibitor enhances AEA in vivo and attenuates colitis through induction of miRNA that downregulates inflammatory pathways (Shamran et al., 2017).Previous studies from our laboratory demonstrated that Delta-9-Tetrahydrocannabinol (THC), the principal psychoactive constituent of cannabis, can suppress SEB-mediated ARDS in mice (Mohammed et al., 2020b;Mohammed et al., 2020d). THC-treated mice showed significant alterations in the expression of miRNA in the lung-infiltrated mononuclear cells (MNCs), which were associated with suppression of lung inflammation (Mohammed et al., 2020a) Together, these studies suggested that cannabinoids have significant potential in the treatment of ARDS. Nonetheless, whether direct administration of endocannabinoids such as AEA can suppress ARDS has not been previously investigated. Such studies are essential because while THC and AEA are both know to activate CB1 and CB2 receptors, AEA has also been shown to act as an agonist for the Transient Receptor Potential Cation Channel Subfamily V member 1 (TRPV1), also known as the vanilloid receptor 1, THC does not modulate TRPV1 (Muller et al., 2018) . In the current study, we, therefore, tested if endocannabinoid administration can suppress inflammation seen in ARDS caused by SEB. We found that AEA was highly

effective in attenuating ARDS and inflammation in the lungs caused by SEB. We found that AEA altered the expression of miRNA in the mononuclear cells (MNC) isolated from the lungs of SEB-treated mice which promoted anti-inflammatory pathways. This study opens the possibility of the use of AEA or FAAH inhibitors in the attenuation of ARDS in a clinical setting.

2.3 MATERIALS AND METHODS

Mice

The mice were purchased from Jackson laboratories with age of (6-8 weeks) C57BL/6 mice . Five animals per cage as a maximum level that were housed under pathogenic –free conditions in the Animal Resource Facility (ARF) at the University of South Carolina. Under the policy approved by the Institutional Animal Care and Use Committee (IACUC) all requirements for the experiments were performed. Mice were housed under a 12 hour light/dark cycle at 18-23°C and 40-60% humidity.

Chemicals, reagents and kits

All chemicals and reagents were purchased as follows: N-arachidonoyl ethanolamine or AEA from Cayman Chemicals (Ann Arbor, Michigan, United States) SEB:from Toxin Technologies (Sarasota, FL); RPMI 1640 supported with L-glutamine: from Corning (New York, NY, USA); Fetal Bovine Serum, Penicillin and Streptomycin: from Invitrogen Life Technologies (CA, USA). True Nuclear Transcription Factor Buffer Set was purchased from Biolegend (San Diego, CA) while Fc Block reagent was purchased from BD Pharmingen (San Diego, CA). EasySep mouse MDSCs (CD11bGr1) selection kit was purchased from STEMCELL technologies (Seattle, WA) for purification of MDSCs. miScript SYBR green PCR kit, miScript primer assays kit, RNA

easy, and miRNA easy kit were purchased from Qiagen (Valencia, CA). Taq DNA Polymerase kit was purchased from Invitrogen Life Technologies (Carlsbad, CA).

Induction of Acute Respiratory Distress Syndrome in mice using Staphylococcus Enterotoxin B (SEB) inhalation and treatment with Anandamide

ARDS was induced in mice as described previously (Rieder et al., 2011). Mice were randomly divided into either vehicle or treatment groups before exposure to SEB. Mice were exposed to SEB intra-nasally (I.N.) with a single dose at a concentration of 50 µg/mouse in 25 µl of Phosphate Buffer Saline (PBS) as previously described (Rieder et al., 2011) on day 0. On day -1, AEA or VEH was given into these mice by the Intra Peritoneal (I.P.) route at a dose of 40 mg/kg body weight. AEA dissolved in ethanol (50 mg/ml) was diluted further in PBS. Each mouse received 0.1 ml consisting of 84 µl of PBS and 16 µl of ethanol containing AEA. The vehicle controls received 0.1 ml consisting of 84 µl of PBS and 16 µl of ethanol without AEA. The dose of AEA was based on our previous studies demonstrating that 40 mg/kg body weight of AEA attenuated T cell-mediated delayed-type hypersensitivity response (Jackson et al., 2014b). The treatment with AEA was repeated on day 0 (SEB exposure day), and day 1. Mice were euthanized on day 2 (48 hrs after SEB exposure) for various studies.

Evaluation of lung function

To evaluate the effect of AEA to attenuate the effects of SEB, clinical parameters of the lungs were measured using whole-body plethysmography (Buxco, Troy, NY, USA), as described (Elliott et al., 2016). A single mouse from each group of Naïve, SEB+VEH, and SEB+AEA was first restrained in a plethysmographic tube and was allowed to acclimatize as previously described (Elliott et al., 2016). The lung

function was calculated for clinical parameters such as Specific Airway Resistance (sRAW), Specific Airway Conductance (sGAW) and Minute per Volume (MV).

Lung Histopathology

Lung tissue was excised from each mouse and directly fixed in 10% formalin without inflation. The lung tissues were then embedded in paraffin and sections were cut at our core facility. The sections were then processed for H & E staining. Briefly, lung tissue sections mounted on slides were first transferred in xylene to deparaffinized the tissue sections. The tissue sections were then rehydrated in alcohol (100%, 95%, and 90 %). The sections were finally stained with Hematoxylin and Eosin (H & E) and dehydrated. H & E stained sections were analyzed using KEYENCE digital microscope VHX-7000 (IL-USA).

Isolation and purification of lung mononuclear cells (MNCs)

These cells were isolated as described previously (Rieder et al., 2012). Briefly, mice were given heparinized PBS to perfuse the lungs. A stomacher 80 biomaster blender (Seward, Fl) was used to homogenize the lung tissue suspended in 10 ml of 1x PBS and 10% Fetal Bovine Serum (FBS). The homogenized lung tissues were centrifuged at 1200 rpm at 4°C for 12 min. The pellet was then washed with PBS and resuspended in PBS post centrifugation. We then used a density gradient centrifugation method to purify lung mononuclear cells (MNCs). In brief, the cells resuspended in sterile PBS were carefully layered using Histopaque-1077 purchased from Sigma-Aldrich (St. Louis, MO) and centrifuged at 500x*g* for 30 minutes at room temperature (25°C). The mononuclear cells were collected at the interface. MNCs mixed with trypan blue were then enumerated using a Biorad TC 20-Automated cell counter.

Detection of cytokines in serum

Blood samples from each group of mice were collected under general anesthesia. The collected blood samples were then centrifuged to collect the sera. The sera were either used immediately or stored at -80°C. The detection of the cytokines was performed using ELISA MAX standards kits from Biolegend.

Flow cytometry Analysis:

Spleen cells and MNCs isolated from the lungs were stained with various fluorescent–conjugated antibodies purchased from Biolegend (SanDiego, CA, USA), which included: For T cell subsets: Allophycocyanin (APC) conjugated anti-CD3, Phycoerythrin (PE) conjugated anti-CD4, PerCP/Cyanine 5.5 (PerCP-CY5.5) conjugated anti-CD8, Fluorescein Isothiocyanate (FITC) conjugated anti-Vβ8, and PE/Dazzle Conjugated anti-NK1.1. For lymphocyte activation markers, T cell memory markers, MDSCs, and Tregs, the following Abs were used: Phycoerythrin (PE) Conjugated anti-CD69, Brilliant Violet-510 Conjugated anti-CD25, Fluorescin Isothiocyanate (FITC) Conjugated anti-CD44, Brilliant Violet-785 Conjugated anti-CD3, Allophycocyanin (APC) Conjugated anti-CD62L, Alexa Fluor 488 Conjugated anti-FoxP3, Phycoerythrin (PE) Conjugated anti-IL10, Fluorescein Isothiocyanate (FITC) Conjugated anti-CD11b, Phycoerythrin (PE) Conjugated anti-Gr1, Alexa Fluor 700 conjugated anti-LY6C, and Phycoerythrin cy5 (PECY5) conjugated anti-LY6G.

The staining of cells for dual markers was performed as described in our previous publications (Al-Ghezi et al., 2019;Becker et al., 2020;Dopkins et al., 2020;Mohammed et al., 2020b). In brief, MNCs and spleen cells were treated with Fc Block reagent (BD Pharmingen, San Diego, CA) followed by staining cells with various antibodies by

incubation at 4°C for 20-30 minutes. Stained cells were washed twice with cold PBS containing 2% FBS (Staining buffer). For IL 10 and FOXP3 staining, we used the Intracellular Cytokine Staining Kit (BD biosciences) consisting of fixation/permeabilization buffer. In brief, the cells were fixed using fixation/permeabilization buffer, followed by washing the cells with PBS and then staining the cells using anti–Foxp3 and anti–IL10 antibodies. The cells were finally suspended in 0.5 ml staining buffer and analyzed using Beckman Coulter FC500 or BD Bioscience FACSCelesta™ , which was followed by analysis on the FlowJo V10 version software.

Induction of Myeoid Derived Suppressor Cells by Anandamide

Mice were injected with Anandamide and SEB, as described earlier. Forty eight hrs later, mice were euthanized and the peritoneal exudate was collected and washed with PBS. The cells were resuspended in 1 mL, treated with Fc block for 10 min at RT. Next, the EasySep CD11b Gr1 selection kit (STEMCELL Technologies, Seattle, WA; catalog number 19867) was used to isolate CD11bGr1 based on the guidelines provided in the kit.

Suppression of T cell proliferation by Myeloid Derived Suppressor Cells in vitro

To test the immunosuppressive effects of MDSCs on T cell proliferation, naive C57BL/6 mice were euthanized and splenic T cells were isolated. Splenic T cells at a concentration of 5×10^5 cells/well were cultured in 96-well tissue culture plates in the presence of Concanavalin A (ConA), a T cell mitogen, at a concentration of (2.5μg/ml) together with different ratios of AEA induced purified MDSCs for 48 hours. [^{3}H]thymidine (2 μCi per well) was added to the cell culture in the last 18 hrs, and the radioactivity was measured using a liquid-scintillation counter (MicroBeta TriLux; PerkinElmer).

Micro-RNAs Arrays and Analysis

miRNA analysis was performed as described previously(Tomar et al., 2015;Alghetaa et al., 2018). Total RNA including miRNA was isolated from lung infiltrating MNCs using miRNeasy kit from Qiagen. A Nanodrop 2000 spectrophotometer (Thermo Fisher Scientific, Wilmington, DE) was used to determine RNA purity and concentration. Next, Affymetrix gene chip miRNA 4.0 array platform was used (Affymetrix Inc, Santa Clara, CA) to determine the miRNA expression profile of lung MNCs and only those miRNAs that were altered more than 1.5-fold or higher were considered for further analysis. Ingenuity Pathway Analysis (IPA) was used for identifying the role of miRNA in various biological pathways using the software available at http://www.ingenuity.com. Also, the microRNA.org database was used to examine the sequence alignment regions between miRNA-23a-3p and miRNA-34a-5p and their respective target genes.

Quantitative-Real Time Polymerase Chain Reaction (qRT-PCR)

This was performed as described previously (Mohammed et al., 2020a). Briefly, to determine the expression of the selected miRNA and respective genes, qRT-PCR was performed using cDNA synthesized from total RNA and miRNA. miScript II RT kit from Qiagen was used to synthesize cDNA using and following the protocol of Qiagen company.

Snord96A and GAPDH were used as endogenous controls. 2ΔΔCt was used to determine fold change in expression (Table 1).

Transfection of miRNA

Transfection was performed as described previously (Busbee et al., 2015). In brief, splenocytes were cultured in complete RPMI 1640 medium (10% FBS, 10 mM L-glutamine, 10 mM Hepes, 50 μM β-mercaptoethanol, and 100μg/ ml penicillin). 2.5 × 10^5 cells/well were seeded in a 24-well plate and transfected with mock control, synthetic mimic mmu-miRNA-23a-3p MSY0000542, synthetic mimic mmu-mmiRNA-34a-5p MIN0000542 using a HiPerFect transfection reagent kit from Qiagen.

Statistical Analysis

Graph Pad Prism 6.0 Software (San Diego,CA,US) was used for statistical analyses. Student's t-test was used for comparison among two groups. One way-ANOVA with post hoc Tukey's test was used to compare between more than two groups. The results were expressed as mean ± SEM. A p-value ≤ of 0.05 was considered statistically significant.

2.4 RESULTS

Anandamide improves lung function, rescues lung damage, and decreases pro-inflammatory cytokines in mice exposed to Staphylococcus Enterotoxin B

We used the following groups of mice to study the effect of AEA on SEB-mediated ARDS: Naïve, SEB+VEH, and SEB+AEA. After forty-eight hours of SEB exposure, the lung function of all groups was evaluated using a Buxco instrument system. We observed that the clinical parameters for lung function including specific airways resistance, specific airway conductance, and minute per volume to be significantly improved in SEB+AEA groups and similar to the naïve group, in comparison to SEB+VEH mice **(2.1 A)**. These data demonstrated that AEA was able to rescue

impairments to the lung function caused by SEB exposure. Further, the total number of mononuclear cells (MNCs) in the lung was significantly decreased in SEB+AEA mice when compared to SEB+VEH mice **(Fig2.1 B).** Histological sections of the lungs are shown in **Fig 2.1C** that are representative pictures of the data presented in **Fig 2.1B**. Analysis of sera obtained from mice showed that there was a significant decrease in the pro-inflammatory cytokines TNFα, IL-2, and IFN-γ in SEB+AEA group when compared to SEB+VEH mice **(Fig 2.1 D).**

Anandamide suppresses the infiltration of inflammatory cells in the lungs and spleens

We then assessed the presence of T cells in the lungs (**Fig 2.2A-D**) and spleens (**Fig 2.2E-H**) by staining with fluorescein-conjugated antibodies and analyzing using flow cytometry. The data have been depicted as a representative flow cytometric analysis followed by percentage of cells/mouse, and total number of cells/mouse in vertical bars. Results showed that there was a significant increase in T cell subset populations, both in percentages and numbers, including CD4+ T cells, CD8+ T cells, V□8+ T cells, and NK T cells in the lungs and spleens of SEB+VEH group when compared to the naïve mice, thereby demonstrating that SEB caused activation and proliferation of these cells **(Fig 2.2 A-H).** Interestingly, SEB+AEA group when compared to the SEB+VEH group, showed a significant decrease in the percentage and numbers of all T cell subsets, including the V□8+ T cells that are specifically activated by SEB. This combined with the fact that SEB+AEA group had a decrease in the total number of infiltrating MNCs in the lungs (**Fig 2.1B**) when compared to SEB+VEH group, clearly demonstrated that AEA decreases both the percentage and total numbers of T cell subsets induced by SEB.

AEA suppresses the proliferation of splenic lymphocytes in vitro

To determine whether the AEA suppresses SEB-activated proliferation of T cells directly, we performed in vitro assays in which splenic lymphocytes, isolated from naïve mice, were pretreated with a dose of 20 μM of AEA and activated 30 minutes later with 1μg/ml of SEB. The cells were then incubated for 24 hrs and 48 hrs. We assessed the effect of AEA on T cell subpopulations, including CD4+ T cells, CD8+ T cells, Vβ8 + T cells, and NKT cells by flow cytometry. We observed that there was a significant decrease in the percentage of all T cell subsets and NKT cells in the SEB+AEA group when compared to the SEB+VEH group at 24 hrs **(Fig 2.3 A-D)**, and this decrease was further augmented at 48 hrs **(Fig 2.3 E-H)**. Next, we investigated activation markers such as CD3, CD69, CD25, CD44, as well as CD62L (L-slectin) which is expressed on naïve CD4+ T cells used for recirculation and binding to high endothelial venules and on central memory T cells. We observed that the percentages of CD3+CD69+, CD69+, CD44+, and CD62L+ cells from the SEB+Veh group were significantly increased when compared to naïve mice indicating that SEB had activated a significant proportion of T and other immune cells. However, in the SEB+AEA group, there was a significant decrease in percentages of these cells when compared to the SEB+VEH group except CD62L+ cells which were enhanced in SEB+AEA mice when compared to the SEB+VEH group (**Fig 2.4**). It should be noted that when we looked at CD25+ cells that were CD69-, these cells were significantly increased SEB+AEA group (33.6%) when compared to SEB+VEH (7.9%) (**Fig 2.4**). Because CD25 is also expressed on Tregs, these data suggested that AEA may increase the proportion of Tregs which is shown in

subsequent Figs. Together, these in vitro studies demonstrated that AEA directly worked on SEB-activated immune cells thereby significantly suppressing their activation.

Anandamide alters the expression of Micro-RNAs in lung infiltrating Mononuclear Cells

We next analyzed miRNA profiles of lung infiltrating MNCs to examine the extent to which AEA attenuates inflammation via miRNA induction. The data were analyzed using Ingenuity Pathway Analysis (IPA) software as described earlier (Rao et al., 2015a). The heat map of miRNAs (>3000) was first generated which showed marked alterations in miRNA expression in SEB+VEH mice when compared to the SEB+AEA mice. Upon analysis of a $\geq$ 1.5 fold increase or decrease in miRNA expression, a marked difference in the upregulation/downregulation of miRNAs between SEB+VEH and SEB+AEA mice was observed **(Fig 2.5A)**. Specifically, there were at least 77 miRNAs that were upregulated and 59 miRNAs that were downregulated in SEB+AEA mice when compared to SEB+VEH mice **(Fig 2.5B)**. Next, we analyzed select miRNAs for their targets especially those involved in the regulation of inflammation, using the IPA software from Qiagen and observed that some of the downregulated miRNAs, specifically miRNA-23a-3p targeted TGF- β2 and ARG1, and miRNA-34a-5p (synonym: miRNA-449c based on IPA classification) targeted FoxP3 **(Fig 2.5C).** Also, we found miRNA-34a-5p to target GATA3 involved in Th2 differentiation and miRNA-30c-5p which was down-regulated to target SOCS1, a suppressor of cytokine signaling. These data suggested that AEA, by downregulating these miRNAs, may induce several of these anti-inflammatory molecules such as TGF- β2, ARG1, GATA3, and SOCS1.

Validation of Micro-RNAs and their target genes

We further confirmed miRNA-23a-3p and miRNA-34a-5p specific target genes using miRNA.org or TargetScan software. miRNA-23a-3p showed a strong binding affinity with its complementary 3'UTR region of TGF- β2 gene and miRNA-34-5pa showed a strong binding affinity with the 3'UTR region of the FoxP3 gene (**Fig 2.6 A,E**). We then validated the expression of miRNA-23a-3p and miRNA-34a-5p and their respective genes (ARG1, TGF-β2, and FoxP3) by performing qRT-PCR using MNCs isolated from the lungs. Both miRNA-23a-3p and miRNA- 34a-5p were significantly downregulated in SEB+AEA mice when compared to SEB+VEH counterparts **(Fig 2.6B, F)**. Upon analysis of their respective target genes including ARG1, TGF- β2, and FoxP3 in the lung MNCs, there was a significant upregulation of both genes in cells from SEB+AEA mice when compared to SEB+VEH mice **(Fig 2.6 C, D, G).**

Analysis of Micro-RNA-23a-3p and Micro-RNAs-34a-5p and their specific target gene expression

To corroborate that miRNA-23a-3p and miRNA-34a-5p specifically regulate the respective target genes (ARG1, TGF-β2, and FoxP3), we performed a series of transfection assays. To this end, SEB at a concentration of 1μg/ml was used to activate splenocytes following overnight incubation. The following day, activated cells were then transfected with mock, mimic or inhibitor of miRNA-23a-3p, or miRNA-34a-5p. Forty-eight hours after transfection, we collected the cells for qRT-PCR. Based on the qRT-PCR analysis, we observed that there was a significant increase in miR-23a **(Figure 2.7A)** and miR-34a-5p expression **(Figure 2.7D)** in cells transfected with their respective mimics. In contrast, the cells that were transfected with respective inhibitors

showed a significant decrease in miRNA-23a and miRNA-34a-5p expression. Upon analysis of their target genes, we noted that there was significant suppression of TGF-β2 and ARG1 in miR-23a mimic-transfected cells **(Fig 2.7 B, C)** as well as FoxP3 expression in miRNA-34-5p mimic-transfected cells **(Fig 2.7 E),** whereas there was complete reversal (increase) in their expression **(Fig 2.7 B, C, E)** following inhibition of their respective miRNAs. These findings indicated a direct relationship with miRNA-23a-3p and miRNA-34a-5p expression with their target genes ARG1, TGF-β2, and FoxP3.

Anandamide induces Myeloid Derived Suppressor Cells and T regulatory cells

The above studies indicated that AEA-regulated miRNAs might induce anti-inflammatory genes leading to the generation of suppressor cells such as MDSCs and T regulatory cells (Tregs). To test this, MNCs from the lungs of both SEB+AEA and SEB+VEH mice were assessed for the generation of MDSCs and their subsets (CD11b+Gr1+ and LY6C+LY6G+). Flow cytometry data showed that there was a significant increase in the percentage of MDSCs (CD11b+Gr1+) in SEB+AEA mice when compared to SEB+VEH mice in both the lungs and spleen **(Fig 2.8A, E)**. Additionally, we noted that AEA caused increased percentages of both $Ly6G^{+}Ly6C^{low}$ granulocytic and $Ly6G^{-}Ly6C^{high}$ monocytic MDSCs **(Fig 2.8B).** Furthermore, upon analysis of Tregs, there was a significant increase in CD4+FoxP3+ cells in SEB+AEA mice **(Fig 2.8 C)** when compared to the SEB+VEH group. A significant increase of CD4+IL10+ cells, a phenotype of regulatory Type 1 (Tr1)-like cells, was observed as well in SEB+AEA mice when compared to SEB+VEH mice, **(Fig 2.8 D).** To confirm that the MDSCs induced by AEA were immunosuppressive, we performed an in vitro

assay in which spleen T cells from naïve mice were activated with ConA in the presence of varying proportions of purified MDSCs. The Data shown in Fig 8F demonstrated that the MDSCs caused a dose-dependent decrease in T cell proliferation. These data together suggested that AEA was inducing immunosuppressive MDSCs and Tregs, consistent with the data shown in miRNA experiments.

2.5 Discussion

In the present study, we explored the effect of AEA treatment in a SEB-induced mouse model of ARDS. Our results indicated that AEA indeed broadly improves clinical outcomes of lung function and inflammatory status following exposure to SEB. Mechanistically, AEA reduces the infiltration of proinflammatory T cell subsets and further suppresses splenic lymphocyte proliferation induced by SEB. Additional analyses suggested that such inflammatory control may be mediated, at least in part, via the suppression of two specific miRNAs, miRNA-23a-3p and miRNA-34a-5p, which directly regulate the expression of gene targets ARG1, TGF-β2, and FoxP3. As a result, the regulation of these miRNAs by AEA allows for an increase in immunosuppressive Tregs and MDSC populations.

ARDS is a life-threatening form of respiratory failure that affects heterogeneous populations. Currently, there is no FDA-approved drug to treat ARDS leading to high rates of mortality (Rao et al., 2015a). Treatment options are still limited because of which the mortality rate is almost 40% and according to US healthcare data, the annual cost of treatment is more than $5 billion/year due to a long time of hospitalization and intensive medical care (Thornton Snider et al., 2012). With the advent of COVID-19, the additional

healthcare burden will continue to rise (Bartsch et al., 2020) due to its ability to induce ARDS-like clinical features. ARDS is caused by a variety of insults which include pneumonia, sepsis, trauma, and certain viral infections. The common feature of ARDS also includes systemic heightened immune response leading to inflammation in the lungs, edema, alveolar damage, and respiratory failure. Staphylococcus Enterotoxin B (SEB) acts as a superantigen and activates a large proportion of T cells having certain Vβ T cell receptor-expressing cells (Vβ8) leading to cytokine storm and systemic inflammation (Nagarkatti et al., 2009;Rao et al., 2015a).

Cannabinoids have extensively been tested for their anti-inflammatory properties (Nagarkatti et al., 2009). Recently, we reported that Tetrahydrocannabinol (THC), the psychotropic compound found in cannabis that activates both CB1 and CB2, can suppress SEB-mediated ARDS (Mohammed et al., 2020a) . However, whether endocannabinoids can suppress ARDS has not been tested previously. Such studies are important because the levels of endocannabinoids such as AEA can be regulated by inhibitors of Fatty Acid Amide Hydrolase (FAAH), an enzyme that breaks down AEA. AEA has a chemical structure that is different from THC, has lower affinity for CB_1 receptors, and a much shorter duration of action both *in vitro* and *in vivo* (Justinova et al., 2005). Thus, while we found that 20mg/kg of THC can block SEB-mediated ARDS when given even the same day as SEB (Mohammed et al., 2020a), with AEA, we found that it was necessary to give a higher dose of 40mg/kg body weight, and also inject AEA prior to antigenic challenge (Jackson et al., 2014b). In this study, we used the endocannabinoid, AEA, as a mode of treatment for mice with ARDS due to the possibility that its levels can be increased using FAAH inhibitors. In fact, in a previous study, we noted that FAAH

knockout mice or administration of FAAH inhibitor could upregulate endogenous AEA leading to suppression of autoimmune hepatitis (Hegde et al., 2008). The suppressive effect of AEA on TNFα and alveolar macrophages as well as on inflammatory cytokines IL6 and IL12 have been demonstrated in previous studies (Chiurchiu et al., 2015). AEA was also shown to activate CB1 receptors and and cause a decrease in the production and release of IL-12 and IL-23 which induce inflammatory T cells namely Th1 and Th17 cells, respectively (Chiurchiu et al., 2016). In these studies, treatment of keratinocytes with AEA in vitro led to decreased induction of IFN-γ and IL-17 producing Th1 and Th17 cells respectively (Chiurchiu et al., 2016)). The other key endocannabinoid, 2-AG, has also been shown to mediate anti-inflammatory properties. We have reported that naïve immune cells produced low levels of 2-AG but upon activation, they produced higher levels which in turn suppressed T cell proliferation (Sido et al., 2016)). Also, 2-AG treatment (40 mg/kg) suppressed methylated Bovine Serum Albumin (BSA)-induced delayed-type hypersensitivity (DTH) response mediated by Th1 and Th17 cells (Sido et al., 2016). These studies suggested that immune cells upon activation may produce endocannabinoids which may act as negative regulators of the immune response (Sido et al., 2016).

In the current study, we noted that AEA induced significant levels of MDSCs. MDSCs are heterogeneous cells generated during inflammation and cancer development (Yang et al., 2020). Because of their remarkable ability to suppress T cell response (Bird, 2020), they are believed to promote tumor growth in cancer patients and suppress inflammation in autoimmune and inflammatory diseases (Elliott et al., 2018;De Cicco et al., 2020). Further, a previous study has shown that AEA induces MDSCs and cause

immunosuppression during DTH response (Jackson et al., 2014a). There are two types of MDSCs: $Ly6G^{+}Ly6C^{low}$ granulocytic and $Ly6G^{-}Ly6C^{high}$ monocytic (Bird, 2020). We found that AEA increased the percentages of both these subsets but the granulocytic were induced to a greater extent when compared to the monocytic. There are many mechanisms through which MDSCs mediate the suppression of inflammation. Tumor-induced MDSC inhibit T cell proliferation by causing L-arginine depletion through arginase-1 activity (Ostrand-Rosenberg and Fenselau, 2018) , and in the current study, we did find that AEA induced increased expression of arginase-1. MDSCs also produce immunosuppressive cytokines such as IL-10 and TGF-β (Eggert et al., 2020), and we found that AEA also induced increased expression of IL-10. The IL-10 produced by MDSCs has also been shown to induce Tregs (Park et al., 2018), which is consistent with the current study where we noted an increase in Tregs as well. It should be noted that both LPS and SEB have been used as a model to study lung inflammation. While LPS primarily induces neutrophils in the lungs, and SEB primarily induces mononuclear cells, SEB can also trigger, to a lesser extent, neutrophils when compared to LPS (Neumann et al., 1997). In the current study, we did not study the effect of AEA on neutrophils, which is a limitation.

In recent years, several studies including those from our lab have shown the critical role of miRNAs in gene expression (Singh et al., 2015;Alghetaa et al., 2018). We have shown that miRNAs are involved in the regulation of immune responses and in the upregulation of anti-inflammatory genes. However, there are limited studies on whether endocannabinoid-mediated attenuation of inflammation is associated with alterations in the miRNA of activated immune cells and there are no such studies in the regulation of

inflammatory cells in the lungs seen during ARDS. In the current study, we, therefore, investigated the role of AEA in the regulation of miRNAs in lung infiltrating MNCs. We observed that treatment with AEA significantly altered the expression of several miRNAs in lung MNCs. AEA treatment led to upregulation of 59 miRNAs and downregulation of 77 miRNAs in comparison to VEH-treated counterparts. Using IPA analysis, we were able to narrow down our studies to miRNA-23a-3p which was downregulated and targeted ARG1 and TGFβ2 genes, while miRNA-34a-5p, also downregulated, targeted the FOXP3 gene. It is interesting to note that we found in a previous study that THC treatment was also able to decrease the expression of miRNA-34a-5p and induce FoxP3 (Mohammed et al., 2020a), similar to the action of AEA seen in the current study, thereby suggesting that miRNA-34a-5p is a critical miRNA that may be downregulated following treatment with cannabinoids such as THC and AEA. ARG1 encodes for arginase produced by the MDSCs which inhibits T cell proliferation by L-arginine depletion (Grzywa et al., 2020). These data were consistent with our observation that AEA also increased the proportions of MDSCs in the lung MNCs. FOXP3 is a transcription factor belonging to the forkhead/winged-helix family of transcriptional factors and is considered a master regulator of the development of Tregs (Ono, 2020). Moreover, it has been shown that FOXP3 expression is essential for Tregs development and function in mice (Fontenot et al., 2003). Additionally, TGFβ2 has been shown previously to drive Treg induction (Becker et al., 2018)). In this study, we observed that treatment with AEA induced an increase in the percentages of FOXP3+ Tregs in the lungs of mice injected with SEB, consistent with the miRNA data. Importantly, we found using transfection studies involving mimic and inhibitor that miRNA-23a-3p

targeted ARG1 and TGFβ2 expression, while miRNA-34a-5p targeted the FOXP3. The induction of Tregs and MDSCs by AEA is consistent with a previous observation that cannabinoids are potent inducers of these immunosuppressive cells. For example, both tetrahydrocannabinol (THC) and cannabidiol (CBD) have been shown to induce MDSCs (Hegde et al., 2010;Hegde et al., 2011;Hegde et al., 2015;Rao et al., 2015b;Sido et al., 2015a;Elliott et al., 2018;Mohammed et al., 2020a) . Also, AEA was shown to induce MDSCs even in naïve mice following i.p. injection through activation of mast cells to release MCP-1 (Jackson et al., 2014a). There are not many reports on the role of miRNA-23a on the regulation of inflammation. Interestingly, during septic insult, miRNA-23a expression was found to be decreased which was associated with increased autophagy and suppression of inflammatory mediators (Si et al., 2018). In this study, miRNA-23a was shown to target Autophagy related 12 (ATG12), which regulates autophagy(Si et al., 2018).

In summary, data from this study shows that AEA can effectively suppress SEB-induced ARDS in mice. Upon analysis of molecular mechanisms, we observed the role of miRNA-23a-3p in the regulation of TGF-β2 and ARG1 genes which in turn suppressed the inflammatory properties of SEB-induced MNCs in the lung. Similarly, miRNA-34a-5p directly regulates FOXP3 in lung infiltrating MNCs and the suppression of this miRNA by AEA might induce Tregs in the promotion of immune suppression following exposure to SEB.

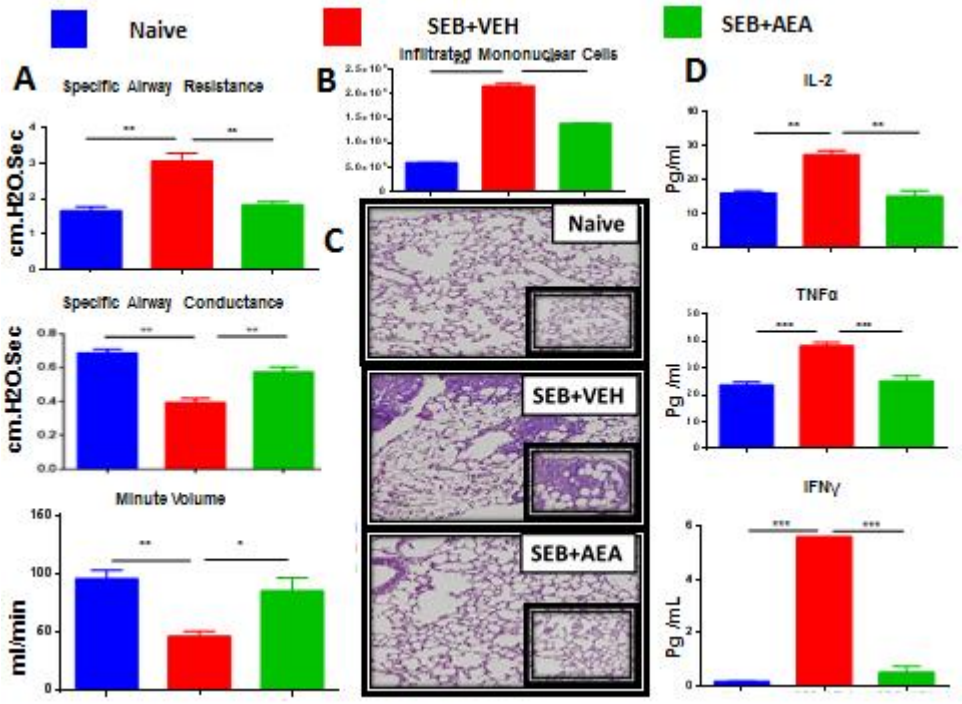

Figure 2. 1: AEA attenuates SEB-induced ALI in mice. Mice were exposed to SEB intra-nasally with a single dose of 50 µg/mouse on day 0. On days -1, 0 and 1, AEA or VEH was given into these mice i.p at a dose of 40 mg/kg body weight. Mice were euthanized on day 2 for various studies. (A) Showing clinical functions of the lung including Specific Airways Resistance (sRAW), Specific Airways Conductance (sGAW), and Minute per Volume (MV). (B) Comparison between the groups for the total number of Mononuclear Cells isolated from the lungs. (C) Representative images of histopathological H & E staining of excised lung tissue (20X magnification). (D) Measurement of cytokines IL2, IL6, and TNFα in the serum. Five mice in each group were used and the data confirmed in three independent experiments. *p≤ o.o5, p**≤ o.o1, ***p≤ o.oo1.

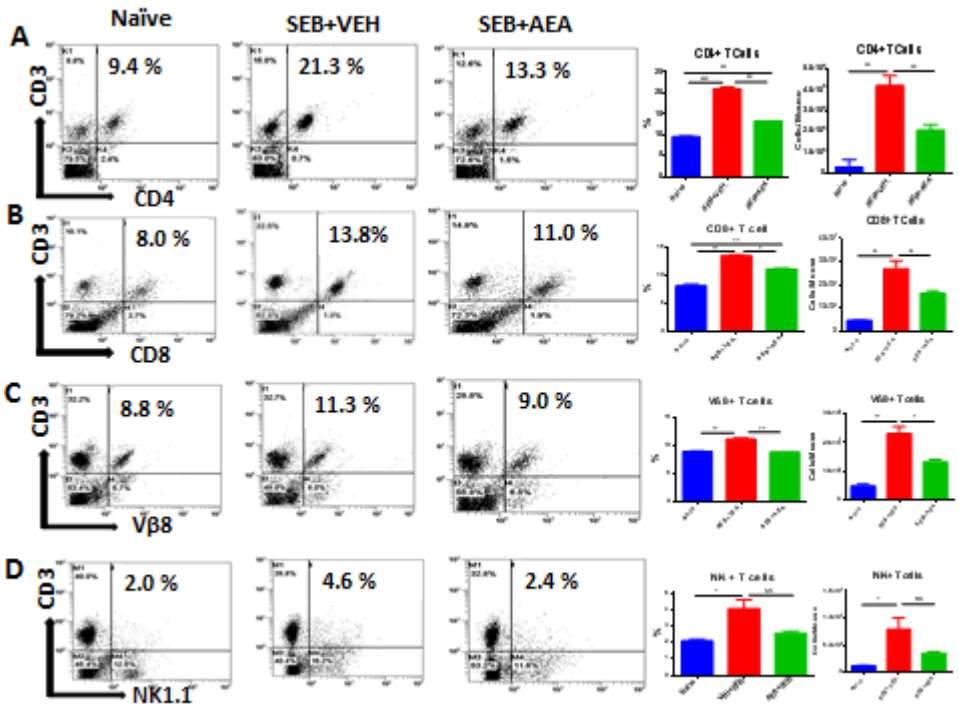

Figure 2. 2: AEA decreases T cell subpopulations in the lungs and spleens. Mice were treated with SEB and AEA as described in Fig 1 legend. Each panel shows a representative experiment depicting lung MNCs and splenocytes analyzed for various T cell markers. Data from 5 mice/group is presented in the form of vertical bars with Mean+/-SEM. Panels A-D and E-H show data from the lungs and spleens, respectively. (A) CD3+CD4+ T cells (B) CD3+CD8+ T cells, (C) CD3+Vβ8+ T cells, (D) CD3+NK1.1+ cells. Five mice in each group were used and the data was confirmed in three independent experime. *p≤ o.o5, p**≤ o.o1, ***p≤ o.oo1 .

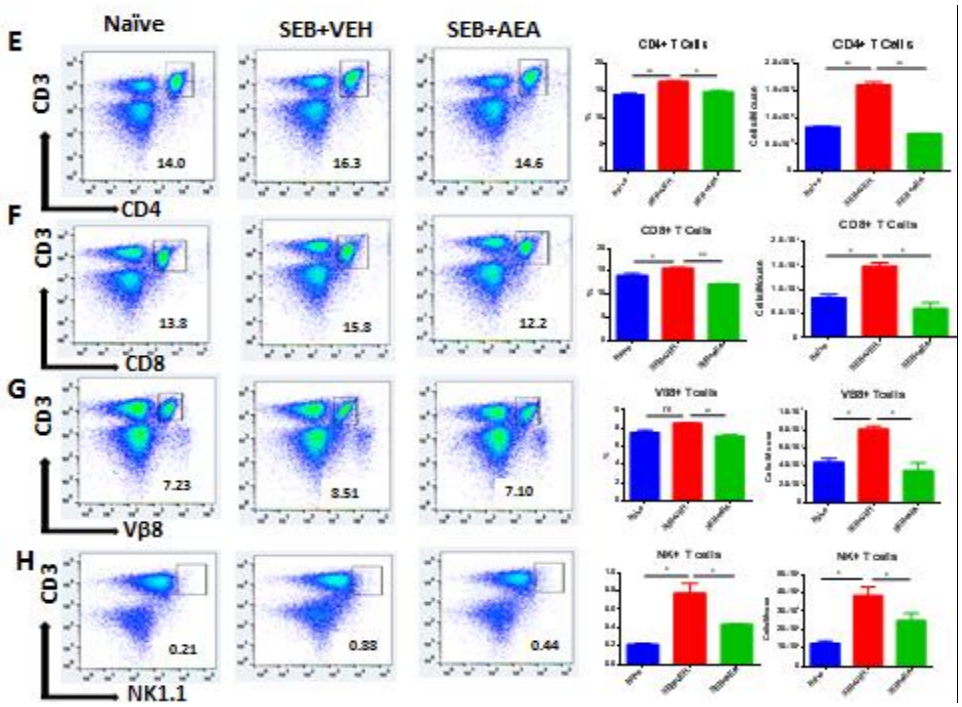

Figure 2.2: AEA decreases T cell subpopulations in the lungs and spleens. Mice were treated with SEB and AEA as described in Fig 1 legend. Each panel shows a representative experiment depicting lung MNCs and splenocytes analyzed for various T cell markers. Data from 5 mice/group is presented in the form of vertical bars with Mean+/-SEM. Panels A-D and E-H show data from the lungs and spleens, respectively. (E) CD3+CD4+ T cells (F) CD3+CD8+ T cells, (G) CD3+Vβ8+ T cells, (H) CD3+NK1.1+ cells. Five mice in each group were used and the data was confirmed in three independent experiments. *p≤ o.o5, p**≤ o.o1, ***p≤ o.oo1.

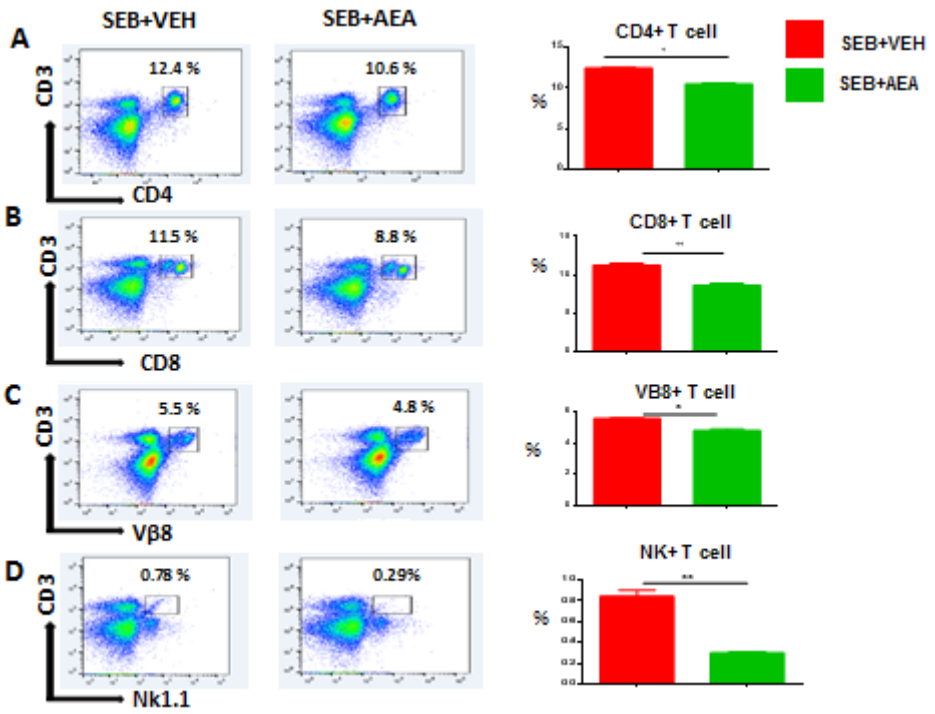

Figure 2. 3: AEA decreases T cell subsets in the splenocytes activated with SEB in vitro. Spleen cells isolated from naïve mice were pretreated with AEA in vitro followed by activation with SEB, and then cultured for 24 (A-D) or 48 (E-H) hrs, and stained for various markers. Each panel shows a representative experiment using flow cytometry and the vertical bars depict data from groups of 5 mice with Mean+/-SEM. (A) CD3+CD4+ cells. (B) CD3+CD8+ cells. (C) CD3+Vβ8+ cells (D) CD3+NK+ cells. The data was confirmed in three independent experiments. *p≤ o.o5, p**≤ o.o1.

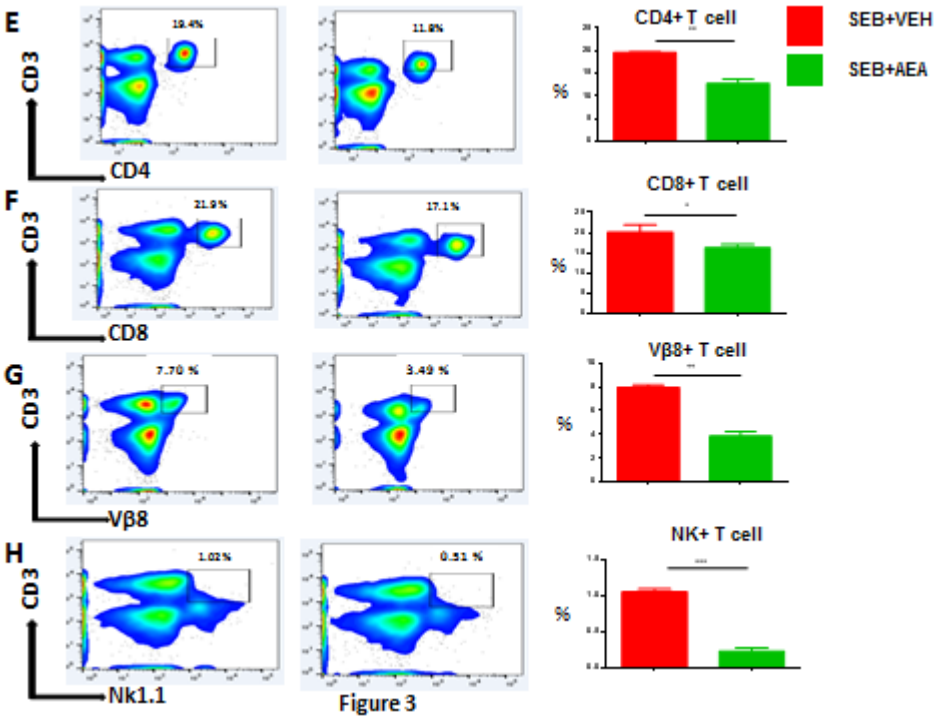

Figure 2.3: AEA decreases T cell subsets in the splenocytes activated with SEB in vitro. Spleen cells isolated from naïve mice were pretreated with AEA in vitro followed by activation with SEB, and then cultured for 24 (A-D) or 48 (E-H) hrs, and stained for various markers. Each panel shows a representative experiment using flow cytometry and the vertical bars depict data from groups of 5 mice with Mean+/-SEM. (E) CD3+CD4+ cells. (F) CD3+CD8+ cells. (G) CD3+Vβ8+ cells (D,H) CD3+NK+ cells. The data was confirmed in three independent experiments. *p≤ o.o5, p**≤ o.o1.

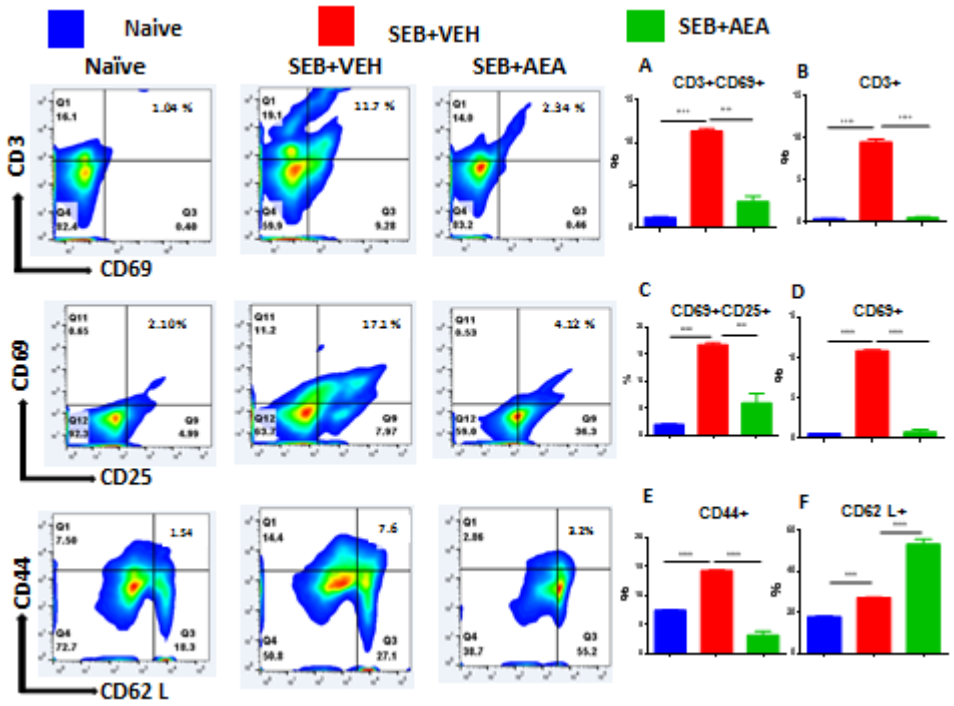

Figure 2. 4: AEA suppresses T cell activation markers in splenocytes activated with SEB. The spleen cells were pretreated with AEA and then activated with SEB in vitro for 48 hrs as described in Fig 3 legend. The cells were stained for various activation markers. Each panel shows a representative experiment using flow cytometry, and the vertical bars depict percentage data from groups of 5 mice with Mean+/-SEM. (A) CD3+CD69+ cells, (B) CD3+ cells, (C) CD69+25+ cells, (D) CD69+ cells, (E) CD44+ cells, (F) CD62L+ cells. *p≤ o.o5, p**≤ o.o1, ***p≤ o.oo1.

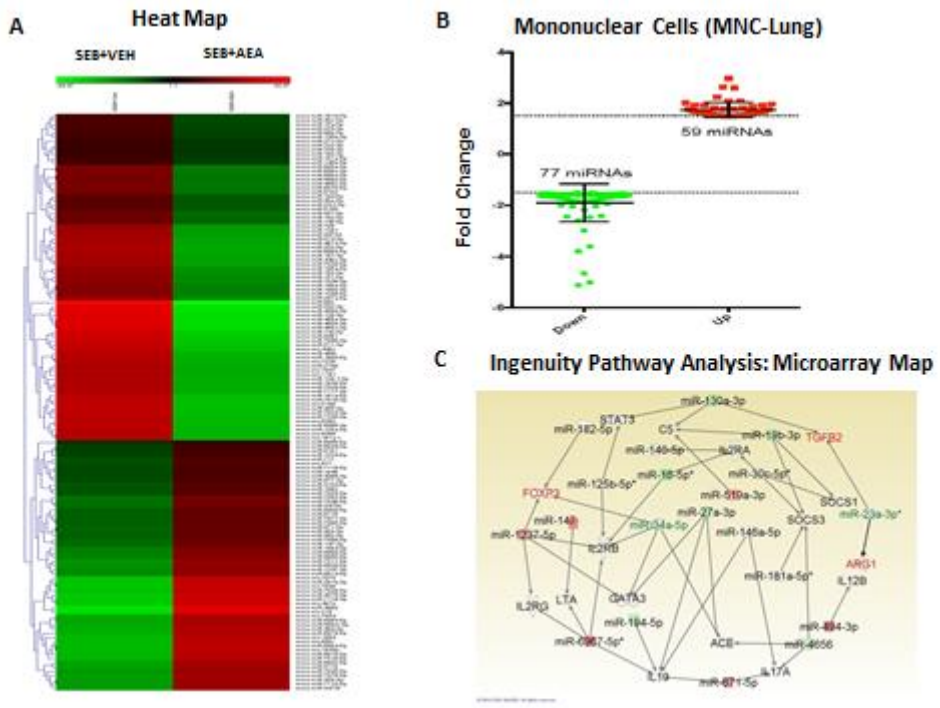

Figure 2. 5: AEA alters miRNA expression in the mononuclear cells isolated from the lungs of SEB injected mice. Mice were treated with SEB and AEA as described in Fig 1 legend. Isolated mononuclear cells of the lung were screened for miRNA expression as described in methods (A). The heat map that shows all of the altered and unchanged miRNAs in the VEH+SEB and AEA+SEB groups. (B) Diagram of miRNAs with 1.5 fold change showing 59 miRNAs upregulated while 77 miRNAs downregulated. (C) Networking of the miRNAs with their targeted genes including anti-inflammatory genes, the map showing the main miRNAs including miRNA 23a-3p targeting ARG1 and TGFβ2 gene while miRNA 34a-5p targeting FOXP3 gene.

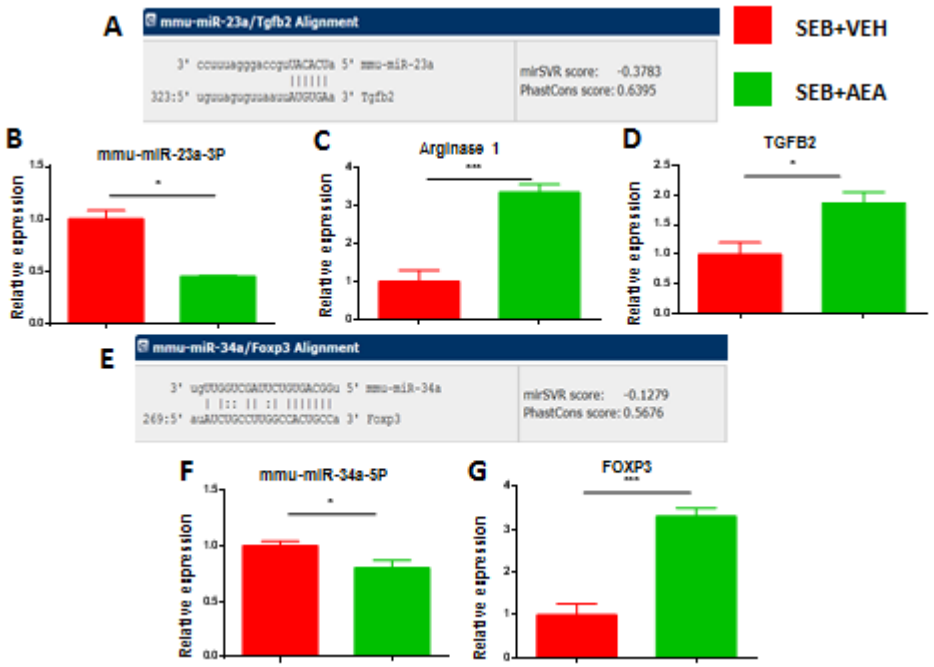

Figure 2. 6: Validation of select miRNAs and targeted genes. Mice were treated with SEB and AEA as described in Fig 1 legend. Mononuclear cells from the lungs of both groups were isolated and screened for expression of miRNA expression with their targeted genes by qRT-PCR. (A) Binding affinity between miRNA 23a-3p and targeted genes including ARG1 and TGFβ2. (B) miRNA 23a-3p expression. (C,D) Expression of ARG1 and TGFβ2. (E) Binding affinity between miRNA 34a-5p and targeted gene FOXP3. (F) Expression of miRNA 34a-5p. (G) Expression FOXP3. Statistical significances as p≤ o.o5, p**≤ o.o1, ***p≤ o.oo1.

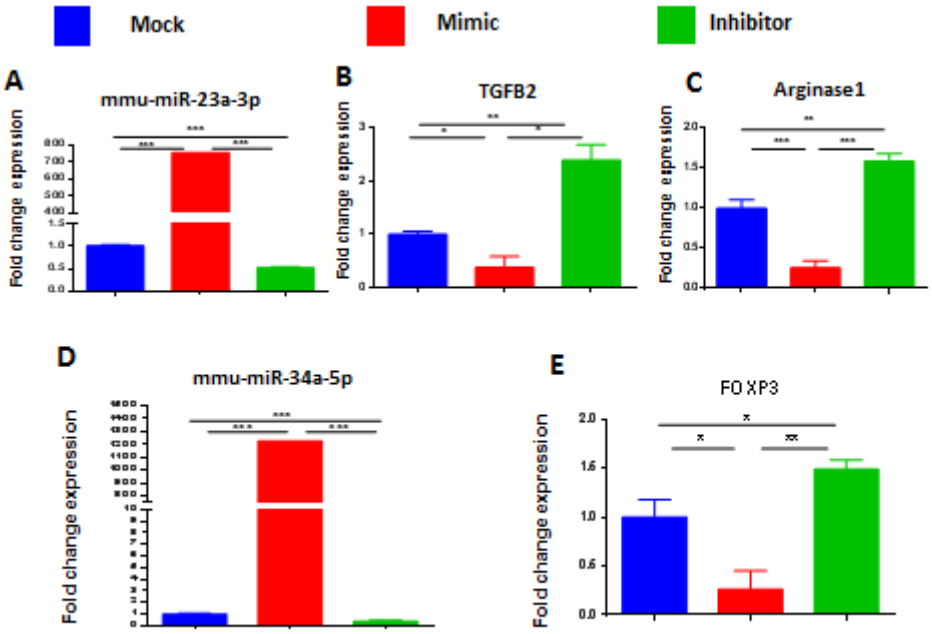

Figure 2. 7: Validation of the genes targeted by miRNA 23a-3p and miRNA 34a-5p. Splenocytes of C57BL6 mice, cultured and activated with SEB overnight were transfected with mock, mimic and inhibitor of each of miRNA 23a-3p and miRNA 34a-5p. qRT-PCR was used to detect the levels of targeted genes. (A) Expression of miRNA 23a-3p. (B) Expression of TGFB2 gene. (C) Expression of Arginase 1 gene (D) Expression of miRNA 34a-5p. (E) Expression of FOXP3. Statistical significances as p≤ o.o5, p**≤ o.o1, ***p≤ o.oo1.

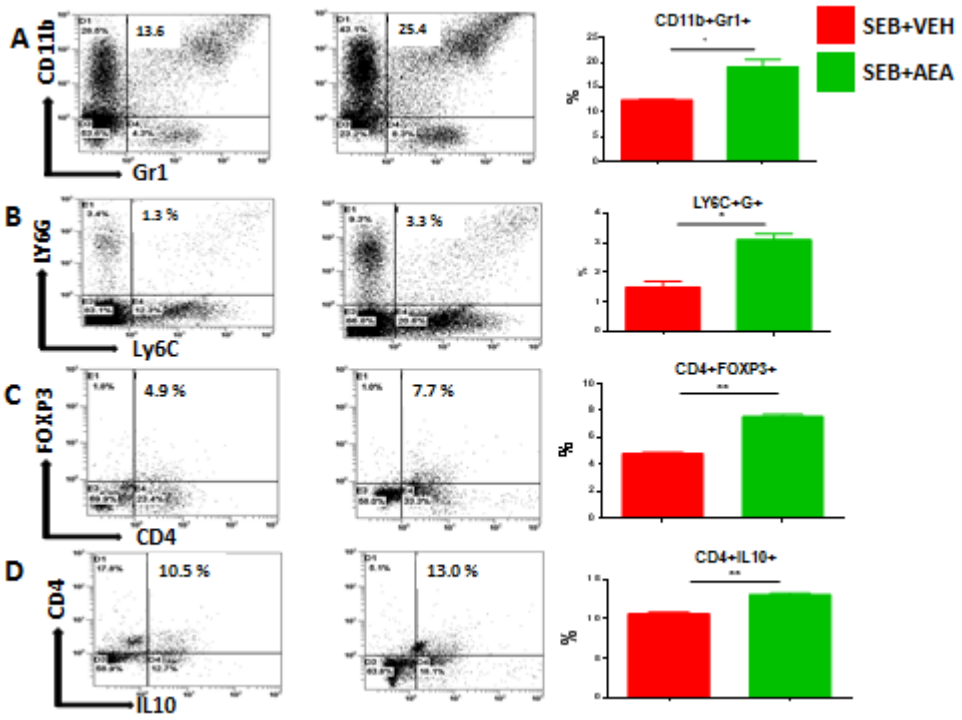

Figure 2. 8: AEA induces MDSCs and Tregs in the lungs of SEB administered mice. Mice were treated with SEB and AEA as described in Fig 1 legend. The lung MNCs were next stained for markers to detect MDSCs and Tregs. Each panel shows a representative experiment depicting lung MNCs analyzed for various T cell markers. Data from 5 mice/group is presented in the form of vertical bars with Mean+/-SEM. (A) Cells double-stained for CD11b and Gr1. A representative experiment using flow cytometry(B) Cells double-stained for LY6C and LY6G. (C) Cells double-stained for CD4 and FOXP3. (D) Cells double-stained for CD4 and IL10. (E) Cells from the spleens were double-stained for CD11b and Gr1. Vertical bars show data from 5 mice. (F) AEA-induced MDSCs were incubated with splenic T cells that were activated with ConA at different ratios to create different Tcell:MDSC ratios. T cell proliferation was assessed by 3H- Thymidine Incorporation Assay. Data from 5 mice/group is presented in the form of vertical bars with Mean+/-SEM. *p≤ 0.05, p**≤ 0.01, p***≤ 0.001

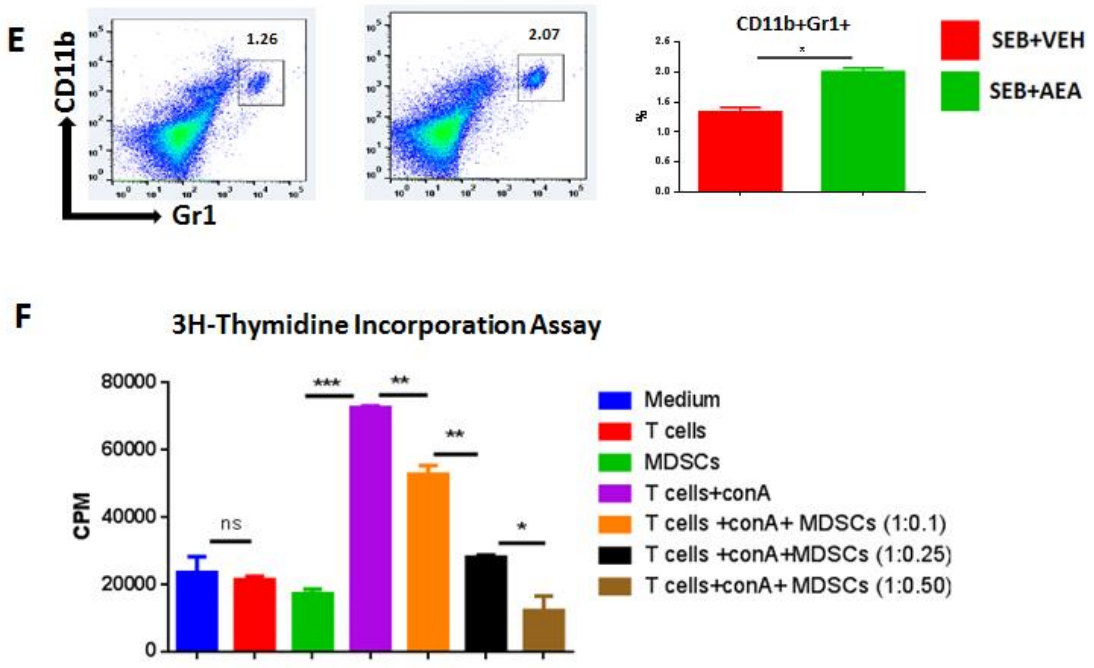

Figure 2.8: AEA induces MDSCs and Tregs in the lungs of SEB administered mice. Mice were treated with SEB and AEA as described in Fig 1 legend. The lung MNCs were next stained for markers to detect MDSCs and Tregs. Each panel shows a representative experiment depicting lung MNCs analyzed for various T cell markers. Data from 5 mice/group is presented in the form of vertical bars with Mean+/-SEM. (A) Cells double-stained for CD11b and Gr1. A representative experiment using flow cytometry (B) Cells double-stained for LY6C and LY6G. (C) Cells double-stained for CD4 and FOXP3. (D) Cells double-stained for CD4 and IL10. (E) Cells from the spleens were double-stained for CD11b and Gr1. Vertical bars show data from 5 mice. (F) AEA-induced MDSCs were incubated with splenic T cells that were activated with ConA at different ratios to create different Tcell:MDSC ratios. T cell proliferation was assessed by 3H- Thymidine Incorporation Assay. Data from 5 mice/group is presented in the form of vertical bars with Mean+/-SEM. *$p \leq 0.05$, p**≤ 0.01, p***≤ 0.001

Table 2. 1: Primer sequences used for RT-qPCR

Name of the gene	Primer	Sequence
GAPDH	Forward	5- AGGTCGGTGTGAACGGATTTG-3
	Reverse	5-TGTAGACCATGTAGTTGAGGTCA-3
FOXP3	Forward	5 - CCCATCCCCAGGAGTCTTG-3
	Reverse	5-ACCATGACTAGGGGCACTGTA-3
TGFβ2	Forward	5-CTTCGACGTGACAGAGGCT-3
	Reverse	5-GCAGGGGCAGTGTAAACTTATT-3
ARG1	Forward	5-CGGGTTAAATTCGGGTTATC-3
	Reverse	5-CGAACTACCGCGATTCTAATC-3

CHAPTER 3

Endocannabinoid Anandamide Attenuates Acute Respiratory Distress Syndrome Through Modulation of Microbiome in the Gut-Lung Axis

3.1 ABSTRACT

ARDS is a serious lung condition characterized by severe hypoxemia leading to limitations of oxygen needed for lung function. In this study, we investigated the effect of AEA, an endogenous cannabinoid, on SEB mediated ARDS in the mouse. Single Cell RNA sequencing data showed that the lung epithelial cells from AEA treated mice showed increased levels of Anti-Microbial Peptides (AMPs) and tight junction proteins. Miseq sequencing data on 16s RNA and LeFSe analysis demonstrated that SEB caused significant alterations in the microbiota with increases in pathogenic bacteria both in the lungs and the gut while treatment with AEA reversed this effect and induced beneficial bacteria. AEA treatment suppressed inflammation both in the lungs as well as gut-associated mesenteric lymph nodes (MLNs). AEA triggered several bacterial species that produced increased levels of SCFAs, including butyrate. Also, administration of butyrate alone could attenuate SEB-mediated ARDS. Taken together, our data indicate that AEA treatment attenuates SEB-mediated ARDS by suppressing inflammation and preventing dysbiosis both in the lungs and the gut through the induction of AMPs, tight junction proteins, and SCFAs that stabilize the gut-lung microbial axis driving the immune homeostasis.

3.2 INTRODUCTION

ARDS is defined as a form of respiratory failure that is caused by a variety of insults including pneumonia, sepsis, trauma and certain viral infections (Nagarkatti et al., 2020). One of the common features of ARDS includes hyperactivation of immune response systemically and in the lungs leading to the development of pulmonary edema, alveolar damage, and respiratory failure (Nagarkatti et al., 2020). ARDS is considered to be a major health problem in the field of clinical respiratory medicine worldwide (Confalonieri et al., 2017). ARDS affects approximately 200,000 patients every year in the United States and causes over 75,000 deaths annually (Fan et al., 2018). Thus, it is difficult to treat ARDS and nearly 37% of the ARDS patients die annually. Globally, 10% of intensive care unit admissions represent ARDS, which account for over 3 million patients annually (Fan et al., 2018).

COVID-19 caused by SARS-CoV2 has triggered global pandemic with more than 209 million infections and has killed over 4 million people to date. People who get the severe form of COVID-19 develop ARDS and manifest systemic hyperimmune response with cytokine storm which is difficult to treat leading to high rates of mortality. While the precise cause of hyperimmune response is unclear, there is evidence to support the possibility that hyperactivation of immune response may result from alterations in the microbiota and advancement of secondary infections. The prevalence of coinfection can account for up to 50% among patients who die from COVID-19 (Lai et al., 2020). The

coinfection can result from pathogens such as *Streptococcus pneumoniae*, *Staphylococcus aureus*, and *Klebsiella pneumoniae* (Lai et al., 2020). *Staphylococcus* produces Staphylococcus enterotoxin B (SEB) that acts as a superantigen thereby activating a large proportion of T cells, causing cytokine storm, ARDS, multiorgan failure and often death (Taub and Rogers, 1992;Lang et al., 2003;Sultan et al., 2021). Staphylococcus Enterotoxins produced by *Staphylococcus aureus* is also known to cause food poisoning and toxic shock syndrome (Pinchuk et al., 2010). Staphylococcus Enterotoxin B (SEB) is classified as a biological threat agent due to its ability to cause fatal toxic effects (Verreault et al., 2019). Our laboratory has investigated multiple murine models of SEB-mediated ARDS and has found that cannabinoids are highly effective in attenuating ARDS (Rao et al., 2015b;Mohammed et al., 2020a;Sultan et al., 2021) .

Cannabinoids are compounds that activate two types of G-protein-coupled receptors, CB1 and CB2 that are expressed primarily in the CNS, and cells of the immune system, respectively (Nagarkatti et al., 2009;Cristino et al., 2020). They are found naturally produced in the body (endocannabnoids) or in the cannabis plant (phytocannabinoids). The cannabis plant has over 120 phytocannabinoids of which Δ9-tetrahydrocannabinols (THC) is very well characterized for its ability to activate CB1 and thereby mediate psychoactive properties. THC can also activate the CB2 receptors expressed on immune cells and mediate anti-inflammatory effects (Becker et al., 2020;Mohammed et al., 2020a;Becker et al., 2021). The endocannabinoids, which are host-derived lipid hormones, are found in all tissues, organs and bodily fluids and control a wide range of physiological functions including appetite, pain, sleep, mood and memory(Finn et al., 2021;Rahman et al., 2021). The two most well-studied

endocannabinoids are the arachidonic acid derivatives, *N*-arachidonoylethanolamine (AEA) and 2-arachidonoylglycerol (2-AG). We and others have shown that endocannabinoids can also act as potent anti-inflammatory agents (Pandey et al., 2009;Jackson et al., 2014a;Sido et al., 2016;Ahmed et al., 2021;Osafo et al., 2021). Recently, we demonstrated that AEA can attenuate SEB-mediated ARDS in the mouse model by targeting miRNA which trigger anti-inflammatory pathways involving immunosuppressive cells such as the MDSCs and the Regulatory T cells (Tregs) (Sultan et al., 2021). Recent studies have shown that the diversity of the gut microbiota may be regulated by endocannabinoids (Finn et al., 2021;Minichino et al., 2021). This raises an important question of whether endocannabinoids can alter the microbiota in the gut and the lungs during ARDS thereby providing increased protection from pathogenic bacteria as well as by suppressing hyperinflammation. In the current study, we tested this hypothesis and our results demonstrated that AEA-mediated attenuation of SEB-induced ARDS may result from causing increased abundance of beneficial bacteria that produce SCFA that are anti-inflammatory and by inducing AMPs and tight junctions proteins that prevent the emergence of pathogenic bacteria. The current study also provides evidence on the cross talk of the microbiota in the gut-lung axis during ARDS.

3.3 MATERIALS AND METHODS

Mice housing and grouping

Female C57BL/6 mice, 6-8 weeks old, were purchased from Jackson laboratories. Mice were housed at a density of 5 animals per cage under pathogenic–free conditions in the Animal Resource Facility (ARF) at the University of South Carolina School of Medicine. These studies were approved by the Institutional Animal Care and

Use Committee (IACUC). Mice were housed under a 12-hour light/dark cycle at 18-23°C and 40-60% humidity. The mice were randomized and then assigned for specific treatments.

Induction of SEB-mediated ARDS in mice and treatment with AEA

ARDS was induced in mice as described previously (Rieder et al., 2011;Sultan et al., 2021). Mice were given a single dose of SEB intranasally at a concentration of 50 µg/mouse in 25 µl of Phosphate Buffer Saline (PBS) on day 0. On day-1, AEA (40 mg/kg body weight) or vehicle (VEH) was given into these mice by the intra-peritoneal (I.P.) route. AEA dissolved in ethanol (50 mg/ml) and was diluted further in PBS. Each mouse received 0.1 ml consisting of 84 µl of PBS and 16 µl of ethanol containing AEA. The vehicle controls (VEH) received 0.1 ml consisting of 84 µl of PBS and 16 µl of ethanol without AEA. The dose of AEA was based on our previous studies demonstrating that 40 mg/kg body weight of AEA attenuated T cell-mediated delayed-type hypersensitivity response and SEB-mediated ARDS (Jackson et al., 2014a). The treatment with AEA was repeated on day 0 (SEB exposure day), and day 1. Mice were euthanized on day 2 (48 h after SEB exposure) for various studies.

Evaluation of lung function in mice

To evaluate the effect of AEA on the functions of the lung, the whole-body plethysmography (Buxco, Troy, NY, USA) was used as described previously (Elliott et al., 2016). In brief, mice from each group were first restrained, in a plethysmography tube and were allowed to acclimatize. The clinical parameters of the lung including peak Inspiratory Flow (PIF), Peak Expiratory Flow (PEF), and Tidal Volume (TV) were evaluated.

Collection of Serum and Broncho Alveolar Lavage Fluid (BALF)

To collect blood, mice were kept under anesthesia and then were bled through the retroorbital orifice. Broncho Alveolar Lavage Fluid (BALF) was collected as previously described (Rao et al., 2015a), Briefly BALF was collected 48 hrs. post-SEB exposure, after the mice were euthanized. The lung was excised as an intact unit along with the trachea. To collect BALF, sterile ice-cold PBS was injected through the trachea.

Lung and Colon Histopathology

The lung and colon were excised after perfusion and the tissues were kept directly in 10 % formalin followed by embedding the tissues in paraffin. The sections of lungs and colon were cut in the Core facility and then processed for Hematoxylin and Eosin (H & E) staining as described previously (Sultan et al., 2021). Briefly, the lung and colon tissues were first mounted on glass slides and then the slides were transferred into xylene to deparaffinized the tissue sections. The tissue sections were then rehydrated in alcohol (100%, 95%, and 90%). The sections were finally stained with H & E and followed by dehydration. H & E-stained sections were analyzed using KEYENCE (IL-US) digital microscope VHX-7000. Histopathological scoring parameters for lung and colon were evaluated as previously described (Akgun et al., 2005;Matute-Bello et al., 2011).

Capillary Leak Measurement

Evans blue assay was used to measure the capillary leak as described previously (Rieder et al., 2012). Mice were injected intravenously with 1% Evans blue dye in PBS. The mice were sacrificed under general anesthesia after 2 hours. The lungs were removed after perfusion with heparinized PBS and transferred in formamide and kept at 37°C for 24 hrs. The calculation of leaked dye was measured by determining the absorbance of

supernatant at 620 nm and then following equation was applied to calculate the percent increase in the capillary leak: (OD sample-OD control)/OD control)*10.

Gut Leakage Measurement

Gut permeability in vivo was measured as described previously (Busbee et al., 2020). Briefly, C57BL/6 mice were administered FITC dextran (Sigma Aldrich) dissolved in 100 ul of PBS by oral gavage, then four hours later, blood was collected from mice and then the concentration of FITC-dextran was determined using spectrophotometer (PerkinElmer Life Science) with excitation wavelength at 480 nm.

Isolation of Mesenteric Lymph Nodes (MLNs) and Flow cytometric analysis

MLNs were isolated from euthanized mice and single cells were prepared in complete medium following squeezing the tissue through Stomacher 80 Biomaster blender (Steward, FL, USA). The cells were filtered using 70 um filter and centrifuged for 10 mins, at 1300 rpm. The pellet was resuspended in complete medium, and the cells were counted using Bio-Rad TC 20 automated cell counter (Herculus-CA-USA).

The MLN cells were stained using fluorescent conjugated antibodies (anti-CD3 Brilliant Violet 785, anti-CD4 Phycoerythrin (PE), anti-CD8 Alexa Fluor 700, anti-Vβ8 FITC (Fluorescein isothiocyanate), anti-NK1.1-PE/Dazzle. The staining of cells for dual markers was performed as described previously (Abdulla et al., 2021a). In brief, Fc receptor block was added to the MLN cells and incubated for 10 mins at room temperature followed by staining of the cells using appropriate antibodies and then incubated at 4°C for 20-30 minutes. Stained cells were washed twice with cold PBS containing 2% Fetal Bovine Serum (FBS) Staining buffer.

Single Cell RNA Sequencing (scRNA-seq) and Analysis

scRNA-Seq was performed as describe previously (Teodoro et al., 2020). The whole lung tissue from mice were smashed using a Stomacher 80 Biomaster blender (Steward, FL, USA). The tissues were then filtered with a 70 µm filter twice and then centrifuged at 1300 RPM for 7 minutes. Cell pellets were treated with RBC lysis on ice for five minutes, and then washed twice in 10x buffer. Dead cells were removed using a Stem Cell Technologies dead cell removal kit (STEM CELL,sunrise-FL-USA) and the cell viability was measured using TC 20 automated cell counter. The cell viability was 92-95%. A target number of 3000 cells from each group was then loaded into the Chromium Controller (10x Genomics) and 10X Genomics was used to process the cells. Following the manufacturer's protocol, the chromium single cell 5′ reagent kits (10 × Genomics) were used to process samples into single-cell RNA-seq (scRNAseq) libraries. The sequencing of these libraries was performed using the NextSeq 550 instrument (Illumina) with a depth of 20-50 k reads per cell. The base call files generated from sequencing the libraries were then processed in the 10 × Genomics Cell Ranger pipeline (version 2.0) to create FASTQ files. The FASTQ files were then aligned to the mm10 mouse genome, and the read count for each gene in each cell was generated. Each group was aggregated using the aggr pipeline in Cell Ranger, and the output was browsed in Loupe Browser 4.2.0. This allowed us to identify clusters and illustrated the differentially expressed genes between each cluster and groups.

Miseq Sequencing of Gut-Lung Axis

First, the microbial DNA from the cecal flush were isolated as described previously (Mohammed et al., 2020b;Alghetaa et al., 2021). In brief, genomic DNA from

the colon samples were isolated using QIAamp DNA Stool Mini Kit and following the protocol of the company (Qiagen). DNA from lungs tissue were isolated using ZR Bacterial DNA MidiPrep from Zymo Research and following the manufacturer's instructions. The concentration of DNA was determined using Nanodrop (Thermo Fisher Scientific, Waltham, MA). The isolated DNA was either used immediately or stored at −20°C for use in future. The 16S rRNA sequencing was performed on V3- V4 hypervariable regions of bacterial DNA of both lungs and gut. Amplification of DNA was performed, and Illumina adapter overhang nucleotide sequences (San Diego, CA) were added. The sequencing was then performed on Illumina MiSeq Platform and as described previously (Mohammed et al., 2020c).

Quantitate -Real Time Polymerase Chain Reaction (qRT-PCR)

qRT-PCR was performed as described previously (Abdulla et al., 2021b;Sultan et al., 2021). Briefly, cDNA was synthesized from total RNAs using miScript II RT kit from Qiagen and following the protocol of the Qiagen company (Germantown-MD-USA). The details of primers used are presented in Table 3.1.

Identification and Quantification of Short Chain Fatty Acids (SCFA)

Quantification of SCFAs was performed as described previously (Mehrpouya-Bahrami et al., 2017). Briefly, 100 mg of cecal content was collected and then acidified by metaphosphoric acid and kept on ice for 30 mins. Centrifugation at 12000× *g* for 15 min at 4°C was performed and then supernatant was collected and filtered using MC filters at 12000× *g* for 4 mins at 4°C. The filtered samples were then transferred into glass vials then Methyl Tert Butyl Ether (MTBE) purchased from Sigma Aldrich

(St.Louis,MO-United States) was added and were centrifuged at 1300 rpm for 5 mins at RT. The top organic layer was transferred to a new vial. The standard mixtures and internal standards were used to detect the response factors and linearity for each SCFA standard acid. To perform analysis of SCFAs, HP 5890 gas chromatography configured with a flame-ionization detector (GC-FID) was used and 0.1mM 2-ethyl butyric acid was used as an internal standard (IS) for all samples and standards. To quantify, the concentration of SCFA, Varian MS workstation (version 6.9.2) was used.

Pretreatment with Butyrate and treatment with SEB.

Mice were treated with butyrate or vehicle (PBS) through oral gavage on day -1 at a dose of 200 mg/kg. On day 0, mice were given another dose of butyrate with same dose and 3 hrs later, the mice received 50 □g SEB in 25 ul of PBS intranasally. On day 1, these mice received another dose of butyrate or vehicle based on the groups. The mice were then euthanized on day 2 (48 hrs after SEB exposure) for further analysis of ARDS. Dose was based on our previous studies (Abdulla et al., 2021a).

Statistical Analysis

We used Graph Prism Software (San Diego, CA, United States). In this study, t-test was applied to compare the two groups, while One–way ANOVA with post-hoc Tukey's test to compare between three groups. Data were expressed as Mean ± SEM and statistically significant differences were illustrated in figures as *$p<0.05$, **$p<0.01$, ***$p<0.001$, ****$p<0.0001$.

3.4 RESULTS

Anandamide attenuates SEB-mediated inflammation in the lungs

Recently, we reported that AEA attenuates SEB-mediated acute lung injury (Sultan et al., 2021). The goal of this study was to explore the role of microbiota in this model, and to that end, we first performed experiments that corroborated our previous findings that AEA can suppress inflammation in the lungs and improve lung functions following exposure to SEB. Mice were exposed to SEB+ Veh or SEB+AEA as described in Methods and 48 hr later, the lung functions were evaluated using Buxco Instrument System. Peak Inspiratory Flow, Peak Expiratory Flow and Tidal Volume were measured. All parameters significantly improved in SEB+AEA, when compared to SEB+VEH (**Figure 3.1 A-C)**. These data demonstrated the ability of Anandamide to improve lung functions affected by SEB exposure. Next, we analyzed for the expression of IL-6, a key cytokine induced during ARDS by SEB (Mohammed et al., 2020d) and found that it was highly induced following SEB treatment and was significantly attenuated following treatment with AEA both in the serum (**Figure 3.1 D**) and BALF (**Figure 3.1 E**).

Effect of Anandamide on the Lung and Colon in SEB- exposed mice

Because SEB causes systemic cytokine storm and pathogenesis, we tested the effect of Anandamide (AEA) on lung and colon in SEB-exposed mice. Histopathological analysis and scores of the lungs demonstrated that AEA decreased the infiltration of inflammatory cells in SEB +AEA group, when compared to the SEB+VEH group (**Figure 3.2A**). Interestingly, data obtained from the colon demonstrated that SEB exposure caused significant infiltration of inflammatory cells in the colon of SEB+VEH group, when compared to Naïve group. AEA treatment decreased the SEB-mediated

infiltration of the inflammatory cells in the colon (**Figure 3.2 B).** Upon analysis of vascular and gut leakage, we noted that Anandamide significantly decreased the leakage in the lungs (**Figure 3.2D**) and the gut (**Figure 3.2E**) in the SEB+AEA group, when compared to SEB+VEH group.

Anandamide attenuates SEB-activated T cells in the mesenteric lymph nodes (MLNs)

To further investigate the effect of AEA on gut-associated immune response, we analyzed the effect of AEA on the mesenteric lymph nodes (MLNs). The data showed that AEA significantly decreased the percentage and absolute numbers of CD4+ T cells, CD8+T cells, V□8+ T cells, and NK T cells in the SEB+AEA group, when compared to SEB+VEH group of mice (**Figure 3.3 A-D).**

scRNA-seq of cells isolated from the lungs

Using scRNA-seq we first looked at the different types of cell clusters in the lungs of SEB+VEH and SEB+AEA mice. As seen from **Figure 3.4A** we detected 12 different types of cells isolated from the lungs and criteria used is detailed in the Figure legend. The data showed that some of the cell clusters were different between the SEB+VEH vs SEB+AEA group. Of significant note, there was an increase in the cluster numbered 6 (Regulatory cell 2) in SEB+AEA when compared to SEB+VEH, consistent with our previous studies that AEA induces Tregs (Sultan et al., 2021). Also, there was significant decrease in the clusters numbered 8 and 9 (Macrophages 2 and 3 respectively) in SEB+AEA group when compared to SEB+VEH. Lung epithelial cells play an important role such as barrier protection, fluid balance, clearance of particulate matter, and protection against infection (Guillot et al., 2013). Furthermore, they produce

antimicrobial peptides (AMPs), which act as antibiotics to kill pathogenic bacteria (Beisswenger and Bals, 2005). We therefore performed scRNA-seq of epithelial cells (cluster 10) from the lungs to study the expression of AMPs. The data demonstrated that AEA significantly upregulated the expression of AMP-related genes in the lung epithelial cells (**Figure 3.4B**). The AMP-related genes including Tracheal Antimicrobial Peptide (TAP1) (**Figure 3.4B**), Tracheal Antimicrobial Peptide 2 (TAP2) (**Figure 3.4C**), Lysozyme 2 (LYZ 2) (**Figure 3.4D**), and murine Beta Defensin 2 (MBD2) (**Figure 3.4H)**. We also noted increased expression of tight junction proteins such as Claudin 1 (CLDN1) (**Figure 3.4F)** and Cadherin 1(CDH1) (**Figure 3.4G)**, as well as Secretory Leukocyte Peptidase Inhibitor (SLPI) (**Figure 3.4E**) in SEB+AEA group when compared to the SEB+VEH group. Moreover, these data were confirmed by performing q-RT-PCR (**Figure 3.4B-H).**

The effect of AEA on microbial profile in the lungs and the gut

Because we noted significant induction of AMPs following AEA treatment, we next investigated the microbial profile in the lungs and the gut following SEB treatment. SEB treatment increased the abundance of microbiota in the lungs, and AEA significantly reversed this as shown using Chao1 rare fraction measure (**Figure 3.5A)**. Beta diversity analysis that measures the similarity or dissimilarity between various groups showed that all 3 groups were well separated, with the SEB+AEA group clustered away from the SEB+VEH group (**Figure 3.5B**). Additionally, Caulobacterales and Pesudomonodales at the level of order, were significantly decreased in the SEB+AEA group when compared to SEB+VEH (**Figure 3.5 C, D).** To distinguish significantly altered bacteria among the three groups, Linear discriminant analysis effect size (LefSe) analysis (**Figure**

3.6A) was performed and the corresponding cladogram (**Figure 3.6B)** was generated. Data showed that there were several bacteria found to be distinctly expressed in each of the 3 groups. Our LefSe analysis of the lungs indicated that beneficial bacteria such as Muribaculaceae(s24-7) was indicated in the SEB+AEA group only. Also, some beneficial bacteria such as Lachnospiraceae, Clostridia which produce butyrate were indicated in the SEB+AEA group but not in the Naïve or SEB+VEH group. Interestingly, some pathogenic bacteria such as Pseudomonas and Enterobacteriaceae were indicated in the SEB+VEH group only but not in the Naïve or SEB+AEA.

Role of Anandamide in the regulation of microbial dysbiosis in the Gut

Previously we have shown that there is cross talk between the gut and lung microbiota which regulates ARDS (Alghetaa et al., 2021). To that end, we investigated if SEB caused similar alterations in the gut and if AEA would reverse these changes. SEB treatment decreased the abundance of microbiota in the gut and AEA failed to reverse this as shown using Chao1 rare fraction measure (**Figure 3.7A).** Beta diversity analysis showed that all 3 groups were well separated with the SEB+AEA group clustered away from the SEB+VEH group (**Figure 3.7B**). The analysis of microbiota using MiSeq of 16s-RNA of microbiota of the gut indicated that Anaeroplasmatacae at the family level and Tenericutes at the phylum level were significantly increased in the SEB+VEH group when compared to the naïve mice, and treatment with AEA reversed this change (**Figure 3.7 C-D)**. To distinguish significantly altered bacteria among the three groups, LefSe analysis (**Figure 3.8A)** was performed and the corresponding cladogram (**Figure 3.8B)** was generated. Our LefSe analysis of the gut indicated that Muribaculaceae (S24-7) was indicated in the gut of SEB+AEA group. Anaeroplasma and Tenericutes which are

pthogenic bacteria, were seen in the gut of SEB+VEH only but not in the Naïve or SEB+AEAgroup. These data showed that there were distinct bacteria found to be uniquely expressed in each of the 3 groups (**Figure 3.8**).

Effect of Anandamide on Short Chain Fatty Acids SCFAs) in the Gut

Gut microbiota are known to produce SCFAs that suppress inflammation (Dang and Marsland, 2019;Kim, 2021). To that end, we measured the levels of SCFAs in Naïve, SEB+VEH and SEB+AEA and we found that Butyric acid, Valeric acid and Iso-Valeric acid levels were significantly decreased in the SEB+VEH group when compared to the naïve mice while in the SEB+AEA group, the levels of these SCFAs increased significantly when compared to SEB+VEH group (**Figure 3.9).**

The Role of Butyrate in the Amelioration of SEB-mediated ARDS

We next tested the role of butyrate in attenuating ARDS by directly administering it into SEB-injected mice. The data showed that administration of butyrate significantly improved the SEB-mediated ARDS as seen from decreased infiltration of inflammatory cells and histological scores in the lungs (**Figure 3.10A**). The Butyrate also improved the clinical lung parameters such as Specific Airways Resistance (**Figure 3.10B**) and Specific Airways Conductance (**Figure 3,10C).**

3.5 DISCUSSION

ARDS is a hypoxemic respiratory failure characterized by severe lung inflammatory responses leading to high mortality that may reach up to 60% (Fan et al., 2018). ARDS is triggered by a variety of insults such as pneumonia, sepsis, trauma and certain viral infections. SARS-CoV-2 infection that causes COVID-19 has also been shown to trigger viral pneumonia leading to ARDS in patients with the severe form of the disease (Gibson et al., 2020). ARDS can also cause alterations in the microbiota in the lungs leading to secondary infections. The prevalence of coinfection varies among COVID-19 patients as indicated in different studies, but it can account for up to 50% among patients who die from COVID-19 (Lai et al., 2020). The co-pathogens include *Staphylococcus aureus* (Lai et al., 2020) which produces SEB that can also promote ARDS and cytokine storm. Thus, characterization of lung microbiome is an important aspect to understand the mechanisms involved in ARDS. SEB can also alter the gut microbiota and thereby alter the lung-gut axis that drives the immune homeostasis. It is for these reasons, the current study focused on the role of SEB in altering the microbiota in the lungs and the gut, and further address if AEA-mediated attenuation of ARDS is associated with microbiome profile. It should be noted that the effect of AEA on microbiota in the gut and lungs has not been investigated before.

The results obtained from the current study based on clinical lung parameters were consistent with our previous studies (Sultan et al., 2021) demonstrating that AEA treatment significantly improved all the parameters of ARDS in the lung including peak

inspiratory flow, peak expiratory flow, and tidal volume. In the current study, the expression of IL-6, one of the proinflammatory cytokines, was significantly increased in mice with ARDS, and AEA treatment significantly decreased IL-6 expression in both serum and BALF of mice. IL-6 has been shown to be highly expressed in respiratory infections including SARS-CoV-2/COVID-19 patients and other respiratory infections (Gubernatorova et al., 2020;McGonagle et al., 2020).

AMPs are produced primarily by the epithelial cells that play an important role in host defense against infections (Geitani et al., 2020). AMPs have been applied as a therapeutic agent against lung infections (Mahlapuu et al., 2016). In the current study, using scRNAseq, we found that AEA increased the expression of several AMPs by the lung epithelial cells. TAP1 and TAP2 are among the AMPs produced by lung epithelial cells exclusively in the respiratory system that are specifically protective against pathogens such as Pseudomonas spp (Diamond et al., 1991;Diamond et al., 1993). SLPI which has also been shown previously to play an important role against pathogenic bacteria including Pseudomonas during respiratory infections (Weldon et al., 2009;Camper et al., 2016). Interestingly, in the current study we noted that SEB+VEH group had increased abundance of Pseudomonas spp while it was absent in the naïve and SEB+AEA group. These data suggested that SEB may promote the growth of Pseudomonas and that AEA may suppress its growth by inducing AMPS. Additionally, mBD2 which is an antimicrobial peptide not only inhibits the growth of pathogenic bacteria such as *Pseudomonas aeruginosa*, but also promotes macrophage functions (Wu et al., 2018). In the current study, we noted that AEA treatment increased the expression of mBD2 which was associated with decreased *Pseudomonas* in SEB+AEA group when

compared to SEB+VEH group. Similarly, LYZ2, another AMP which was induced by AEA has been shown to play a key role in increasing bacterial killing in the lungs and prevent the spread of the infection (Akinbi et al., 2000;Jaeger et al., 2020). Additionally, S24_7 (Muribaculaceae) which is a beneficial bacteria (Ormerod et al., 2016;Lagkouvardos et al., 2019) was seen in the SEB+AEA group in both the gut and the lungs suggesting that there may be a cross talk between gut and lung microbiome. Our Lefse analysis indicated that Enterobacteriaceae and Pseudomonas which were both indicated in the lungs of SEB+VEH group but not in the naïve or SEB+AEA, and it is interesting to note that they are considered as a cause for pneumonia and lung diseases (Karnad et al., 1987;von Baum et al., 2010). Additionally, Tenericutes which is considered to be pathogenic (Clarke et al., 2012)was indicated in the SEB+VEH only but not in the Naïve or SEB+AEA of the gut. Lachnospiraceae and Clostridia which are one of the main producers of butyrate (Guo et al., 2020) were indicated after AEA treatment but not in SEB+VEH group. Together, these data suggested that SEB may trigger harmful bacteria, and AEA not only prevents these but also induces beneficial bacteria in the lungs and the gut.

Tight junctions plays an important role in the intestinal barrier functions which control the permeability (Rober et al., 2018, Adam et al., 2020). In the current study, we noted that Claudin and E-cadherin were upregulated by AEA. CLDN1 is one of the main tight junctions that maintains the intestinal epithelial homeostasis (Fernando et al.,2018). Decrease in CLDN1 expression leads to an increase in the leakiness during lung injury (Desin et al, 2020). E-cadherin (CDH1) plays a critical role in the epithelial cell barrier

functions (Jefferson et al 2015) and losing of E-cadherin function can lead to respiratory disorders (Post et al., 2018).

Crosstalk in the Gut-Lung Axis is one of the important pathways to maintain the immune homeostasis (Enaud et al., 2020). Physiological pathways of gut-lung axis are considered as bidirectional and establish a well-maintained relationship between gut and lung as well as playing a crucial role in maintaining the health and homeostasis (Silver et al., 2021). Gut-Lung Axis has been investigated before including previous studies from our lab indicated that cannabinoids, specifically THC, was able to modulate the microbiome profile of both gut and lung in a similar way during ARDS (Mohammed et al., 2020c). To date, there are no studies showing the immune modulation effect of the endocannabinoid, AEA, on the microbiome profile of the Gut-Lung axis.

In the current study, we noted that some bacteria were common in both the lungs and the gut of naïve mice such as Betaproteobacteria. Also, S24_7 (Muribaculaceae) beneficial bacteria, was seen both in the lungs and the gut of SEB+AEA group. These findings supported the concept of a cross talk between gut and lung microbiome.

Our study also indicated that AEA treatment led to a decrease in the abundance of the order Pseudomonas and Caulobacterlaes, which are both considered to cause human respiratory tract infections (Li et al., 2020;Mohammed et al., 2020c). In the current study, we also noted that there was increased abundance in the gut, the family Anaplasmataceae, which are α-proteobacteria, classified in the order Rickettsiales, and currently contains five genera, some of which contain members that are known to infect humans (Patterson et al., 2021) *Anaplasmataceae* members are well recognized for causing tick-borne life-threatening zoonotic diseases in the United States

(Patterson et al., 2021). Thus, it was interesting to note that AEA prevented the increase in Anaplasmataceae induced by SEB. We also noted that SEB caused an increase in the phylum Tenericutes in the gut, which consist of wall-less bacteria. Their members establish commensal or highly virulent relationships in animals and humans (Skennerton et al., 2016). Also, in the lungs, SEB caused an increase in Caulobacteraceae which are gram-negative proteobacteria that can include a variety of pathogenic bacteria (Liu et al., 2021) as well as an increase in Pseudomonadales, some members of which are pathogens (do Nascimento et al., 2020). Interestingly, AEA reversed the effect of SEB on these bacteria. In the current study, we also noted that AEA treatment increased the abundance of S24_7, currently called *Muribaculaceae*, a family of bacteria within the order Bacteroidales (Lagkouvardos et al., 2019). These bacteria are normally found in the gut (Lagkouvardos et al., 2019) but interestingly, we also found these in the lungs of AEA treated mice which also suggested gut-lung axis and crosstalk. Also, *Muribaculaceae* are known to promote fermentation pathways to produce SCFAs (Smith et al., 2019), which was also found to be increased following AEA treatment.

In this study, analysis of gut microbiome as well as LefSe demonstrated that AEA treatment increased the Bacteroidetes and Clostridia, which are the main bacteria that produce butyrate (Chai et al., 2019). Additionally, we found that AEA induced the abundance of Lachnospiraceae, a family of anaerobic bacteria in the order Clostridiales that ferment diverse plant polysaccharides to SCFA (Vacca et al., 2020), which were found to be increased in mice treated with AEA. Thus, the gut-lung axis may allow the SCFA to get access into the blood stream, and into the lungs and suppress inflammation in the lungs. To that end our studies also demonstrated that direct administration of

butyrate into SEB-injected mice, suppressed the ARDS. Sodium Butyrate is very well known for its anti-inflammatory and immune modulatory properties (Marjitie et al 2019).

Lymph nodes are considered as the site of immune response initiation against pathogens (Buettner and Bode, 2012). Previous studies from our lab have demonstrated the role of MLNs in the modulation of microbiome (Adulla et al., 2021). Another important study has shown that mesenteric lymph nodes significantly attenuated inflammatory biomarkers of the lung to preserve the barriers in a septic model of rats (Liu et al., 2020). Additionally, another study demonstrated that gut-associated lymph nodes serve as a main source for initiation of systemic inflammatory responses specifically against acute lung injury (Jin et al., 2020). Thus, in the current study, we investigated the immune responses in MLNs specifically the response of T cells after AEA treatment. AEA significantly decreased the T cell subsets including CD4+T cells, CD8+T cells, V□8+ T cells, and NK+ T cells in the MLNs, when compared to SEB+VEH group

In summary, the current study demonstrates that SEB, a bacterial superantigen, induces ARDS triggering inflammation not only in the lungs but also in the gut. Interestingly, SEB also caused alterations in the lung and gut microbiota, specifically causing an abundance of pathogenic bacteria such as Pseudomonas while AEA reversed this effect. AEA induced several antimicrobial peptides and it is likely that this effect may have prevented the emergence of pathogenic bacteria following SEB treatment. AEA also promoted the abundance of beneficial bacteria that produce SCFAs such as butyrate. Thus, AEA may attenuate SEB-mediated ARDS not only through direct suppression of inflammation in the lungs but also by altering the microbiota in the lungs

and the gut. Our studies also suggest that increasing the endogenous AEA through use of inhibitors such as *Fatty Acid Amide Hydrolase* (*FAAH*) may serve as effective treatment modalities against ARDS.

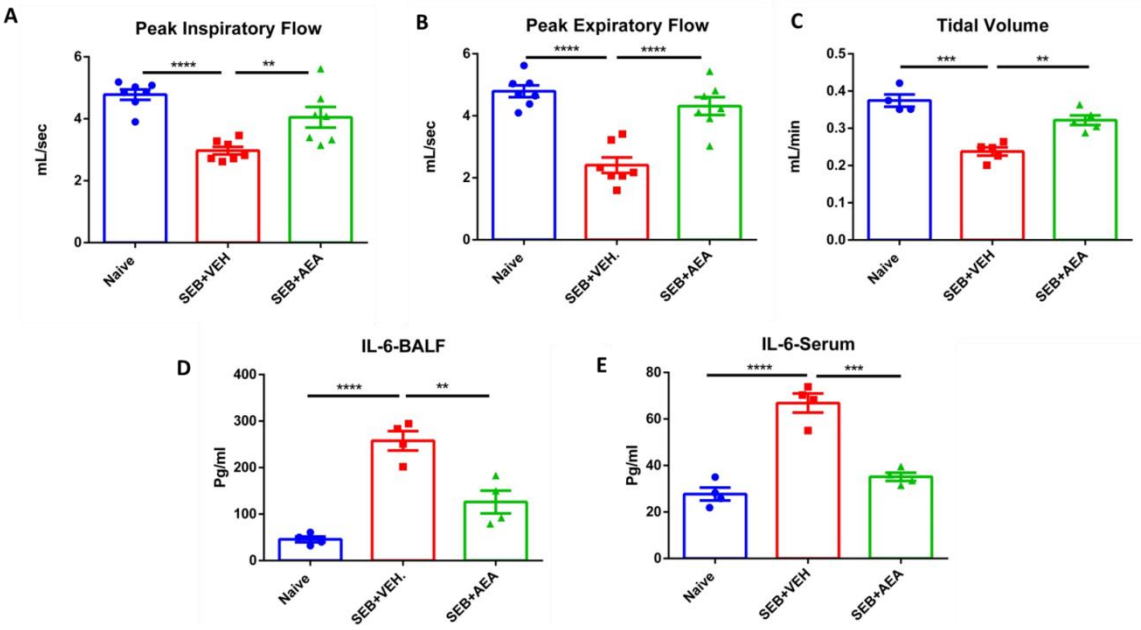

Figure 3. 1: AEA improves the clinical symptoms of ARDS in the lungs induced by SEB. On day -1, 0, and 1, mice received 40mg/kg of AEA or VEH i.p. and SEB at a dose of 50 ug/mouse intranasally on day 0. Mice were euthanized 48 hrs after SEB exposure. The lung functions were assessed using Plethysmography. The data shown include clinical functions of the lung including (A) Peak Inspiratory Flow, (B) Peak Expiratory Flow, and (C) Tidal Volume (TV). (D) Measurement of cytokines IL6, in the sera and BALF. Seven mice in each group were used and the data confirmed in three independent experiments. *p≤ 0.05, p**≤ 0.01, ***p≤ 0.00

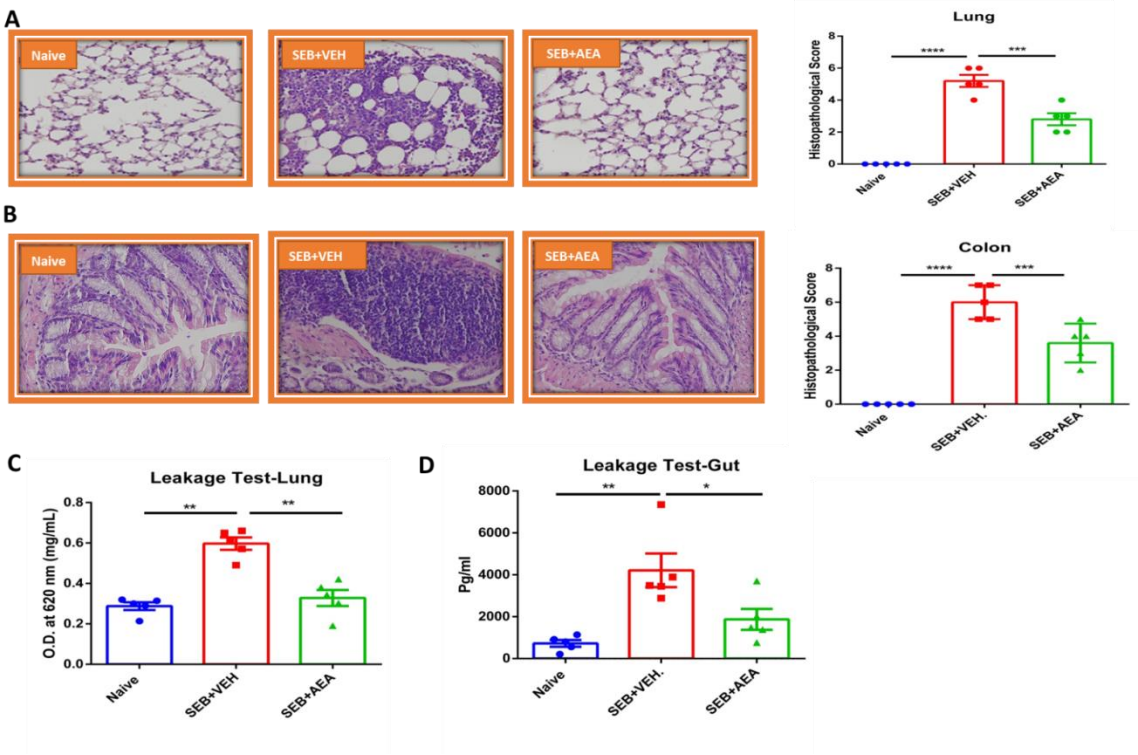

Figure 3. 2: AEA decreases inflammatory parameters of Gut and Lung. Mice were treated with SEB and AEA as described in Fig 1 legend. (A) Representative histopathological images and scores for the lung sections of Naïve, SEB+VEH, SEB+AEA mice stained with H & E. (B) Representative histopathological images and scores for the colon tissue from Naïve, SEB+VEH, SEB+AEA mice. (C) Gut leakage in the gut. (D) Capillary Leakage in the lung of Naïve, SEB+VEH and SEB+AEA. Five mice in each group were used and the data was confirmed in three independent experiments. *p≤ 0.05, p**≤ 0.01, ***p≤ 0.001.

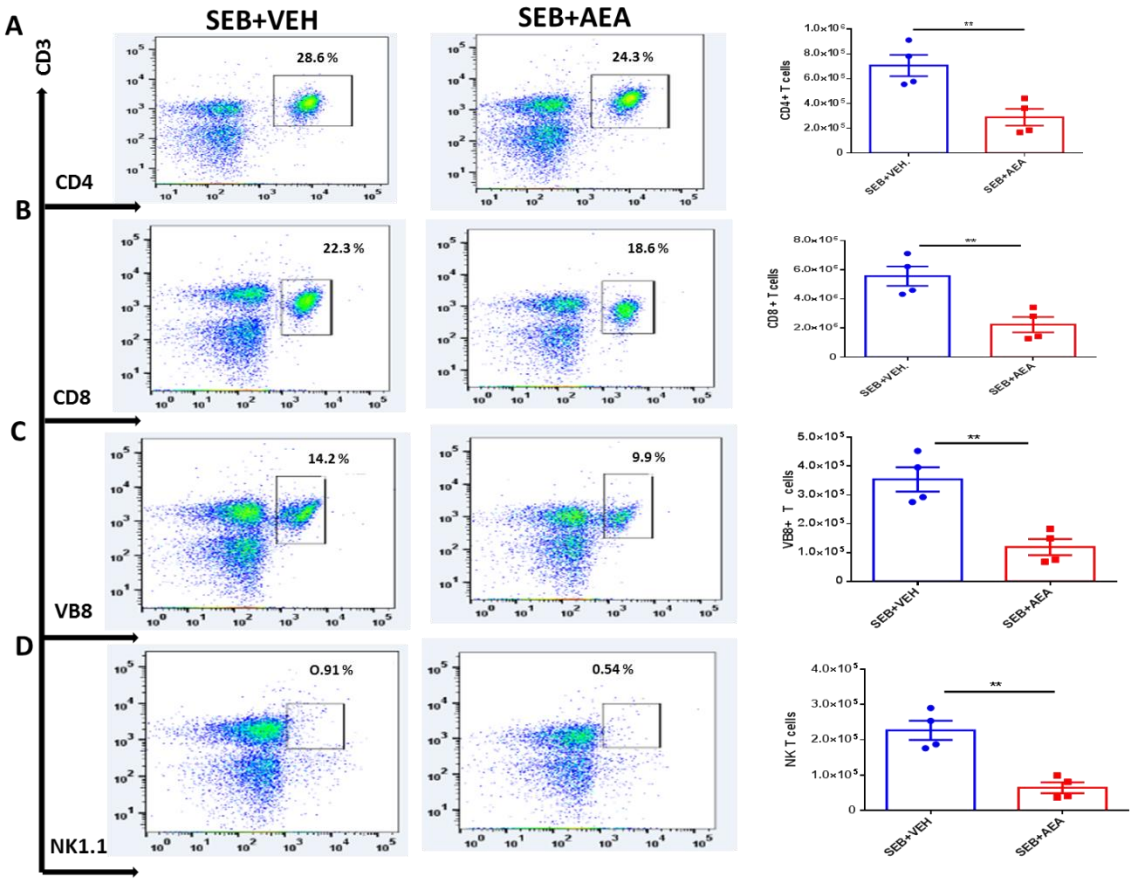

Figure 3. 3: AEA decreases T cell subpopulations in the MLN. Mice were treated with SEB and AEA as described in Fig 1 legend. Each panel shows a representative experiment depicting MLN analyzed for percentages of various T cell markers. The data on total cellularity from 5 mice/group is presented in the form of vertical bars with Mean+/-SEM. (A) CD3+CD4+ T cells (B) CD3+CD8+ T cells, (C) CD3+Vβ8+ T cells, (D) CD3+NK1.1+ cells. Five mice in each group were used and the data was confirmed in three independent experiments. *p≤ 0.05, p**≤ 0.01, ***p≤ 0.001.

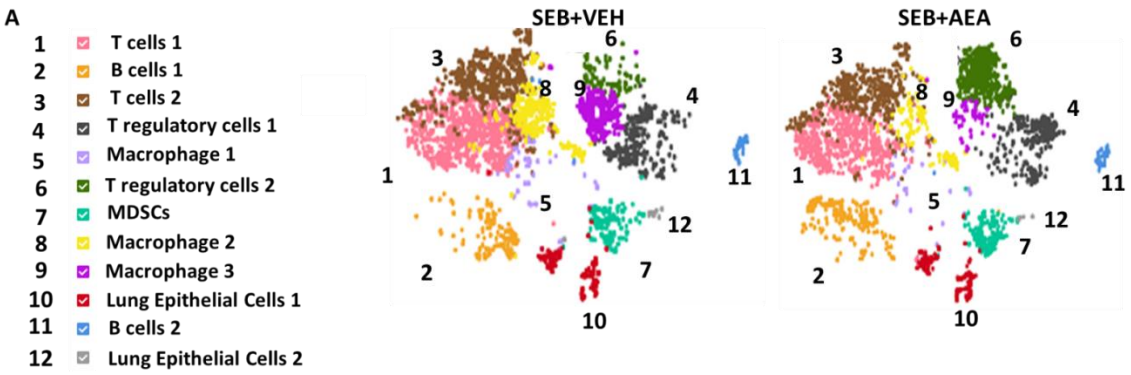

Figure 3. 4: AEA-mediated induction of AMPs and tight junction proteins during ARDS, analyzed using scRNA-Seq of the lungs and qRT-PCR. Mice were treated with SEB and AEA as described in Fig 1 legend. (A) Different types of cell clusters in the lungs of SEB+VEH and SEB+AEA mice. The cells were classified based on markers as follows: Panel (A) 1) T cells 1 (CD3 +,CD8+,CD44+,Trbc1) , 2) B cells1 (CD19+,CD38,PAX5), 3) T cells 2 (CD3+,Trbc2, CD8+, IFNG,Trbc1), 4) T regulatory cells 1 (CD4+, SATB1+, FOXP3+, MAF+, SELL +, CLTA4+,STAT5B, IKZf2, Lag3, Nt5e), 5) Macrophage 1 (F4/80, Fth,Ftl,CD68), 6) T regulatory cells 2 (CD4+ SATB1,MAF+, SELL +, CLTA4+, STAT5B, IKZf2,CCr4,Gata3), 7)Myeloid Derived Suppressor Cells (MDSCs) (CD11B+,GR1+,ARG1+,LY6C+), 8) Macrophage 2 (F4/80, Fth, Ftl, Siglec F), 9) Macrophage 3 (F4/80), 10) Lung Epithelial cells1 (TAP1+, TAP2+, SLPI+, Lyz2+,MBD2, LTF, CDH1, CLDN1), 11) B cells 2 (CD19+,PAX5), 12) Lung Epithelial cells2 (TAP2+, SLPI+, Lyz2+,MBD2, EPCAM+, CDH1). Panels B-G represent various molecules studied on epithelial cells from the lungs using scRNA-Seq (upper panels) and validated using qRT-PCR (lower panels). The qRT-PCR data was obtained from 5 mice. *p≤ 0.05, p**≤ 0.01, ***p≤ 0.001.

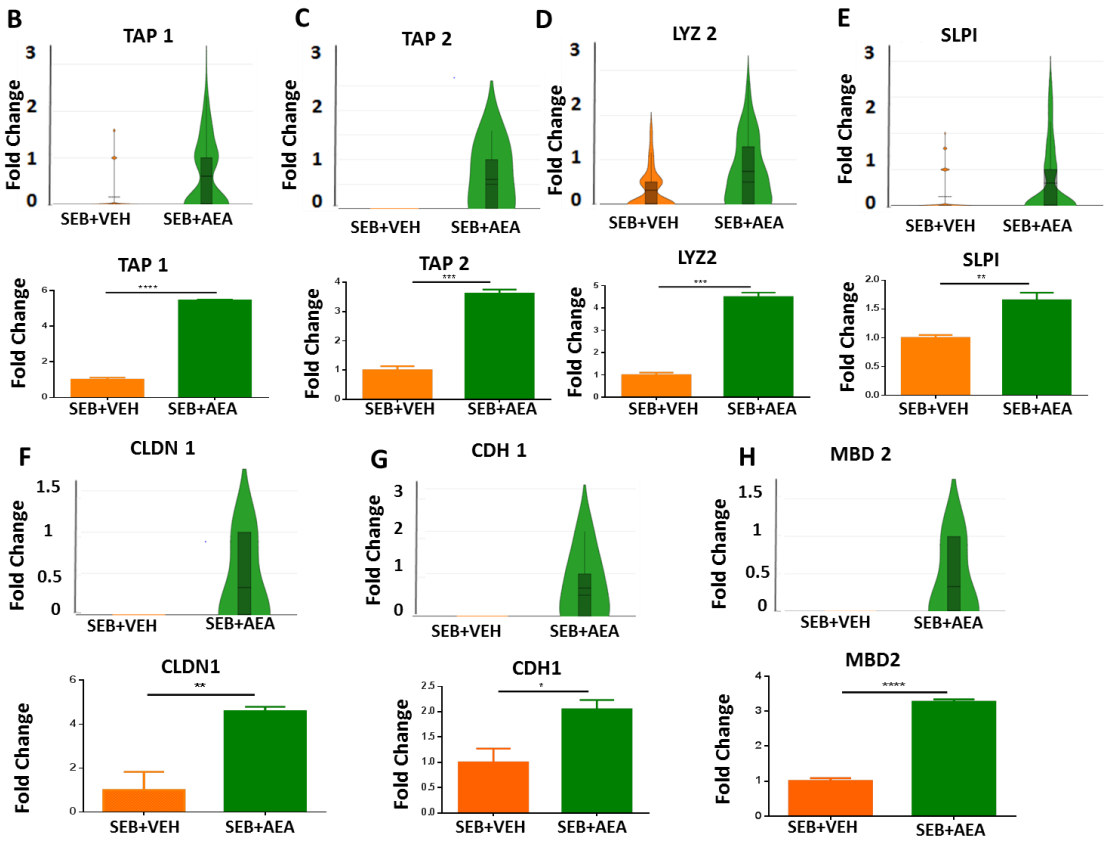

Figure 3.4: AEA-mediated induction of AMPs and tight junction proteins during ARDS, analyzed using scRNA-Seq of the lungs and qRT-PCR. Mice were treated with SEB and AEA as described in Fig 1 legend. (A) Different types of cell clusters in the lungs of SEB+VEH and SEB+AEA mice. The cells were classified based on markers as follows: Panel (A) 1) T cells 1 (CD3 +,CD8+,CD44+,Trbc1) , 2) B cells1 (CD19+,CD38,PAX5), 3) T cells 2 (CD3+,Trbc2, CD8+, IFNG,Trbc1), 4) T regulatory cells 1 (CD4+, SATB1+, FOXP3+, MAF+, SELL +, CLTA4+,STAT5B, IKZf2, Lag3, Nt5e), 5) Macrophage 1 (F4/80, Fth,Ftl,CD68), 6) T regulatory cells 2 (CD4+ SATB1,MAF+, SELL +, CLTA4+, STAT5B, IKZf2,CCr4,Gata3), 7)Myeloid Derived Suppressor Cells (MDSCs) (CD11B+,GR1+,ARG1+,LY6C+), 8) Macrophage 2 (F4/80, Fth, Ftl, Siglec F), 9) Macrophage 3 (F4/80), 10) Lung Epithelial cells1 (TAP1+, TAP2+, SLPI+, Lyz2+,MBD2, LTF, CDH1, CLDN1), 11) B cells 2 (CD19+,PAX5), 12) Lung Epithelial cells2 (TAP2+, SLPI+, Lyz2+,MBD2, EPCAM+, CDH1). Panels B-G represent various molecules studied on epithelial cells from the lungs using scRNA-Seq (upper panels) and validated using qRT-PCR (lower panels). The qRT-PCR data was obtained from 5 mice. *p≤ 0.05, p**≤ 0.01, ***p≤ 0.001.

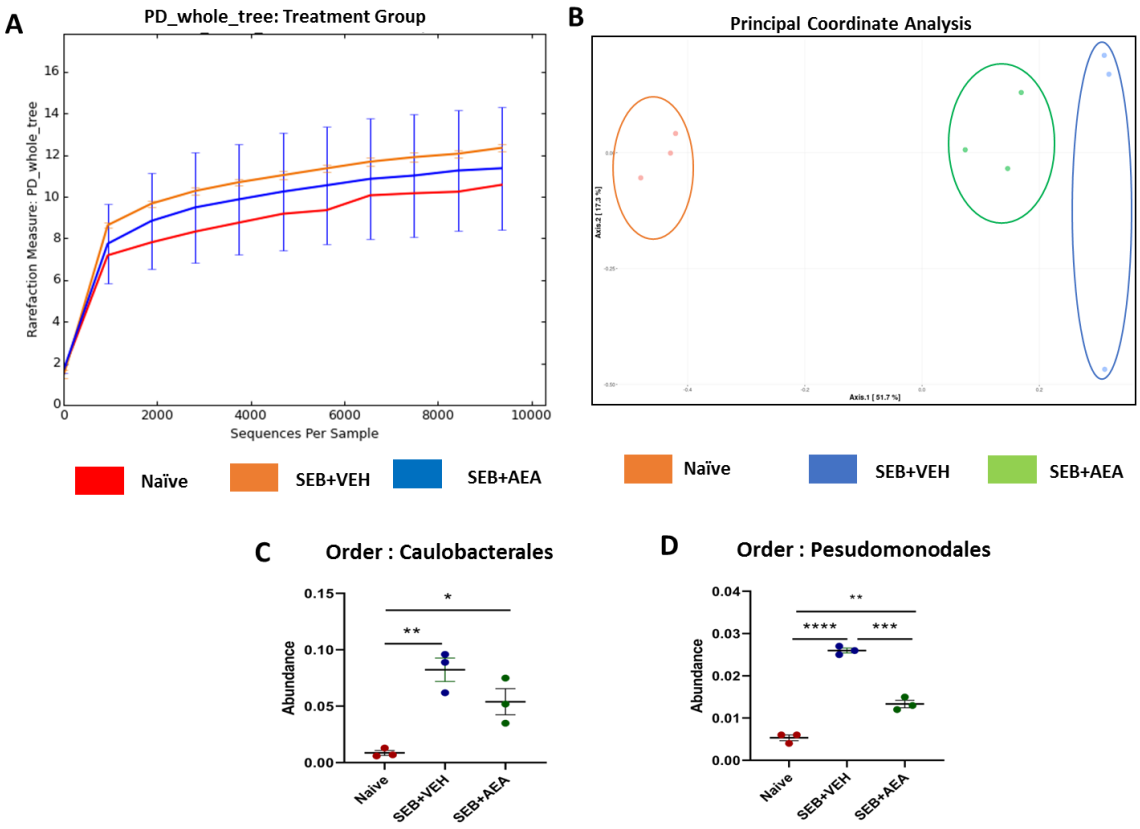

Figure 3. 5: The role of AEA on the abundance of microbiota in the lungs of ARDS induced by SEB. Mice were treated with SEB and AEA as described in Fig 1 legend. The lungs were collected and 16S rRNA sequencing and using Nephele platform were used to analyze and generate: (A) Rarefaction curves depicting alpha diversity within groups (Chao1 index). (B) Principal coordinate analysis which reveals the clustering of bacteria in lungs based on their 16S rRNA content similarity. Graph prism was used to analyze the abundancy of microbiome in panels C and D. We used 3 mice for each group and one way ANOVA was applied for the statistics. *p≤ 0.05, p**≤ 0.01, ***p≤ 0.001.

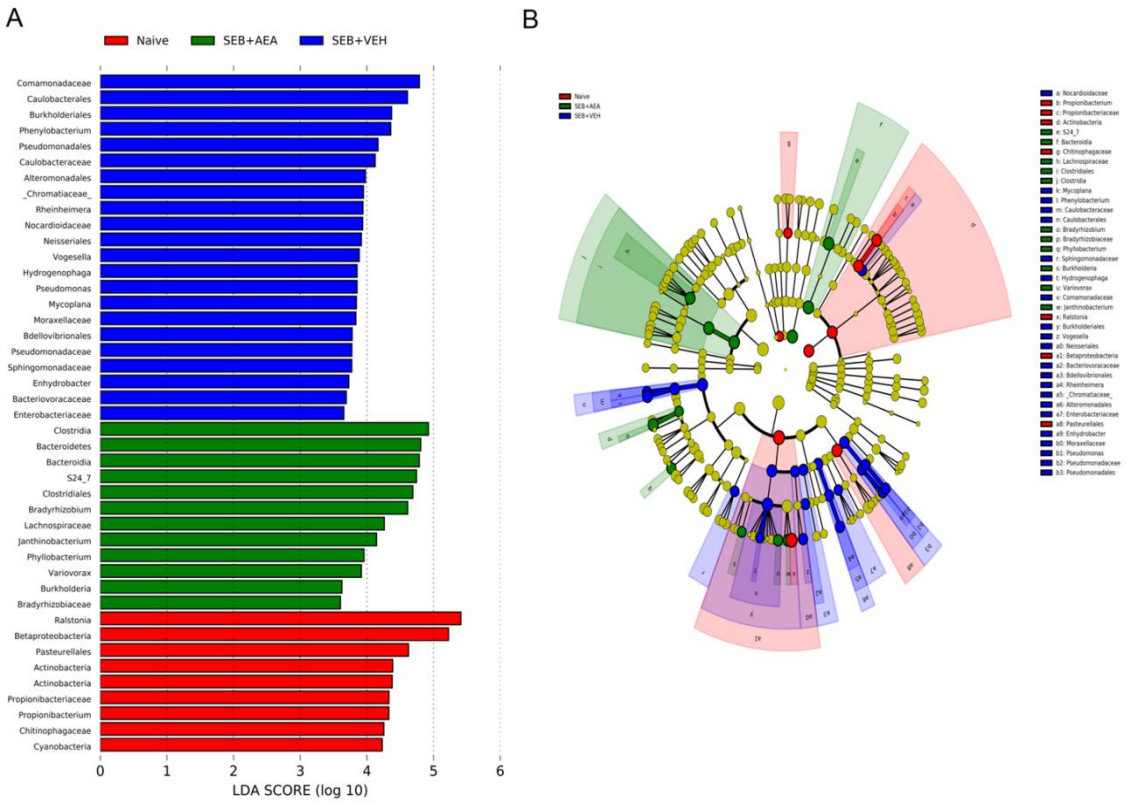

Figure 3. 6: Linear discriminant analysis of effect size (LefSE) in the lungs. (A) LefSE-generated linear discrimination analysis (LDA) scores for differentially expressed taxa. (B) LeFSE-generated cladogram for operational taxonomic units (OTUs) showing phylum, class, order, family, genus and species from outer to inner swirl. For LefSe data, the alpha factorial Kruskal-Wallis test among classes was set to 0.05, and the threshold on the logarithmic LDA score for discriminative features was set at 3.

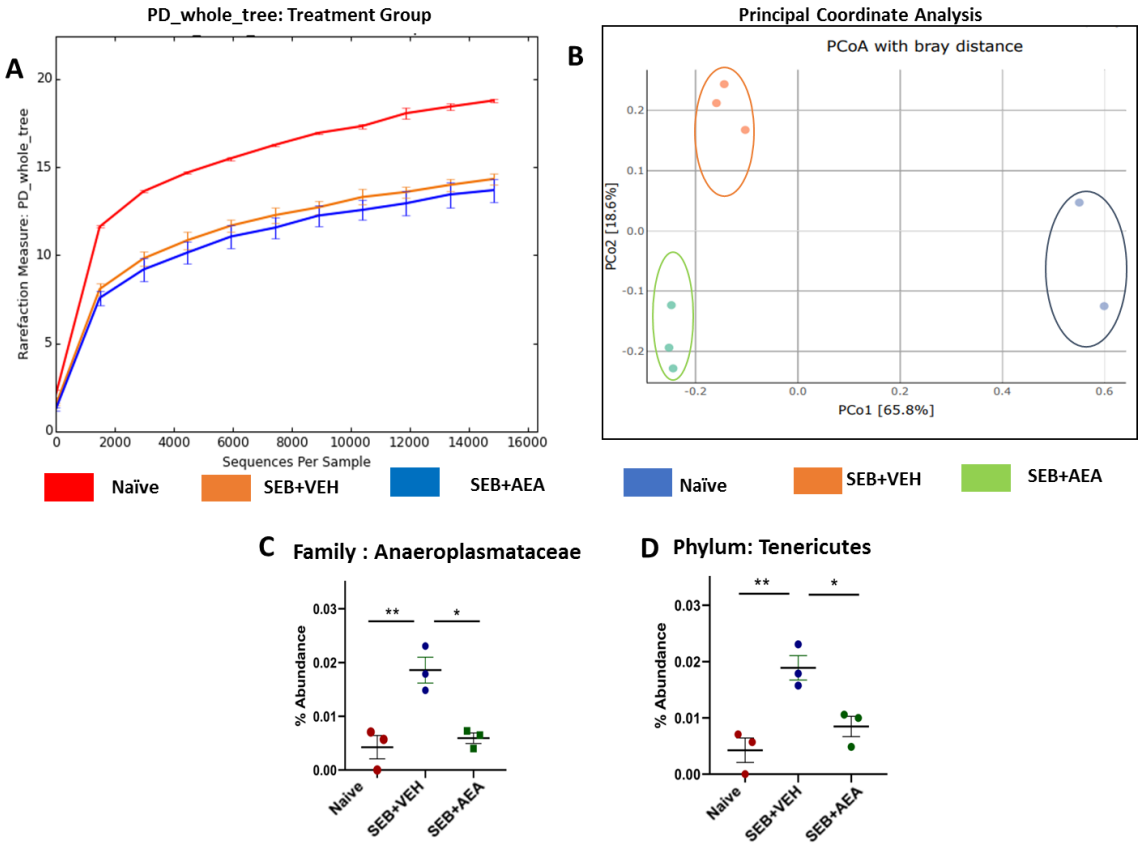

Figure 3. 7: Effect of AEA on the abundance of microbiota in colon/cecal flush of mice with SEB-mediated ARDS. Mice were treated with SEB and AEA as described in Fig 1 legend. The samples of cecal flush were collected and using 16S rRNA sequencing and Nephele platform, data were analyzed: (A) Rarefaction curves depicting alpha diversity within groups (Chao1 index). (B) Principal coordinate analysis which reveals the clustering of bacteria in lungs based on their 16S rRNA content similarity. Graph prism was used to analyze the abundancy of microbiome in panels C and D. We used 3 mice for each group and one way ANOVA was applied for the statistics. *p≤ 0.05, p**≤ 0.01, ***p≤ 0.001.

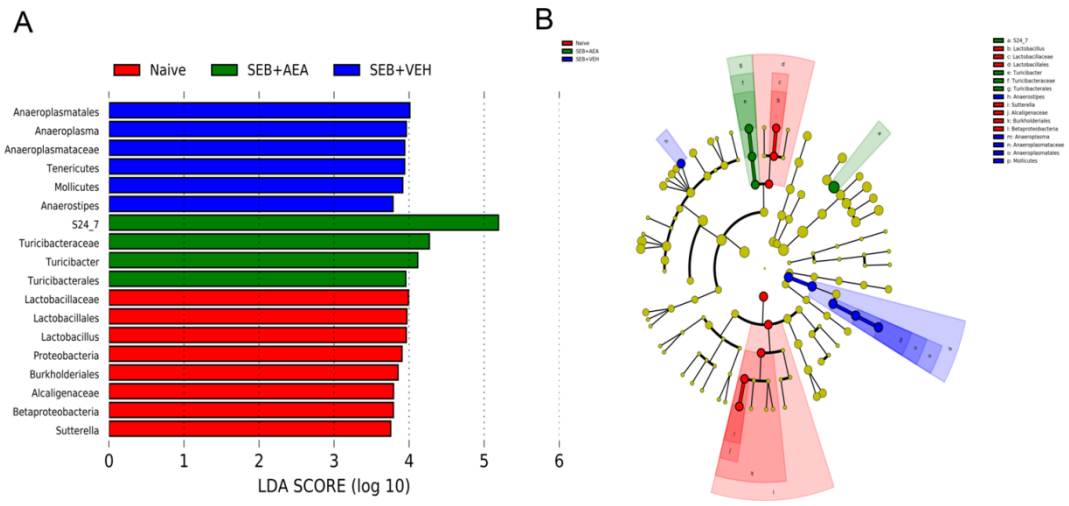

Figure 3. 8: Linear discriminant analysis of effect size (LefSE) in the cecal flush of mice with ARDS. Mice were treated with SEB and AEA as described in Fig 1 legend. (A) LefSE-generated linear discrimination analysis (LDA) scores for differentially expressed taxa. (B) LeFSE-generated cladogram for operational taxonomic units (OTUs) showing phylum, class, order, family, genus and species from outer to inner swirl. For LefSe data, the alpha factorial Kruskal-Wallis test among classes was set to 0.05, and the threshold on the logarithmic LDA score for discriminative features was set at 3.

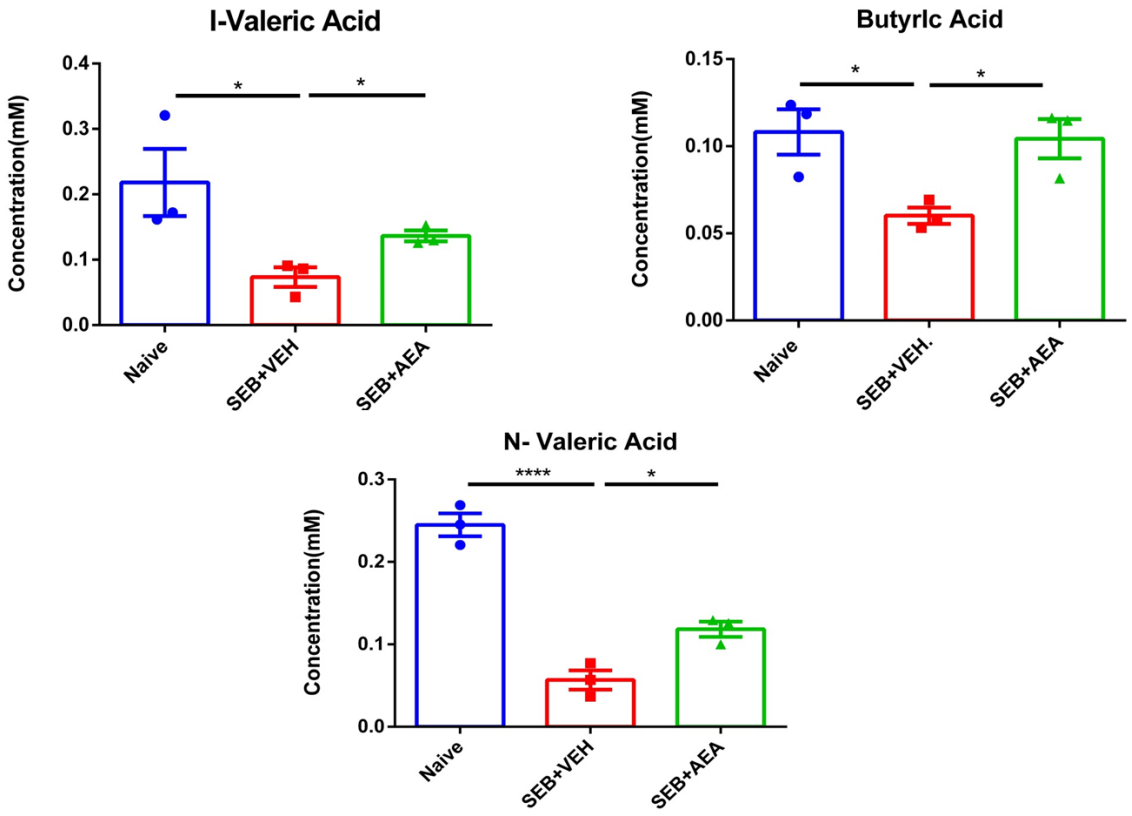

Figure 3. 9: Analysis of SCFAs from cecal flushes of mice with ARDS. Mice were treated with SEB and AEA as described in Fig 1 legend. Concentrations of SCFAs from the cecal flushes were measured. Vertical bars represent mean ± SEM from 3 mice/group and significant differences between groups are shown with asterisks (*p < 0.05, **p < 0.01, ***p < 0.001, ****p < 0.0001) based on one-way ANOVA.

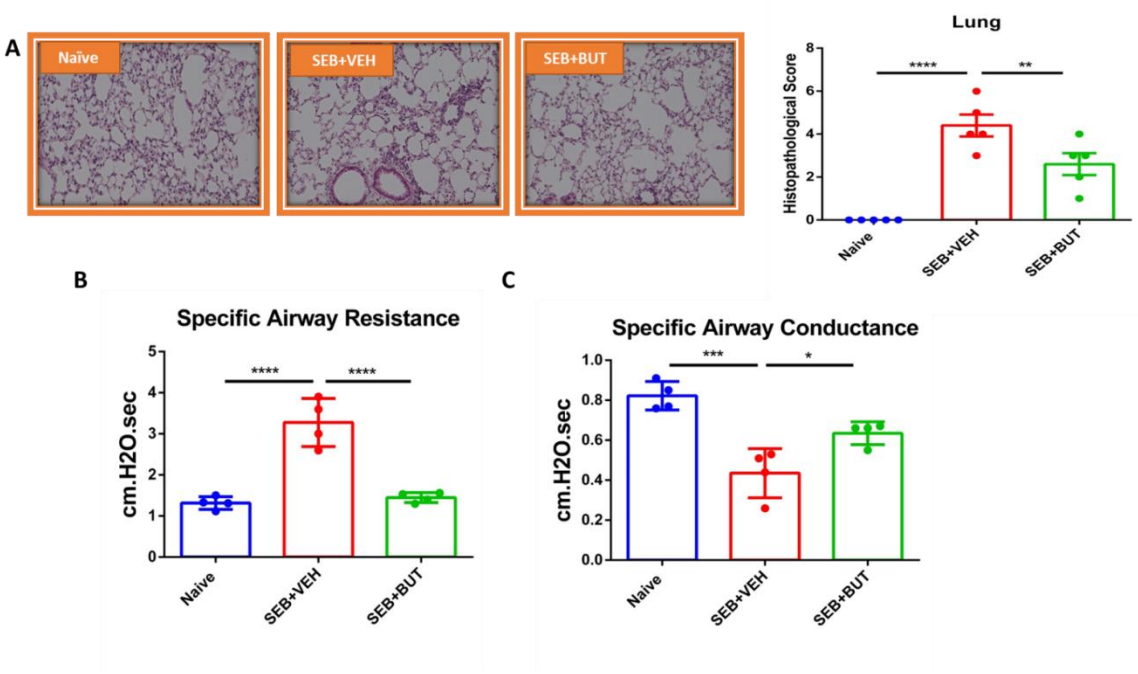

Figure 3. 10: Effect of butyrate on ARDS induced by SEB. On day -1, 0, and 1, mice received 200 mg/kg of butyrate (BUT) or VEH through oral gavage, while SEB in a dose of 50 ug/mouse was given intranasally on day 0. Mice were euthanized on day 2 for various studies (48 hrs after SEB exposure). (A) Representative histopathological images and scores with H & E staining of excised lung tissue. (B) Use of Plethysmography to measure the clinical function of the lung including (B) Specific Airway Resistance and (B) Specific Airway Conductance. Five mice in each group were used and the data confirmed in three independent experiments. *p≤ 0.05, p**≤ 0.01, ***p≤ 0.00.

TABLE 3.1: Primer sequences used for RT-qPCR.

Name of the gene	Primer	Sequence
Tracheal Anti Microbial Peptide 1(TAP1)	Forward	5-GGA CTT GCC TTG TTC CGA GAG-3
	Reverse	5-GCT GCC ACA TAA CTG ATA GCG-3
Tracheal Anti Microbial Peptide2 (TAP2)	Forward	5-CTC CCA CTT TTA GCA GTC CCC-3
	Reverse	5-CTG GCG ATG GCT TTA CTT-3
Secretory Leukocyte Peptidase Inhibitor (SLPI)	Forward	5-TAC GGC ATT GTG GCT TCT CAA-3
	Reverse	5-TAC GGC ATT GTG GCT TCT CAA-3
Lysozyme 2	Forward	5-ATG GAA TGG CTG GCT ACT ATG-G 3
	Reverse	5-ACC AGT ATC GGC TAT TGA TCT GA-3
Claudin 1(CLDN1)	Forward	5-GGG GAC AAC ATC GTG ACC G-3
	Reverse	5-AGG AGT CGA AGA CTT TGC ACT-3
Epithelial Cadherin (ECDH)	Forward	5-CAG GTC TCC TCA TGG CTT TGC -3
	Reverse	5-CTT CCG AAA AGA AGG CTG TCC-3
Murine Beta Defensine 2 (MBD2)	Forward	5-AGA ACA AGG GTA AAC CAG ACC T-3
	Reverse	5-ACT TCA CCT TAT TGC TCG GGT-3

CHAPTER 4

CONCLUSION AND SUMMARY

In the current study, we investigated the role of endogenous cannabinoids, specifically AEA, to attenuate SEB-mediated ARDS. We investigated the role of AEA in the amelioration of ARDS through modulation of microRNAs targeting the inflammatory pathways as well as the role of AEA in the amelioration of ARDS through modulation of the microbiome profile in the gut-lung axis through induction of AMPs and SCFAs

ARDS is characterized by hypoxemia, bilateral pulmonary infiltration, pulmonary edema, and cytokine storm. The current treatment protocols are not effective in controlling ARDS, and only supportive care and mechanical ventilation are the most commonly used clinical options. In December of 2019, the World Health Organization (WHO) declared that COVID-19 had emerged as a pandemic and considered as a significant international threat to human lives. COVID-19 was found to be a highly infectious respiratory disease that caused high rates of mortality in humans due to its ability to trigger ARDS. The United States of America was the epicenter for COVID-19 related ARDS with 18.2 million cases and 322,218 deaths as of December 2020. As of today, while the vaccine has been effective in preventing death, COVID-19 continues to

kill people who are not vaccinated because of the development of ARDS which is challenging to treat. Due to unavailability to find an effective treatment against ARDS, it

is important to investigate an alternative approach. This study presents a novel use of AEA to treat ARDS which was found to be highly efficacious to attenuate ARDS and the cytokine storm. In the current study, we demonstrate for the first time the therapeutic efficacy of AEA in SEB-induced ARDS and identify two critical mechanisms including a role for miRNA and the microbiota.

Our data showed that AEA improved clinical lung functions, reduced immune cell infiltration in the lung tissue, decreased the proinflammatory levels of the cytokines in the sera, and decreased the percentages and absolute cell count of T cell subsets in the lungs and spleen while increasing the percentages of the T regulatory cells and MDSC population, in mice with SEB-mediated ARDS. Mechanistically, AEA significantly modulated the microarray profile of miRNA expression of the lung mononuclear cells which showed significantly downregulated miR 23a-3p that caused an upregulation of Arg1, a marker for MDSCs and upregulation of TGFB2 which induces T regulatory cells. AEA also caused downregulation of miR 34a-5p which caused an upregulation of the FOXP3 gene, a specific marker for Tregs. Transfection of T cells using the mimics and inhibitors of miR 23a-3p and miR 34a-5p confirmed that these miRNA targeted ARG1, TGFB2, and FOXP3, leading to an upregulation of anti-inflammatory genes and induction of anti-inflammatory biomarkers.

The human microbiota consists of trillions of micro-organisms which regulate the immunophysiological homeostasis. The role of gut and lung microbiota during SEB-mediated ARDS and the effect of AEA on microbiota during ARDS has not been investigated before. The current study demonstrated that AEA ameliorated ARDS through modulation of the microbiome profile of the gut-lung axis. AEA significantly decreased the infiltration of the inflammatory cells not only in the lungs but also in the gut. AEA has been decreased the gut leakage and capillary leakage in the lungs. Single Cell RNA Sequencing (Sc-RNA) of the lung tissue revealed that AEA treatment significantly upregulated the induction of AMPs in the lung epithelial cells. Interestingly, our results shown that AMPs such as Tracheal Antimicrobial Peptides 1 and 2 (TAP1, TAP2) were induced by AEA which was associated with a decrease in pathogenic bacteria such as pseudomonas sp during ARDS. Lysozyme 2 is another AMP which also protects against a broad range of gram positive and gram-negative bacteria, and AEA caused upregulation of Lysozyme 2. Serum Leukocyte Protease Inhibitor (SLPI), also known to mediate antimicrobial properties was also induced by AEA. Together, we noted that the AMPs were significantly increased in the airway mucosa specifically by the lung epithelial cells after AEA treatment. Furthermore, Miseq sequencing data of the 16s Ribosomal RNA suggested that AEA modulated the microbiome profile of the gut and lung when compared to the controls to increase butyrate producing bacteria such as S24-7, Lachnospirceae, and Turibacter in both the gut and lungs. Our Lefse analysis confirmed the sequencing of Miseq 16S rRNA. Correlating with the AMP induction by AEA treatment, we also noted the increased abundance of beneficial bacteria and decrease in pathogenic bacteria in the lungs and the gut. The beneficial role of butyrate

was also confirmed by demonstrating that administration of butyrate into SEB-treated mice led to attenuation of the ARDS.

Collectively, our study demonstrates that AEA may play a protective role against ARDS induced by SEB through modulation of miRNA profile of the mononuclear cells in the lung in such a way as to suppress inflammatory pathways. Additionally, AEA also increases the tight junction proteins, and alters the microbiome profile of the gut and lung by promoting AMPs which prevent pathogenic bacteria while increasing the abundance of beneficial bacteria that produce SCFAs such as butyrate which can also suppress ARDS. The current study is highly significant considering that the ongoing pandemic caused by COVID-19 also triggers ARDS, which is challenging to treat. Our studies suggest that administering AEA or enhancing the levels of AEA in vivo through use of FAAH, which hydrolyzes AEA, may serve as novel therapeutic modality to treat ARDS.

REFERENCES

Abdulla, O.A., Neamah, W., Sultan, M., Alghetaa, H.K., Singh, N., Busbee, P.B., Nagarkatti, M., and Nagarkatti, P. (2021a). The Ability of AhR Ligands to Attenuate Delayed Type Hypersensitivity Reaction Is Associated With Alterations in the Gut Microbiota. *Front Immunol* 12**,** 684727.

Abdulla, O.A., Neamah, W., Sultan, M., Chatterjee, S., Singh, N., Nagarkatti, M., and Nagarkatti, P. (2021b). AhR Ligands Differentially Regulate miRNA-132 Which Targets HMGB1 and to Control the Differentiation of Tregs and Th-17 Cells During Delayed-Type Hypersensitivity Response. *Front Immunol* 12**,** 635903.

Abohalaka, R., Bozkurt, T.E., Nemutlu, E., Onder, S.C., and Sahin-Erdemli, I. (2020). The effects of fatty acid amide hydrolase and monoacylglycerol lipase inhibitor treatments on lipopolysaccharide-induced airway inflammation in mice. *Pulm Pharmacol Ther* 62**,** 101920.

Ahmed, I., Rehman, S.U., Shahmohamadnejad, S., Zia, M.A., Ahmad, M., Saeed, M.M., Akram, Z., Iqbal, H.M.N., and Liu, Q. (2021). Therapeutic Attributes of Endocannabinoid System against Neuro-Inflammatory Autoimmune Disorders. *Molecules* 26.

Akgun, E., Caliskan, C., Celik, H.A., Ozutemiz, A.O., Tuncyurek, M., and Aydin, H.H. (2005). Effects of N-acetylcysteine treatment on oxidative stress in acetic acid-induced experimental colitis in rats. *J Int Med Res* 33**,** 196-206.

Akinbi, H.T., Epaud, R., Bhatt, H., and Weaver, T.E. (2000). Bacterial killing is enhanced by expression of lysozyme in the lungs of transgenic mice. *J Immunol* 165**,** 5760-5766.

Al-Ghezi, Z.Z., Miranda, K., Nagarkatti, M., and Nagarkatti, P.S. (2019). Combination of Cannabinoids, Delta9- Tetrahydrocannabinol and Cannabidiol, Ameliorates Experimental Multiple Sclerosis by Suppressing Neuroinflammation Through Regulation of miRNA-Mediated Signaling Pathways. *Front Immunol* 10**,** 1921.

Alam, M.M., and O'neill, L.A. (2011). MicroRNAs and the resolution phase of inflammation in macrophages. *Eur J Immunol* 41**,** 2482-2485.

Alghetaa, H., Mohammed, A., Sultan, M., Busbee, P., Murphy, A., Chatterjee, S., Nagarkatti, M., and Nagarkatti, P. (2018). Resveratrol protects mice against SEB-induced acute lung injury and mortality by miR-193a modulation that targets TGF-beta signalling. *J Cell Mol Med* 22**,** 2644-2655.

Alghetaa, H., Mohammed, A., Zhou, J., Singh, N., Nagarkatti, M., and Nagarkatti, P. (2021). Resveratrol-mediated attenuation of superantigen-driven acute respiratory distress syndrome is mediated by microbiota in the lungs and gut. *Pharmacol Res* 167**,** 105548.

Alrafas, H.R., Busbee, P.B., Nagarkatti, M., and Nagarkatti, P.S. (2020). Resveratrol Downregulates miR-31 to Promote T Regulatory Cells during Prevention of TNBS-Induced Colitis. *Mol Nutr Food Res* 64**,** e1900633.

Amatngalim, G.D., Van Wijck, Y., De Mooij-Eijk, Y., Verhoosel, R.M., Harder, J., Lekkerkerker, A.N., Janssen, R.A., and Hiemstra, P.S. (2015). Basal cells

contribute to innate immunity of the airway epithelium through production of the antimicrobial protein RNase 7. *J Immunol* 194**,** 3340-3350.

Ameri, A. (1999). The effects of cannabinoids on the brain. *Prog Neurobiol* 58**,** 315-348.

Astarita, G., Ahmed, F., and Piomelli, D. (2008). Identification of biosynthetic precursors for the endocannabinoid anandamide in the rat brain. *J Lipid Res* 49**,** 48-57.

Barko, P.C., Mcmichael, M.A., Swanson, K.S., and Williams, D.A. (2018). The Gastrointestinal Microbiome: A Review. *J Vet Intern Med* 32**,** 9-25.

Barrie, N., and Manolios, N. (2017). The endocannabinoid system in pain and inflammation: Its relevance to rheumatic disease. *Eur J Rheumatol* 4**,** 210-218.

Bartel, D.P. (2009). MicroRNAs: target recognition and regulatory functions. *Cell* 136**,** 215-233.

Bartsch, S.M., Ferguson, M.C., Mckinnell, J.A., O'shea, K.J., Wedlock, P.T., Siegmund, S.S., and Lee, B.Y. (2020). The Potential Health Care Costs And Resource Use Associated With COVID-19 In The United States. *Health Aff (Millwood)* 39**,** 927-935.

Becker, W., Alrafas, H.R., Busbee, P.B., Walla, M.D., Wilson, K., Miranda, K., Cai, G., Putluri, V., Putluri, N., Nagarkatti, M., and Nagarkatti, P.S. (2021). Cannabinoid Receptor Activation on Haematopoietic Cells and Enterocytes Protects against Colitis. *J Crohns Colitis* 15**,** 1032-1048.

Becker, W., Alrafas, H.R., Wilson, K., Miranda, K., Culpepper, C., Chatzistamou, I., Cai, G., Nagarkatti, M., and Nagarkatti, P.S. (2020). Activation of Cannabinoid Receptor 2 Prevents Colitis-Associated Colon Cancer through Myeloid Cell De-activation Upstream of IL-22 Production. *iScience* 23**,** 101504.

Becker, W., Nagarkatti, M., and Nagarkatti, P.S. (2018). miR-466a Targeting of TGF-beta2 Contributes to FoxP3(+) Regulatory T Cell Differentiation in a Murine Model of Allogeneic Transplantation. *Front Immunol* 9**,** 688.

Beisswenger, C., and Bals, R. (2005). Antimicrobial peptides in lung inflammation. *Chem Immunol Allergy* 86**,** 55-71.

Bird, L. (2020). MDSC metabolite stuns T cells. *Nat Rev Immunol* 20**,** 352-353.

Buettner, M., and Bode, U. (2012). Lymph node dissection--understanding the immunological function of lymph nodes. *Clin Exp Immunol* 169**,** 205-212.

Busbee, P.B., Menzel, L., Alrafas, H.R., Dopkins, N., Becker, W., Miranda, K., Tang, C., Chatterjee, S., Singh, U., Nagarkatti, M., and Nagarkatti, P.S. (2020). Indole-3-carbinol prevents colitis and associated microbial dysbiosis in an IL-22-dependent manner. *JCI Insight* 5.

Busbee, P.B., Nagarkatti, M., and Nagarkatti, P.S. (2015). Natural indoles, indole-3-carbinol (I3C) and 3,3'-diindolylmethane (DIM), attenuate staphylococcal enterotoxin B-mediated liver injury by downregulating miR-31 expression and promoting caspase-2-mediated apoptosis. *PLoS One* 10**,** e0118506.

Camper, N., Glasgow, A.M., Osbourn, M., Quinn, D.J., Small, D.M., Mclean, D.T., Lundy, F.T., Elborn, J.S., Mcnally, P., Ingram, R.J., Weldon, S., and Taggart, C.C. (2016). A secretory leukocyte protease inhibitor variant with improved activity against lung infection. *Mucosal Immunol* 9**,** 669-676.

Cannell, I.G., Kong, Y.W., and Bushell, M. (2008). How do microRNAs regulate gene expression? *Biochem Soc Trans* 36**,** 1224-1231.

Carthew, R.W., and Sontheimer, E.J. (2009). Origins and Mechanisms of miRNAs and siRNAs. *Cell* 136**,** 642-655.

Chai, L.J., Lu, Z.M., Zhang, X.J., Ma, J., Xu, P.X., Qian, W., Xiao, C., Wang, S.T., Shen, C.H., Shi, J.S., and Zheng-Hong, X. (2019). Zooming in on Butyrate-Producing Clostridial Consortia in the Fermented Grains of Baijiu via Gene Sequence-Guided Microbial Isolation. *Front Microbiol* 10**,** 1397.

Chakravorty, S., Helb, D., Burday, M., Connell, N., and Alland, D. (2007). A detailed analysis of 16S ribosomal RNA gene segments for the diagnosis of pathogenic bacteria. *J Microbiol Methods* 69**,** 330-339.

Chiurchiu, V., Battistini, L., and Maccarrone, M. (2015). Endocannabinoid signalling in innate and adaptive immunity. *Immunology* 144**,** 352-364.

Chiurchiu, V., Rapino, C., Talamonti, E., Leuti, A., Lanuti, M., Gueniche, A., Jourdain, R., Breton, L., and Maccarrone, M. (2016). Anandamide Suppresses Proinflammatory T Cell Responses In Vitro through Type-1 Cannabinoid Receptor-Mediated mTOR Inhibition in Human Keratinocytes. *J Immunol* 197**,** 3545-3553.

Clarke, S.F., Murphy, E.F., Nilaweera, K., Ross, P.R., Shanahan, F., O'toole, P.W., and Cotter, P.D. (2012). The gut microbiota and its relationship to diet and obesity: new insights. *Gut Microbes* 3**,** 186-202.

Confalonieri, M., Salton, F., and Fabiano, F. (2017). Acute respiratory distress syndrome. *Eur Respir Rev* 26.

Costola-De-Souza, C., Ribeiro, A., Ferraz-De-Paula, V., Calefi, A.S., Aloia, T.P., Gimenes-Junior, J.A., De Almeida, V.I., Pinheiro, M.L., and Palermo-Neto, J.

(2013). Monoacylglycerol lipase (MAGL) inhibition attenuates acute lung injury in mice. *PLoS One* 8**,** e77706.

Cristino, L., Bisogno, T., and Di Marzo, V. (2020). Cannabinoids and the expanded endocannabinoid system in neurological disorders. *Nat Rev Neurol* 16**,** 9-29.

Dang, A.T., and Marsland, B.J. (2019). Microbes, metabolites, and the gut-lung axis. *Mucosal Immunol* 12**,** 843-850.

Dasilva, M., Grieve, K.L., Cudeiro, J., and Rivadulla, C. (2014). Anandamide activation of CB1 receptors increases spontaneous bursting and oscillatory activity in the thalamus. *Neuroscience* 265**,** 72-82.

De Cicco, P., Ercolano, G., and Ianaro, A. (2020). The New Era of Cancer Immunotherapy: Targeting Myeloid-Derived Suppressor Cells to Overcome Immune Evasion. *Front Immunol* 11**,** 1680.

De Petrocellis, L., Melck, D., Bisogno, T., Milone, A., and Di Marzo, V. (1999). Finding of the endocannabinoid signalling system in Hydra, a very primitive organism: possible role in the feeding response. *Neuroscience* 92**,** 377-387.

Devane, W.A., Hanus, L., Breuer, A., Pertwee, R.G., Stevenson, L.A., Griffin, G., Gibson, D., Mandelbaum, A., Etinger, A., and Mechoulam, R. (1992). Isolation and structure of a brain constituent that binds to the cannabinoid receptor. *Science* 258**,** 1946-1949.

Di Marzo, V. (2018). New approaches and challenges to targeting the endocannabinoid system. *Nat Rev Drug Discov* 17**,** 623-639.

Diamond, G., Jones, D.E., and Bevins, C.L. (1993). Airway epithelial cells are the site of expression of a mammalian antimicrobial peptide gene. *Proc Natl Acad Sci U S A* 90**,** 4596-4600.

Diamond, G., Zasloff, M., Eck, H., Brasseur, M., Maloy, W.L., and Bevins, C.L. (1991). Tracheal antimicrobial peptide, a cysteine-rich peptide from mammalian tracheal mucosa: peptide isolation and cloning of a cDNA. *Proc Natl Acad Sci U S A* 88**,** 3952-3956.

Diamond, M., Peniston Feliciano, H.L., Sanghavi, D., and Mahapatra, S. (2020). "Acute Respiratory Distress Syndrome," in *StatPearls*. (Treasure Island (FL)).

Do Nascimento, L.E., Amaral, R.R., Ferreira, R., Trindade, D.V.S., Do Nascimento, R.E., Da Costa, T.S., and Souto, R.N.P. (2020). Ants (Hymenoptera: Formicidae) as Potential Mechanical Vectors of Pathogenic Bacteria in a Public Hospital in the Eastern Amazon, Brazil. *J Med Entomol* 57**,** 1619-1626.

Donaldson, G.P., Lee, S.M., and Mazmanian, S.K. (2016). Gut biogeography of the bacterial microbiota. *Nat Rev Microbiol* 14**,** 20-32.

Dopkins, N., Becker, W., Miranda, K., Walla, M., Nagarkatti, P., and Nagarkatti, M. (2020). Tryptamine Attenuates Experimental Multiple Sclerosis Through Activation of Aryl Hydrocarbon Receptor. *Front Pharmacol* 11**,** 619265.

Dumas, A., Bernard, L., Poquet, Y., Lugo-Villarino, G., and Neyrolles, O. (2018). The role of the lung microbiota and the gut-lung axis in respiratory infectious diseases. *Cell Microbiol* 20**,** e12966.

Eggert, T., Dorn, H., Sauter, C., Schmid, G., and Danker-Hopfe, H. (2020). RF-EMF exposure effects on sleep - Age doesn't matter in men! *Environ Res* 191**,** 110173.

Elliott, D.M., Nagarkatti, M., and Nagarkatti, P.S. (2016). 3,39-Diindolylmethane Ameliorates Staphylococcal Enterotoxin B-Induced Acute Lung Injury through Alterations in the Expression of MicroRNA that Target Apoptosis and Cell-Cycle Arrest in Activated T Cells. *J Pharmacol Exp Ther* 357**,** 177-187.

Elliott, D.M., Singh, N., Nagarkatti, M., and Nagarkatti, P.S. (2018). Cannabidiol Attenuates Experimental Autoimmune Encephalomyelitis Model of Multiple Sclerosis Through Induction of Myeloid-Derived Suppressor Cells. *Front Immunol* 9**,** 1782.

Enaud, R., Prevel, R., Ciarlo, E., Beaufils, F., Wieers, G., Guery, B., and Delhaes, L. (2020). The Gut-Lung Axis in Health and Respiratory Diseases: A Place for Inter-Organ and Inter-Kingdom Crosstalks. *Front Cell Infect Microbiol* 10**,** 9.

Fan, E., Brodie, D., and Slutsky, A.S. (2018). Acute Respiratory Distress Syndrome: Advances in Diagnosis and Treatment. *JAMA* 319**,** 698-710.

Fenwick, A.J., Fowler, D.K., Wu, S.W., Shaffer, F.J., Lindberg, J.E.M., Kinch, D.C., and Peters, J.H. (2017). Direct Anandamide Activation of TRPV1 Produces Divergent Calcium and Current Responses. *Front Mol Neurosci* 10**,** 200.

Finn, D.P., Haroutounian, S., Hohmann, A.G., Krane, E., Soliman, N., and Rice, A.S.C. (2021). Cannabinoids, the endocannabinoid system, and pain: a review of preclinical studies. *Pain* 162**,** S5-S25.

Flesch, M., Pernot, M., Provost, J., Ferin, G., Nguyen-Dinh, A., Tanter, M., and Deffieux, T. (2017). 4D in vivo ultrafast ultrasound imaging using a row-column addressed matrix and coherently-compounded orthogonal plane waves. *Phys Med Biol* 62**,** 4571-4588.

Fontenot, J.D., Gavin, M.A., and Rudensky, A.Y. (2003). Foxp3 programs the development and function of CD4+CD25+ regulatory T cells. *Nat Immunol* 4**,** 330-336.

Forman, J.J., Legesse-Miller, A., and Coller, H.A. (2008). A search for conserved sequences in coding regions reveals that the let-7 microRNA targets Dicer within its coding sequence. *Proc Natl Acad Sci U S A* 105**,** 14879-14884.

Fride, E. (2002). Endocannabinoids in the central nervous system--an overview. *Prostaglandins Leukot Essent Fatty Acids* 66**,** 221-233.

Fries, B.C., and Varshney, A.K. (2013). Bacterial Toxins-Staphylococcal Enterotoxin B. *Microbiol Spectr* 1.

Geitani, R., Moubareck, C.A., Xu, Z., Karam Sarkis, D., and Touqui, L. (2020). Expression and Roles of Antimicrobial Peptides in Innate Defense of Airway Mucosa: Potential Implication in Cystic Fibrosis. *Front Immunol* 11**,** 1198.

Gibson, P.G., Qin, L., and Puah, S.H. (2020). COVID-19 acute respiratory distress syndrome (ARDS): clinical features and differences from typical pre-COVID-19 ARDS. *Med J Aust* 213**,** 54-56 e51.

Grzywa, T.M., Sosnowska, A., Matryba, P., Rydzynska, Z., Jasinski, M., Nowis, D., and Golab, J. (2020). Myeloid Cell-Derived Arginase in Cancer Immune Response. *Front Immunol* 11**,** 938.

Gubernatorova, E.O., Gorshkova, E.A., Polinova, A.I., and Drutskaya, M.S. (2020). IL-6: Relevance for immunopathology of SARS-CoV-2. *Cytokine Growth Factor Rev* 53**,** 13-24.

Guillot, L., Nathan, N., Tabary, O., Thouvenin, G., Le Rouzic, P., Corvol, H., Amselem, S., and Clement, A. (2013). Alveolar epithelial cells: master regulators of lung homeostasis. *Int J Biochem Cell Biol* 45**,** 2568-2573.

Guo, P., Zhang, K., Ma, X., and He, P. (2020). Clostridium species as probiotics: potentials and challenges. *J Anim Sci Biotechnol* 11**,** 24.

Hegde, V.L., Hegde, S., Cravatt, B.F., Hofseth, L.J., Nagarkatti, M., and Nagarkatti, P.S. (2008). Attenuation of experimental autoimmune hepatitis by exogenous and endogenous cannabinoids: involvement of regulatory T cells. *Mol Pharmacol* 74**,** 20-33.

Hegde, V.L., Nagarkatti, M., and Nagarkatti, P.S. (2010). Cannabinoid receptor activation leads to massive mobilization of myeloid-derived suppressor cells with potent immunosuppressive properties. *Eur J Immunol* 40**,** 3358-3371.

Hegde, V.L., Nagarkatti, P.S., and Nagarkatti, M. (2011). Role of myeloid-derived suppressor cells in amelioration of experimental autoimmune hepatitis following activation of TRPV1 receptors by cannabidiol. *PLoS One* 6**,** e18281.

Hegde, V.L., Singh, U.P., Nagarkatti, P.S., and Nagarkatti, M. (2015). Critical Role of Mast Cells and Peroxisome Proliferator-Activated Receptor gamma in the Induction of Myeloid-Derived Suppressor Cells by Marijuana Cannabidiol In Vivo. *J Immunol* 194**,** 5211-5222.

Hiemstra, P.S., Amatngalim, G.D., Van Der Does, A.M., and Taube, C. (2016). Antimicrobial Peptides and Innate Lung Defenses: Role in Infectious and Noninfectious Lung Diseases and Therapeutic Applications. *Chest* 149**,** 545-551.

Hillman, E.T., Lu, H., Yao, T., and Nakatsu, C.H. (2017). Microbial Ecology along the Gastrointestinal Tract. *Microbes Environ* 32**,** 300-313.

Hodgson, S.H., Mansatta, K., Mallett, G., Harris, V., Emary, K.R.W., and Pollard, A.J. (2021). What defines an efficacious COVID-19 vaccine? A review of the challenges assessing the clinical efficacy of vaccines against SARS-CoV-2. *Lancet Infect Dis* 21**,** e26-e35.

Hollmann, A., Martinez, M., Maturana, P., Semorile, L.C., and Maffia, P.C. (2018). Antimicrobial Peptides: Interaction With Model and Biological Membranes and Synergism With Chemical Antibiotics. *Front Chem* 6**,** 204.

Huntzinger, E., and Izaurralde, E. (2011). Gene silencing by microRNAs: contributions of translational repression and mRNA decay. *Nat Rev Genet* 12**,** 99-110.

Im, D.S. (2021). GPR119 and GPR55 as Receptors for Fatty Acid Ethanolamides, Oleoylethanolamide and Palmitoylethanolamide. *Int J Mol Sci* 22.

Ipsaro, J.J., and Joshua-Tor, L. (2015). From guide to target: molecular insights into eukaryotic RNA-interference machinery. *Nat Struct Mol Biol* 22**,** 20-28.

Jackson, A.R., Hegde, V.L., Nagarkatti, P.S., and Nagarkatti, M. (2014a). Characterization of endocannabinoid-mediated induction of myeloid-derived suppressor cells involving mast cells and MCP-1. *J Leukoc Biol* 95**,** 609-619.

Jackson, A.R., Nagarkatti, P., and Nagarkatti, M. (2014b). Anandamide attenuates Th-17 cell-mediated delayed-type hypersensitivity response by triggering IL-10 production and consequent microRNA induction. *PLoS One* 9**,** e93954.

Jaeger, N., Mcdonough, R.T., Rosen, A.L., Hernandez-Leyva, A., Wilson, N.G., Lint, M.A., Russler-Germain, E.V., Chai, J.N., Bacharier, L.B., Hsieh, C.S., and Kau,

A.L. (2020). Airway Microbiota-Host Interactions Regulate Secretory Leukocyte Protease Inhibitor Levels and Influence Allergic Airway Inflammation. *Cell Rep* 33**,** 108331.

Jin, C., Chen, J., Gu, J., and Zhang, W. (2020). Gut-lymph-lung pathway mediates sepsis-induced acute lung injury. *Chin Med J (Engl)* 133**,** 2212-2218.

Justinova, Z., Solinas, M., Tanda, G., Redhi, G.H., and Goldberg, S.R. (2005). The endogenous cannabinoid anandamide and its synthetic analog R(+)-methanandamide are intravenously self-administered by squirrel monkeys. *J Neurosci* 25**,** 5645-5650.

Karnad, A., Alvarez, S., and Berk, S.L. (1987). Enterobacter pneumonia. *South Med J* 80**,** 601-604.

Keely, S., Talley, N.J., and Hansbro, P.M. (2012). Pulmonary-intestinal cross-talk in mucosal inflammatory disease. *Mucosal Immunol* 5**,** 7-18.

Kim, C.H. (2021). Control of lymphocyte functions by gut microbiota-derived short-chain fatty acids. *Cell Mol Immunol* 18**,** 1161-1171.

Konopka, K.E., Nguyen, T., Jentzen, J.M., Rayes, O., Schmidt, C.J., Wilson, A.M., Farver, C.F., and Myers, J.L. (2020). Diffuse alveolar damage (DAD) resulting from coronavirus disease 2019 Infection is Morphologically Indistinguishable from Other Causes of DAD. *Histopathology* 77**,** 570-578.

Krol, J., Loedige, I., and Filipowicz, W. (2010). The widespread regulation of microRNA biogenesis, function and decay. *Nat Rev Genet* 11**,** 597-610.

Lagkouvardos, I., Lesker, T.R., Hitch, T.C.A., Galvez, E.J.C., Smit, N., Neuhaus, K., Wang, J., Baines, J.F., Abt, B., Stecher, B., Overmann, J., Strowig, T., and Clavel,

T. (2019). Sequence and cultivation study of Muribaculaceae reveals novel species, host preference, and functional potential of this yet undescribed family. *Microbiome* 7**,** 28.

Lai, C.C., Wang, C.Y., and Hsueh, P.R. (2020). Co-infections among patients with COVID-19: The need for combination therapy with non-anti-SARS-CoV-2 agents? *J Microbiol Immunol Infect* 53**,** 505-512.

Lang, C., Behnke, H., Bittersohl, J., Eberhart, L., Walthers, E., Sommer, F., Wulf, H., and Geldner, G. (2003). [Special features of intensive care of toxic shock syndrome. Review and case report of a TSST-1 associated toxic-shock syndrome with adult respiratory distress syndrome and multiple organ failure from a staphylococcal panaritium]. *Anaesthesist* 52**,** 805-813.

Li, T., Long, C., Fanning, K.V., and Zou, C. (2020). Studying Effects of Cigarette Smoke on Pseudomonas Infection in Lung Epithelial Cells. *J Vis Exp*.

Li, X., and Ma, X. (2020). Acute respiratory failure in COVID-19: is it "typical" ARDS? *Crit Care* 24**,** 198.

Liu, L., Feng, Y., Wei, L., and Zong, Z. (2021). Genome-Based Taxonomy of Brevundimonas with Reporting Brevundimonas huaxiensis sp. nov. *Microbiol Spectr***,** e0011121.

Liu, Y., Chen, C., Sun, Q., Sun, H., Liu, N., Liu, Q., Ma, J., Wang, P., Hu, C., Wu, J., Ouyang, B., Chen, J., Chen, M., and Guan, X. (2020). Mesenteric Lymph Duct Drainage Attenuates Lung Inflammatory Injury and Inhibits Endothelial Cell Apoptosis in Septic Rats. *Biomed Res Int* 2020**,** 3049302.

Lu, T.X., and Rothenberg, M.E. (2018). MicroRNA. *J Allergy Clin Immunol* 141**,** 1202-1207.

Macfarlane, L.A., and Murphy, P.R. (2010). MicroRNA: Biogenesis, Function and Role in Cancer. *Curr Genomics* 11**,** 537-561.

Mahlapuu, M., Hakansson, J., Ringstad, L., and Bjorn, C. (2016). Antimicrobial Peptides: An Emerging Category of Therapeutic Agents. *Front Cell Infect Microbiol* 6**,** 194.

Malek, N., Popiolek-Barczyk, K., Mika, J., Przewlocka, B., and Starowicz, K. (2015). Anandamide, Acting via CB2 Receptors, Alleviates LPS-Induced Neuroinflammation in Rat Primary Microglial Cultures. *Neural Plast* 2015**,** 130639.

Martin, T.R. (1999). Lung cytokines and ARDS: Roger S. Mitchell Lecture. *Chest* 116**,** 2S-8S.

Matthay, M.A., and Zimmerman, G.A. (2005). Acute lung injury and the acute respiratory distress syndrome: four decades of inquiry into pathogenesis and rational management. *Am J Respir Cell Mol Biol* 33**,** 319-327.

Matute-Bello, G., Downey, G., Moore, B.B., Groshong, S.D., Matthay, M.A., Slutsky, A.S., Kuebler, W.M., and Acute Lung Injury in Animals Study, G. (2011). An official American Thoracic Society workshop report: features and measurements of experimental acute lung injury in animals. *Am J Respir Cell Mol Biol* 44**,** 725-738.

Mcgonagle, D., Sharif, K., O'regan, A., and Bridgewood, C. (2020). The Role of Cytokines including Interleukin-6 in COVID-19 induced Pneumonia and Macrophage Activation Syndrome-Like Disease. *Autoimmun Rev* 19**,** 102537.

Meade, K.G., and O'farrelly, C. (2018). beta-Defensins: Farming the Microbiome for Homeostasis and Health. *Front Immunol* 9**,** 3072.

Mechoulam, R., Ben-Shabat, S., Hanus, L., Ligumsky, M., Kaminski, N.E., Schatz, A.R., Gopher, A., Almog, S., Martin, B.R., Compton, D.R., and Et Al. (1995). Identification of an endogenous 2-monoglyceride, present in canine gut, that binds to cannabinoid receptors. *Biochem Pharmacol* 50**,** 83-90.

Mehrpouya-Bahrami, P., Chitrala, K.N., Ganewatta, M.S., Tang, C., Murphy, E.A., Enos, R.T., Velazquez, K.T., Mccellan, J., Nagarkatti, M., and Nagarkatti, P. (2017). Blockade of CB1 cannabinoid receptor alters gut microbiota and attenuates inflammation and diet-induced obesity. *Sci Rep* 7**,** 15645.

Miethke, T., Wahl, C., Heeg, K., Echtenacher, B., Krammer, P.H., and Wagner, H. (1992). T cell-mediated lethal shock triggered in mice by the superantigen staphylococcal enterotoxin B: critical role of tumor necrosis factor. *J Exp Med* 175**,** 91-98.

Millar, A.A., and Waterhouse, P.M. (2005). Plant and animal microRNAs: similarities and differences. *Funct Integr Genomics* 5**,** 129-135.

Minichino, A., Jackson, M.A., Francesconi, M., Steves, C.J., Menni, C., Burnet, P.W.J., and Lennox, B.R. (2021). Endocannabinoid system mediates the association between gut-microbial diversity and anhedonia/amotivation in a general population cohort. *Mol Psychiatry*.

Moffatt, M.F., and Cookson, W.O. (2017). The lung microbiome in health and disease. *Clin Med (Lond)* 17**,** 525-529.

Mohammed, A., Alghetaa, H., Sultan, M., Singh, N.P., Nagarkatti, P., and Nagarkatti, M. (2020a). Administration of Delta9-Tetrahydrocannabinol (THC) Post-Staphylococcal Enterotoxin B Exposure Protects Mice From Acute Respiratory Distress Syndrome and Toxicity. *Front Pharmacol* 11**,** 893.

Mohammed, A., Alghetaa, H.K., Zhou, J., Chatterjee, S., Nagarkatti, P., and Nagarkatti, M. (2020b). Protective effects of Delta(9) -tetrahydrocannabinol against enterotoxin-induced acute respiratory distress syndrome are mediated by modulation of microbiota. *Br J Pharmacol*.

Mohammed, A., Alghetaa, H.K., Zhou, J., Chatterjee, S., Nagarkatti, P., and Nagarkatti, M. (2020c). Protective effects of Delta(9) -tetrahydrocannabinol against enterotoxin-induced acute respiratory distress syndrome are mediated by modulation of microbiota. *Br J Pharmacol* 177**,** 5078-5095.

Mohammed, A., H, F.K.A., Miranda, K., Wilson, K., N, P.S., Cai, G., Putluri, N., Nagarkatti, P., and Nagarkatti, M. (2020d). Delta9-Tetrahydrocannabinol Prevents Mortality from Acute Respiratory Distress Syndrome through the Induction of Apoptosis in Immune Cells, Leading to Cytokine Storm Suppression. *Int J Mol Sci* 21.

Muller, C., Morales, P., and Reggio, P.H. (2018). Cannabinoid Ligands Targeting TRP Channels. *Front Mol Neurosci* 11**,** 487.

Nagarkatti, P., Miranda, K., and Nagarkatti, M. (2020). Use of Cannabinoids to Treat Acute Respiratory Distress Syndrome and Cytokine Storm Associated with Coronavirus Disease-2019. *Front Pharmacol* 11**,** 589438.

Nagarkatti, P., Pandey, R., Rieder, S.A., Hegde, V.L., and Nagarkatti, M. (2009). Cannabinoids as novel anti-inflammatory drugs. *Future Med Chem* 1**,** 1333-1349.

Nawijn, M.C., Hackett, T.L., Postma, D.S., Van Oosterhout, A.J., and Heijink, I.H. (2011). E-cadherin: gatekeeper of airway mucosa and allergic sensitization. *Trends Immunol* 32**,** 248-255.

Neumann, B., Engelhardt, B., Wagner, H., and Holzmann, B. (1997). Induction of acute inflammatory lung injury by staphylococcal enterotoxin B. *J Immunol* 158**,** 1862-1871.

Newell, K.A., Ellenhorn, J.D., Bruce, D.S., and Bluestone, J.A. (1991). In vivo T-cell activation by staphylococcal enterotoxin B prevents outgrowth of a malignant tumor. *Proc Natl Acad Sci U S A* 88**,** 1074-1078.

O'brien, J., Hayder, H., Zayed, Y., and Peng, C. (2018). Overview of MicroRNA Biogenesis, Mechanisms of Actions, and Circulation. *Front Endocrinol (Lausanne)* 9**,** 402.

O'connell, R.M., Rao, D.S., and Baltimore, D. (2012). microRNA regulation of inflammatory responses. *Annu Rev Immunol* 30**,** 295-312.

O'neill, L.A., Sheedy, F.J., and Mccoy, C.E. (2011). MicroRNAs: the fine-tuners of Toll-like receptor signalling. *Nat Rev Immunol* 11**,** 163-175.

O'sullivan, S.E. (2016). An update on PPAR activation by cannabinoids. *Br J Pharmacol* 173**,** 1899-1910.

Ono, M. (2020). Control of regulatory T-cell differentiation and function by T-cell receptor signalling and Foxp3 transcription factor complexes. *Immunology* 160**,** 24-37.

Ormerod, K.L., Wood, D.L., Lachner, N., Gellatly, S.L., Daly, J.N., Parsons, J.D., Dal'molin, C.G., Palfreyman, R.W., Nielsen, L.K., Cooper, M.A., Morrison, M., Hansbro, P.M., and Hugenholtz, P. (2016). Genomic characterization of the uncultured Bacteroidales family S24-7 inhabiting the guts of homeothermic animals. *Microbiome* 4**,** 36.

Osafo, N., Yeboah, O.K., and Antwi, A.O. (2021). Endocannabinoid system and its modulation of brain, gut, joint and skin inflammation. *Mol Biol Rep* 48**,** 3665-3680.

Ostrand-Rosenberg, S., and Fenselau, C. (2018). Myeloid-Derived Suppressor Cells: Immune-Suppressive Cells That Impair Antitumor Immunity and Are Sculpted by Their Environment. *J Immunol* 200**,** 422-431.

Pacher, P., Batkai, S., and Kunos, G. (2006). The endocannabinoid system as an emerging target of pharmacotherapy. *Pharmacol Rev* 58**,** 389-462.

Pandey, R., Mousawy, K., Nagarkatti, M., and Nagarkatti, P. (2009). Endocannabinoids and immune regulation. *Pharmacol Res* 60**,** 85-92.

Park, M.J., Lee, S.H., Kim, E.K., Lee, E.J., Baek, J.A., Park, S.H., Kwok, S.K., and Cho, M.L. (2018). Interleukin-10 produced by myeloid-derived suppressor cells is critical for the induction of Tregs and attenuation of rheumatoid inflammation in mice. *Sci Rep* 8**,** 3753.

Patterson, L.L., Byerly, C.D., and Mcbride, J.W. (2021). Anaplasmataceae: Dichotomous Autophagic Interplay for Infection. *Front Immunol* 12**,** 642771.

Pertwee, R.G. (2015). Endocannabinoids and Their Pharmacological Actions. *Handb Exp Pharmacol* 231**,** 1-37.

Pfalzgraff, A., Brandenburg, K., and Weindl, G. (2018). Antimicrobial Peptides and Their Therapeutic Potential for Bacterial Skin Infections and Wounds. *Front Pharmacol* 9**,** 281.

Pinchuk, I.V., Beswick, E.J., and Reyes, V.E. (2010). Staphylococcal enterotoxins. *Toxins (Basel)* 2**,** 2177-2197.

Post, S., Heijink, I.H., Hesse, L., Koo, H.K., Shaheen, F., Fouadi, M., Kuchibhotla, V.N.S., Lambrecht, B.N., Van Oosterhout, A.J.M., Hackett, T.L., and Nawijn, M.C. (2018). Characterization of a lung epithelium specific E-cadherin knock-out model: Implications for obstructive lung pathology. *Sci Rep* 8**,** 13275.

Rahman, S.M.K., Uyama, T., Hussain, Z., and Ueda, N. (2021). Roles of Endocannabinoids and Endocannabinoid-like Molecules in Energy Homeostasis and Metabolic Regulation: A Nutritional Perspective. *Annu Rev Nutr*.

Rao, R., Nagarkatti, P., and Nagarkatti, M. (2015a). Role of miRNA in the regulation of inflammatory genes in staphylococcal enterotoxin B-induced acute inflammatory lung injury and mortality. *Toxicol Sci* 144**,** 284-297.

Rao, R., Nagarkatti, P.S., and Nagarkatti, M. (2015b). Delta(9) Tetrahydrocannabinol attenuates Staphylococcal enterotoxin B-induced inflammatory lung injury and prevents mortality in mice by modulation of miR-17-92 cluster and induction of T-regulatory cells. *Br J Pharmacol* 172**,** 1792-1806.

Rao, R., Rieder, S.A., Nagarkatti, P., and Nagarkatti, M. (2014). Staphylococcal enterotoxin B-induced microRNA-155 targets SOCS1 to promote acute inflammatory lung injury. *Infect Immun* 82**,** 2971-2979.

Ratajczak, W., Ryl, A., Mizerski, A., Walczakiewicz, K., Sipak, O., and Laszczynska, M. (2019). Immunomodulatory potential of gut microbiome-derived short-chain fatty acids (SCFAs). *Acta Biochim Pol* 66**,** 1-12.

Rieder, S.A., Nagarkatti, P., and Nagarkatti, M. (2011). CD1d-independent activation of invariant natural killer T cells by staphylococcal enterotoxin B through major histocompatibility complex class II/T cell receptor interaction results in acute lung injury. *Infect Immun* 79**,** 3141-3148.

Rieder, S.A., Nagarkatti, P., and Nagarkatti, M. (2012). Multiple anti-inflammatory pathways triggered by resveratrol lead to amelioration of staphylococcal enterotoxin B-induced lung injury. *Br J Pharmacol* 167**,** 1244-1258.

Rozynska, R., and Plusa, T. (2015). [Intoxications caused by Staphylococcal enterotoxin B]. *Pol Merkur Lekarski* 39**,** 165-166.

Rubenfeld, G.D., Caldwell, E., Peabody, E., Weaver, J., Martin, D.P., Neff, M., Stern, E.J., and Hudson, L.D. (2005). Incidence and outcomes of acute lung injury. *N Engl J Med* 353**,** 1685-1693.

Schlingmann, B., Molina, S.A., and Koval, M. (2015). Claudins: Gatekeepers of lung epithelial function. *Semin Cell Dev Biol* 42**,** 47-57.

Schneeberger, E.E., and Lynch, R.D. (2004). The tight junction: a multifunctional complex. *Am J Physiol Cell Physiol* 286**,** C1213-1228.

Shamran, H., Singh, N.P., Zumbrun, E.E., Murphy, A., Taub, D.D., Mishra, M.K., Price, R.L., Chatterjee, S., Nagarkatti, M., Nagarkatti, P.S., and Singh, U.P. (2017). Fatty acid amide hydrolase (FAAH) blockade ameliorates experimental colitis by

altering microRNA expression and suppressing inflammation. *Brain Behav Immun* 59**,** 10-20.

Sharir, H., Console-Bram, L., Mundy, C., Popoff, S.N., Kapur, A., and Abood, M.E. (2012). The endocannabinoids anandamide and virodhamine modulate the activity of the candidate cannabinoid receptor GPR55. *J Neuroimmune Pharmacol* 7**,** 856-865.

Shreiner, A.B., Kao, J.Y., and Young, V.B. (2015). The gut microbiome in health and in disease. *Curr Opin Gastroenterol* 31**,** 69-75.

Si, X., Cao, D., Chen, J., Nie, Y., Jiang, Z., Chen, M.Y., Wu, J.F., and Guan, X.D. (2018). miR23a downregulation modulates the inflammatory response by targeting ATG12mediated autophagy. *Mol Med Rep* 18**,** 1524-1530.

Sido, J.M., Nagarkatti, P.S., and Nagarkatti, M. (2015a). Delta(9)-Tetrahydrocannabinol attenuates allogeneic host-versus-graft response and delays skin graft rejection through activation of cannabinoid receptor 1 and induction of myeloid-derived suppressor cells. *J Leukoc Biol* 98**,** 435-447.

Sido, J.M., Nagarkatti, P.S., and Nagarkatti, M. (2015b). Role of Endocannabinoid Activation of Peripheral CB1 Receptors in the Regulation of Autoimmune Disease. *Int Rev Immunol* 34**,** 403-414.

Sido, J.M., Nagarkatti, P.S., and Nagarkatti, M. (2016). Production of endocannabinoids by activated T cells and B cells modulates inflammation associated with delayed-type hypersensitivity. *Eur J Immunol* 46**,** 1472-1479.

Silver, A., Gangopadhyay, A., Gawarkiewicz, G., Silva, E.N.S., and Clark, J. (2021). Interannual and seasonal asymmetries in Gulf Stream Ring Formations from 1980 to 2019. *Sci Rep* 11**,** 2207.

Singh, N.P., Abbas, I.K., Menard, M., Singh, U.P., Zhang, J., Nagarkatti, P., and Nagarkatti, M. (2015). Exposure to diethylstilbestrol during pregnancy modulates microRNA expression profile in mothers and fetuses reflecting oncogenic and immunological changes. *Mol Pharmacol* 87**,** 842-854.

Skennerton, C.T., Haroon, M.F., Briegel, A., Shi, J., Jensen, G.J., Tyson, G.W., and Orphan, V.J. (2016). Phylogenomic analysis of Candidatus 'Izimaplasma' species: free-living representatives from a Tenericutes clade found in methane seeps. *ISME J* 10**,** 2679-2692.

Smith, B.J., Miller, R.A., Ericsson, A.C., Harrison, D.C., Strong, R., and Schmidt, T.M. (2019). Changes in the gut microbiome and fermentation products concurrent with enhanced longevity in acarbose-treated mice. *BMC Microbiol* 19**,** 130.

Smith, P.B., Compton, D.R., Welch, S.P., Razdan, R.K., Mechoulam, R., and Martin, B.R. (1994). The pharmacological activity of anandamide, a putative endogenous cannabinoid, in mice. *J Pharmacol Exp Ther* 270**,** 219-227.

Steckbeck, J.D., Deslouches, B., and Montelaro, R.C. (2014). Antimicrobial peptides: new drugs for bad bugs? *Expert Opin Biol Ther* 14**,** 11-14.

Sultan, M., Alghetaa, H., Mohammed, A., Abdulla, O.A., Wisniewski, P.J., Singh, N., Nagarkatti, P., and Nagarkatti, M. (2021). The Endocannabinoid Anandamide Attenuates Acute Respiratory Distress Syndrome by Downregulating miRNA that Target Inflammatory Pathways. *Front Pharmacol* 12**,** 644281.

Swaroopa, D., Bhaskar, K., Mahathi, T., Katkam, S., Raju, Y.S., Chandra, N., and Kutala, V.K. (2016). Association of serum interleukin-6, interleukin-8, and Acute Physiology and Chronic Health Evaluation II score with clinical outcome in patients with acute respiratory distress syndrome. *Indian J Crit Care Med* 20**,** 518-525.

Tahamtan, A., Teymoori-Rad, M., Nakstad, B., and Salimi, V. (2018). Anti-Inflammatory MicroRNAs and Their Potential for Inflammatory Diseases Treatment. *Front Immunol* 9**,** 1377.

Tan, J., Mckenzie, C., Potamitis, M., Thorburn, A.N., Mackay, C.R., and Macia, L. (2014). The role of short-chain fatty acids in health and disease. *Adv Immunol* 121**,** 91-119.

Taub, D.D., and Rogers, T.J. (1992). Direct activation of murine T cells by staphylococcal enterotoxins. *Cell Immunol* 140**,** 267-281.

Tejman-Yarden, N., Robinson, A., Davidov, Y., Shulman, A., Varvak, A., Reyes, F., Rahav, G., and Nissan, I. (2019). Delftibactin-A, a Non-ribosomal Peptide With Broad Antimicrobial Activity. *Front Microbiol* 10**,** 2377.

Thornton Snider, J., Romley, J.A., Wong, K.S., Zhang, J., Eber, M., and Goldman, D.P. (2012). The Disability burden of COPD. *COPD* 9**,** 513-521.

Tomar, S., Zumbrun, E.E., Nagarkatti, M., and Nagarkatti, P.S. (2015). Protective role of cannabinoid receptor 2 activation in galactosamine/lipopolysaccharide-induced acute liver failure through regulation of macrophage polarization and microRNAs. *J Pharmacol Exp Ther* 353**,** 369-379.

Toriyama, S. (1992). [Viruses and ambisense RNA genomes of tenuivirus]. *Tanpakushitsu Kakusan Koso* 37**,** 2467-2473.

Tsitsiou, E., and Lindsay, M.A. (2009). microRNAs and the immune response. *Curr Opin Pharmacol* 9**,** 514-520.

Tumurkhuu, G., Koide, N., Dagvadorj, J., Morikawa, A., Hassan, F., Islam, S., Naiki, Y., Mori, I., Yoshida, T., and Yokochi, T. (2008). The mechanism of development of acute lung injury in lethal endotoxic shock using alpha-galactosylceramide sensitization. *Clin Exp Immunol* 152**,** 182-191.

Turner, J.R. (2006). Molecular basis of epithelial barrier regulation: from basic mechanisms to clinical application. *Am J Pathol* 169**,** 1901-1909.

Umbrello, M., Formenti, P., Bolgiaghi, L., and Chiumello, D. (2016). Current Concepts of ARDS: A Narrative Review. *Int J Mol Sci* 18.

Vacca, M., Celano, G., Calabrese, F.M., Portincasa, P., Gobbetti, M., and De Angelis, M. (2020). The Controversial Role of Human Gut Lachnospiraceae. *Microorganisms* 8.

Van Egmond, N., Straub, V.M., and Van Der Stelt, M. (2021). Targeting Endocannabinoid Signaling: FAAH and MAG Lipase Inhibitors. *Annu Rev Pharmacol Toxicol* 61**,** 441-463.

Verreault, D., Ennis, J., Whaley, K., Killeen, S.Z., Karauzum, H., Aman, M.J., Holtsberg, R., Doyle-Meyers, L., Didier, P.J., Zeitlin, L., and Roy, C.J. (2019). Effective Treatment of Staphylococcal Enterotoxin B Aerosol Intoxication in Rhesus Macaques by Using Two Parenterally Administered High-Affinity Monoclonal Antibodies. *Antimicrob Agents Chemother* 63.

Von Baum, H., Welte, T., Marre, R., Suttorp, N., Ewig, S., and Group, C.S. (2010). Community-acquired pneumonia through Enterobacteriaceae and Pseudomonas aeruginosa: Diagnosis, incidence and predictors. *Eur Respir J* 35**,** 598-605.

Voshaar, T., Stais, P., Kohler, D., and Dellweg, D. (2021). Conservative management of COVID-19 associated hypoxaemia. *ERJ Open Res* 7.

Walker, J.M., and Huang, S.M. (2002). Endocannabinoids in pain modulation. *Prostaglandins Leukot Essent Fatty Acids* 66**,** 235-242.

Weldon, S., Mcnally, P., Mcelvaney, N.G., Elborn, J.S., Mcauley, D.F., Wartelle, J., Belaaouaj, A., Levine, R.L., and Taggart, C.C. (2009). Decreased levels of secretory leucoprotease inhibitor in the Pseudomonas-infected cystic fibrosis lung are due to neutrophil elastase degradation. *J Immunol* 183**,** 8148-8156.

Wu, K., Xiu, Y., Zhou, P., Qiu, Y., and Li, Y. (2019). A New Use for an Old Drug: Carmofur Attenuates Lipopolysaccharide (LPS)-Induced Acute Lung Injury via Inhibition of FAAH and NAAA Activities. *Front Pharmacol* 10**,** 818.

Wu, Y., Li, D., Wang, Y., Liu, X., Zhang, Y., Qu, W., Chen, K., Francisco, N.M., Feng, L., Huang, X., and Wu, M. (2018). Beta-Defensin 2 and 3 Promote Bacterial Clearance of Pseudomonas aeruginosa by Inhibiting Macrophage Autophagy through Downregulation of Early Growth Response Gene-1 and c-FOS. *Front Immunol* 9**,** 211.

Yang, Z., Guo, J., Weng, L., Tang, W., Jin, S., and Ma, W. (2020). Myeloid-derived suppressor cells-new and exciting players in lung cancer. *J Hematol Oncol* 13**,** 10.

Zhang, D., Li, S., Wang, N., Tan, H.Y., Zhang, Z., and Feng, Y. (2020). The Cross-Talk Between Gut Microbiota and Lungs in Common Lung Diseases. *Front Microbiol* 11**,** 301.

Zhang, J., Zhou, W., Liu, Y., Liu, T., Li, C., and Wang, L. (2018). Oncogenic role of microRNA-532-5p in human colorectal cancer via targeting of the 5'UTR of RUNX3. *Oncol Lett* 15**,** 7215-7220.

Zhao, Y., Ridge, K., and Zhao, J. (2017). Acute Lung Injury, Repair, and Remodeling: Pulmonary Endothelial and Epithelial Biology. *Mediators Inflamm* 2017**,** 9081521.